Facilitating Non-Covalent Interactions:
'Nanoglue' for DNA-CNT Nanohybrid Complexes

Oliver W. J. Burnham

Master of Science by Research

Chemistry

December 2010

Abstract

Polyamine-terminated first and second generation Newkome dendrimers possessing a perylene core were synthesised. Interactions were probed between carbon nanotubes and the perylene core. The DNA binding ability of the dendrimers was tested.

As with similar, non polyamine terminated perylene containing dendrimers reported in the literature, the first generation dendrimer was shown to solubilise carbon nanotubes.

The first generation dendrimer demonstrated a particularly high DNA binding ability, presumably in part due to covalent and self-assembled multivalency. Theory and observations gave cause for concern regarding the applicability of the ethidium bromide displacement DNA binding assay to systems containing polycyclic aromatic hydrocarbons, due to the possibility of intercalation into the DNA double-helix. This alternate binding mode was investigated. The second generation dendrimer exhibited slightly reduced binding ability relative to its cationic charge, in opposition to the increase in binding strength that would be expected due to increased covalent multivalency, but in accordance with a reduction in intercalation and self-assembled multivalency.

Difficulty was experienced imaging DNA by transmission electron microscopy; accordingly no direct evidence could be produced to demonstrate the existence of DNA dendrimer CNT nano-hybrids. However, the data indicating the formation of CNT-dendrimer complexes and dendrimer-DNA complexes suggest that, in solution, DNA dendrimer CNT nano-hybrids should be present. No evidence could be found to suggest that binding of the dendrimer molecules to carbon nanotubes significantly reduced their affinity for DNA, nor to suggest that binding of the dendrimers to DNA significantly inhibited their CNT binding ability.

Acknowledgements

Many thanks first and foremost to Professor David K. Smith for his ideas, advice, and guidance throughout the project, and to the rest of the Smith group for their help and support in addition to that referenced and acknowledged elsewhere. Thanks also to my Independent Thesis Advisory Panel Member, Dr Anne Routledge, for her advice and suggestions.

Thanks to Meg Stark for advice and assistance with electron microscopy and circular dichroism spectroscopy.

Thanks to Karl Heaton and to Trevor Dransfield for mass spectrometry, particularly regarding the various problems encountered when characterising strongly interacting perylenes.

Thanks to Heather Fish and Amanda Dixon for assistance with nuclear magnetic resonance, again especially regarding problems encountered with strongly interacting perylenes.

Thanks finally to my family and friends, and to Samantha, for their company and support when it was needed most.

Declaration

I declare that the work submitted in this thesis is my own except where otherwise acknowledged or referenced, and, except where referenced, has neither been published nor submitted for a degree or qualification at this or any other university.

Oliver W. J. Burnham

Abbreviations and Chemical Formulae

Ac	Acetate
Boc	*tert*-butoxycarbonyl
CD	Circular dichroism
$CDCl_3$	Deuterated chloroform
CFTR	Cystic fibrosis transmembrane conductance regulator
$CHCl_3$	Chloroform
CNT	Carbon nanotube
δ	Chemical shift
Da	Dalton/atomic mass unit, *ca.* 1.66 x 10^{-27} kg
DAPMA	*N*,*N*-di-(3-aminopropyl)-*N*-(methyl)amine
DCC	Dicyclohexylcarbodiimide
DCM	Dichloromethane
DIPEA	*N*,*N*-Diisopropylethylamine
DMAP	4-Dimethylaminopyridine
DMD	Duchenne muscular dystrophy
d-MeOD	Deuterated methanol
DMSO	Dimethyl sulfoxide
dsDNA	Double-stranded DNA
DNA	Deoxyribonucleic acid
EthBr *	Ethidium bromide
ESI	Electrospray ionisation
EtOAc	Ethyl acetate
f-CNT	Functionalised carbon nanotube
G1, G2, ..., G*n*	First generation, second generation, *n*th generation
HCl	Hydrogen chloride or hydrochloric acid
HOBt	Hydroxybenzotriazole
IR	Infrared
M	mol dm^{-3}
m/z	Mass to charge ratio

MALDI	Matrix-assisted laser desorption ionisation
Me	Methyl
MeOH	Methanol
mRNA	Messenger RNA
MWCNT†	Multi-walled carbon nanotube
NMR	Nuclear magnetic resonance
PBI	Perylene bisimide
PEI	Polyethyleneimine
PEG	Polyethylene glycol
ppm	Parts per million
R_f	Retention factor
RNA	Ribonucleic acid
SDBS	Sodium dodecylbenzene sulfonate
SDS	Sodium dodecyl sulphate
SWCNT‡	Single-walled carbon nanotube
T3P	2-Propanephosphonic acid anhydride
TBTU	Tetramethyl-O-(benzotriazol-1-yl)uronium tetrafluoroborate
TEM	Transmission electron microscopy
TFA	Trifluoroacetic acid
THF	Tetrahydrofuran
UV/Vis	Ultraviolet/visible light

* Abbreviated in some publications as EtBr

†Abbreviated in some publications as MWNT

‡Abbreviated in some publications as SWNT

Contents

1 Introduction

1.1 Nanohybrids

In many areas of chemistry and physics, biology is increasingly a guide and an inspiration for further development. The formation of nanostructures provides the opportunity to create complex systems that promise new functionality and greater degrees of controllability. In biological systems, nanoscale structures range from functional molecules such as proteins and deoxyribonucleic acid (DNA) to larger, near microscale cell organelles. In cooperation with associated cell machinery, DNA and enzymes control the biochemical functions of the cell.

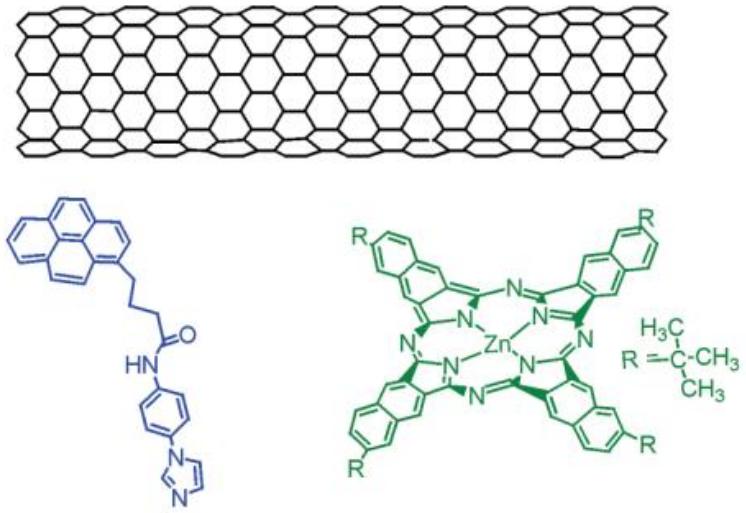

Figure 1: Three components of a carbon nanotube (top), zinc naphthalocyanine (bottom-right) and imidazole (bottom-left) nanohybrid.[1]

Nanohybrids promise a means to construct complex systems from well-defined components, many of which have well-characterised and well understood behaviour and function. For the purpose of this thesis, we will consider a nanohybrid to consist of two or more functionally or structurally distinct sub units. These units, and the resulting hybrid, should be of or near to the nanoscale, and the component parts can be bound together either covalently or non-covalently. To illustrate this principle, non-covalent

π-π stacking interactions have allowed pyrene functionalised imidazole units to be bound to carbon nanotubes (CNTs). Zinc naphthalocyanine can then be bound to the imidazole unit, producing a three-component nanohybrid in which the nanotubes can be reduced by photoinduced electron transfer from the naphthalocyanine (Figure 1).[1] A similar approach has been followed to produce a buckminsterfullerene-CNT nanohybrid via covalent functionalisation of the fullerene unit with a pyrene moiety, and subsequent non-covalent interaction between this pyrene and the nanotube (Figure 2).[2]

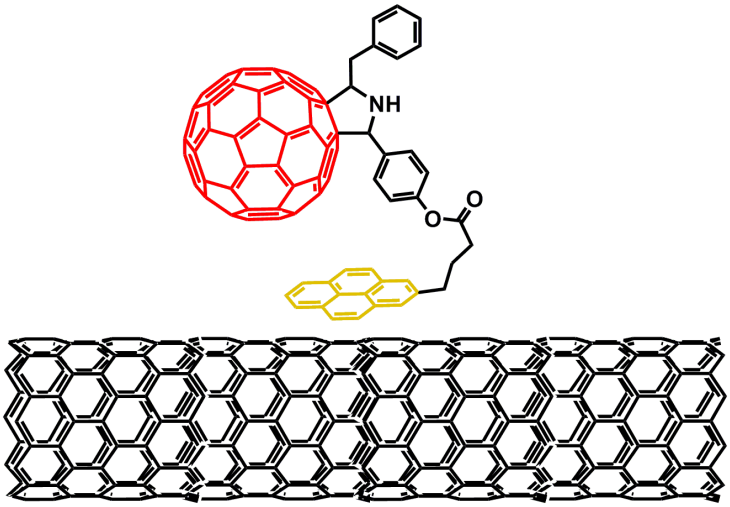

Figure 2: Buckminsterfullerene-CNT nanohybrid, facilitated by covalent functionalisation of the fullerene unit (red) with a pyrene moiety (yellow).[2]

The term *bio-nanohybrid* refers to materials containing both a biological unit and an inorganic substrate, such as composites of layered double hydroxides and DNA, or gold nanoparticles and chitosan.[3] Nanohybrids containing both biological molecules and organic units have also been produced, including complexes consisting of a protein bound to a dendritic polyamine (Figure 3), and numerous polymer-DNA or lipid-DNA complexes.[4–9]

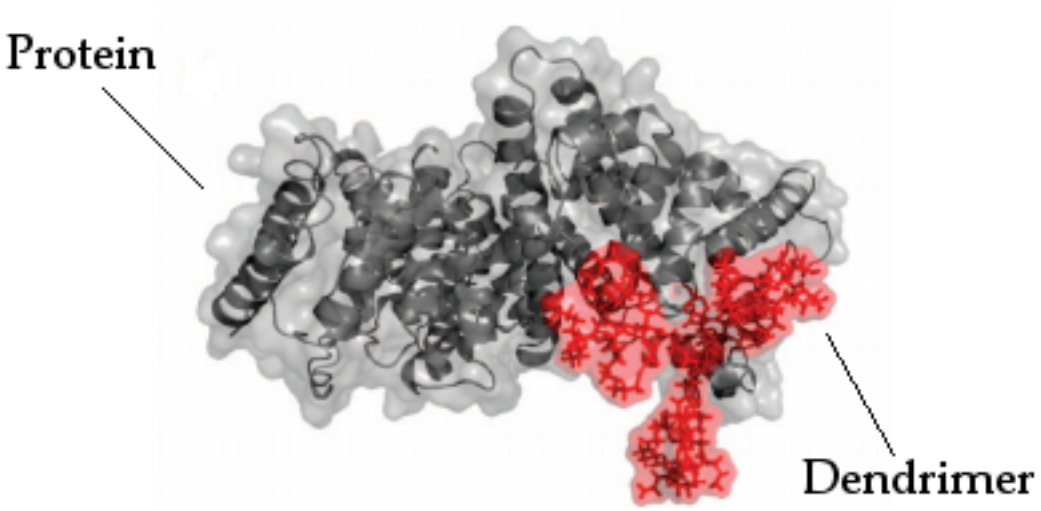

Figure 3: Covalently-bound dendrimer-protein bio-nanohybrid, formed by the attachment of a polyamine-terminated second-generation dendron to bovine serum albumen.[4]

1.2 Nanoscale Architectures

1.2.1 Dendrimers and Dendrons

Dendrimers, historically also known as arborols or cascade molecules, are a class of symmetrical, highly-branched polymers or oligomers. Synthesis is an iterative process, individually adding successive layers or generations to the molecule, allowing for control over both the degree and extent of any branching and thus the overall molecular weight and number of surface groups. Accordingly, unlike most typical polymers, true dendrimers are monodisperse, providing nanoscale building-blocks of known size and behaviour (Figure 4).

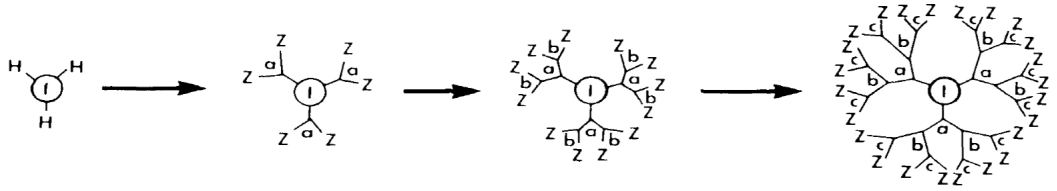

Figure 4: Well-defined, spherical dendrimer produced by an iterative synthesis.[10]

As with polymer derivatisation, surface-group modification of dendritic

molecules provides for some tuneability of their interaction with other molecules. However, the layered structure of dendritic molecules, consisting of *core*, *shell*, and *surface* regions distinguishes them from polymers in that there can be considerably more control over the spatial location of any modifications. This allows for separation of function of the different regions of the vector. Such specialisation has been used to create hydrophobic pockets in a dendrimer's shell, allowing for encapsulation of a toxic, hydrolysable or insoluble drug molecule, while the surface was functionalised with hydrophilic groups, facilitating solubility and biocompatibility and enabling delivery of the drug *in vivo*.[11] Alternatively, dendrimers can be tuned to bind to larger molecules, with surface groups having being added that target specific cell surface proteins,[12] or cores included that are capable of binding large synthetic molecules.[13]

The branching that accompanies the formation of each generation means an exponential increase in the number of terminal groups, rapidly producing molecules with a high-degree of multivalency. This makes dendrimers especially suited to applications where cooperative binding effects are beneficial or desirable, such as receptor binding *in vitro* where dendritic multivalency can allow effective host-guest binding at nanomolar concentrations.[14] The formation of aggregates, either as well-defined dimers or oligomers, or as more amorphous units, has been shown to further enhance the binding ability of many dendrimers, in effect forming a number of non-covalent, highly multivalent supermolecules. Control over the population of these aggregated forms through the introduction of solvophobic moieties, or through increasing the steric bulk of the molecule, is another tool available to chemists, allowing encouragement or reduction of the extent to which their dendrimers interact with each other and with other molecules in solution.

Due to their branching and symmetry, most families of dendrimers will tend towards a spherical morphology as their mass increases (Figure 4). In contrast, dendrons, which can be thought of as a fragment or segment of a dendrimer, are asymmetric with a more easily accessible core. These

characteristics allow dendritic molecules to be further optimised for a given application.

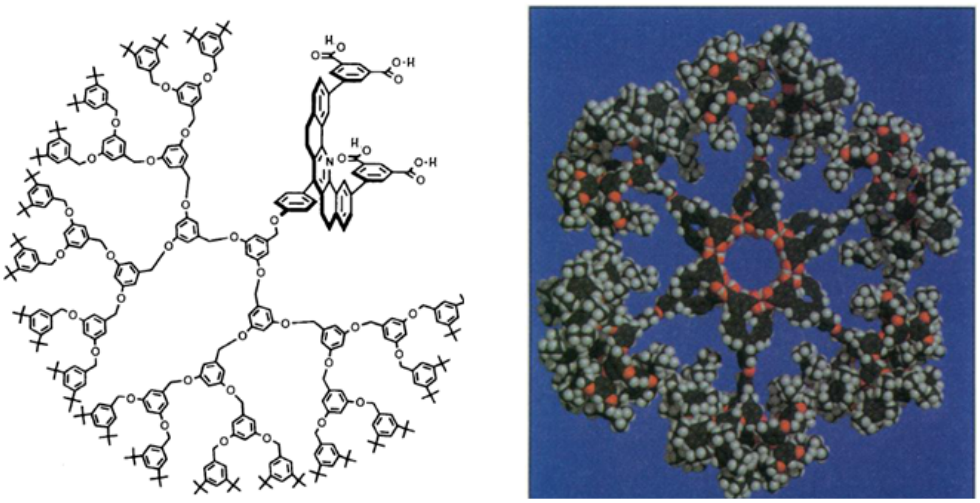

Figure 5: Fréchet-type dendron bearing a tetracarboxylic acid core (left), and the dendritic hexamer produced when six of these dendron units self-assemble (right).[15]

Interactions between complementary dendrons, or between metal ions and multivalent ligands can produce large self-assembled dendrimers (Figure 5).[15,16] This can be an end in itself, or the resulting dendrimer can then be incorporated into larger structures. Cationic dendrimers, either covalently or non-covalently produced, form non-specific complexes with double-stranded DNA, with a number of possible conformations depending on the initial morphology and degree of branching of the dendrimer, and the relative concentrations of DNA and dendrimer.[17]

1.2.2 Carbon Nanotubes

On the nanoscale, there are many types of nanotubes: hollow, pseudo-one dimensional structures with a range of unique properties due to their unusual morphology. Tubular structures, with the atoms arranged in a manner similar to a rolled up sheet of graphite, have been produced from carbon,[18] silicon,[19] and boron nitride,[20] with subtle differences between these isoelectronic analogues. Biological molecules have also been shown to form nanoscale

tubes, with DNA having been formed into programmable structures less than 20 nm across (Section 1.2.3). Naturally occurring structures connect the cytoplasm of adjacent cells in both animals and plants and have been described as nanotubes; however, possessing diameters of up to 700 nm in animals and up to 50 nm in plants, they are considerably wider than many of the synthetically produced structures described above.[21,22]

The first of these synthetic nanotubes were those formed from carbon. Reported by Iijima in 1991, carbon nanotubes are one of several recently discovered carbon allotropes and are closely related to other recently discovered forms of carbon: fullerenes and graphene.[18,23,24] CNTs can exist as single layers, known as single-walled carbon nanotubes (SWCNTs), or multiple layers nested within one another (multi-walled carbon nanotubes, or MWCNTs), with the single-walled variant reported independently and simultaneously in Nature by two groups in 1993.[25,26] Carbon nanotubes possess considerable tensile strength and rigidity and, when unmodified, can act as one-dimensional wires due to their extended aromatic nature.[27,28] Their unique properties render them of great interest in the fabrication of materials and structures across a wide range of scales.

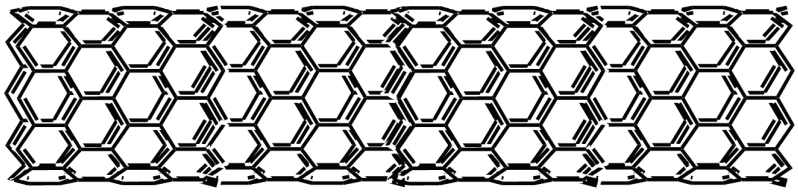

Figure 6: Carbon nanotube, showing the extended graphitic aromatic structure.

Carbon nanotubes have been used to produce ultra-strong fibres,[29] with potential for use in macroscale structures that require otherwise unobtainable tensile strength, such as proposed "space-elevators,"[30,31] as well as being used to reinforce polymer composites.[32] On the nanoscale, carbon nanotubes feature in numerous donor-acceptor nanohybrids, including those described above.[1,2,33] Magnetic nanoparticle-CNT hybrids have been shown to act as improved phenol oxidation catalysts,[34] while many other structural

or functional hybrids between CNTs and a diverse array of nanoscale components such as dendrimers, DNA, or proteins have also been reported.

Hybrids containing carbon nanotubes can be formed by both covalent and non covalent means. Functionalising carbon nanotubes by covalent methods typically involves either oxidation in an acidic medium or 1,3-dipolar cycloaddition, producing substituted structures with much of the carbon nanotubes' unique aromatic character disrupted by the modifying groups,[35–37] although ester-branching dendritic units have been used in order to provide the nanotubes with a high population of functional groups with minimum covalent modification, with highly-branched dendrons "sprouting" from relatively few sites on the CNT surface.[38]

Nevertheless, in some cases even this minimal disruption this may be considered undesirable, particularly if the optoelectronic properties of the nanotube are the focus of interest. As with many nanoscale objects, a large proportion of carbon nanotubes' atoms are on the surface of the molecule - in single-walled carbon nanotubes this is the case for all of the atoms.[39] Consequently, covalent modification of the surface may have significant effects on the properties of the bulk material. It is therefore of great interest to explore routes that allow effective functionalisation of the carbon nanotubes by non-covalent means, as these approaches do not perturb the nanotubes' aromatic framework. Such methods rely on the CNTs' aromatic and hydrophobic character, and in this way make available a wide-range of functionalities and structural additions without chemically modifying the nanotubes' core chemical and physical structure.[39] Non-covalent functionalisation via π-π stacking or van der Waals interactions is, of course, thermodynamically controlled and accordingly suggests potential for CNT containing systems that could be tuned to respond to changes in their chemical or physical environment.[40]

Interactions between carbon nanotubes and common surfactants such as sodium dodecyl sulfate (SDS)[41] or gum arabic, a widely used polysaccharide

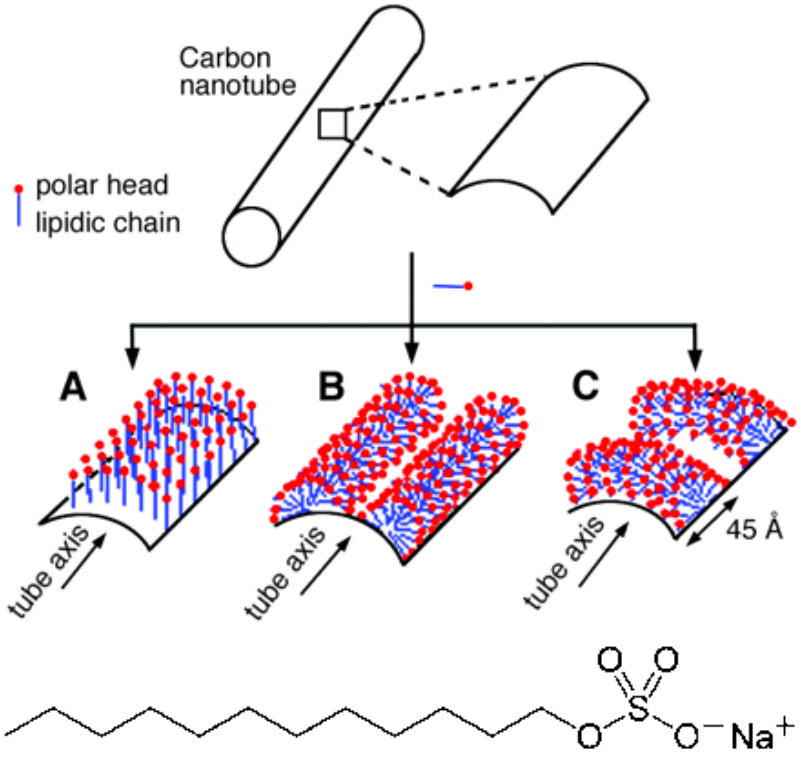

Figure 7: Sodium dodecyl sulphate surfactant (bottom) and illustration of the possible interactions between surfactant molecules and the hydrophobic CNT surface.[41]

food additive[32,42] allow the otherwise strongly aggregating CNTs to be dispersed in aqueous solution (Figure 7). Aside from these lipid derivatives or sugar based polymers, numerous other biological molecules will interact non-covalently with carbon nanotubes. Many proteins will adsorb onto CNTs and this has been exploited in combination with protein DNA interactions to pattern carbon nanotubes onto a DNA scaffold.[32] Direct interactions between CNTs and single-stranded DNA (ssDNA) have been used to create a highly selective and sensitive metal ion sensor. If the fluorescent dye 6-carboxyfluorescein is covalently attached to thymine-rich strands of ssDNA, DNA CNT interactions will keep the dye in close proximity to the aromatic CNT surface, resulting in quenching of the dye's fluorescence. Addition of Hg^{2+} ions promotes the formation of a double-stranded DNA-Hg^{2+} complex due to favourable thymine-mercury-thymine (T-Hg^{2+}-T) interactions, encouraging decomplexation of the modified ssDNA

from the CNT surface and so increasing the total fluorescence of the dye (Figure 8).[43]

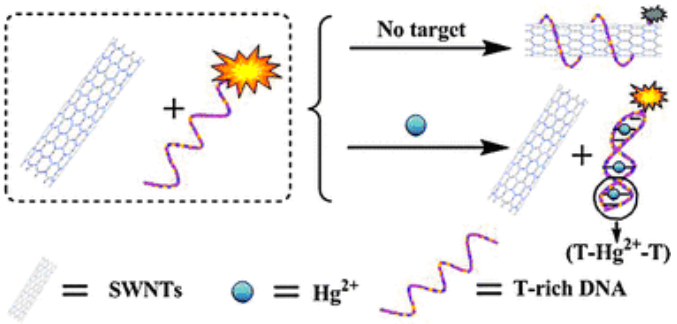

Figure 8: Representation of the possible interactions between modified ssDNA and a carbon nanotube (top-right), and between the same ssDNA and Hg^{2+} ions (bottom-right), indicating the resulting change in fluorescence of the attached dye.[43]

Carbon nanotubes can also form complexes with many biological and non biological species *via* encapsulation. Buckminsterfullerene (C_{60}) has been shown to enter the cavity inside CNTs, with multiple C_{60} units forming a "peapod" structure. Encapsulation has also been demonstrated using larger fullerenes, with "bucky-balls" as large as C_{84} having been observed to enter CNTs. Fullerenes that themselves encapsulate metal atoms have been encouraged to enter carbon nanotubes, creating three-component peapods in which each "pea" contains a shielded metal. Metal salts in solution or in their molten state have been encapsulated directly, as have metal atoms. In one eye-catching investigation, nanoscale thermometers were produced in which a column of liquid gallium was shown to expand linearly with temperature while encapsulated within a carbon nanotube (Figure 9).[40] Liquid water has also been demonstrated to enter carbon nanotubes, demonstrating that the hydrophobic environment within does not necessarily present a barrier to the entry of predominantly hydrophilic compounds.[44]

Small biological molecules have been shown to enter nanotubes, as well as adhering to the outer surface. DNA octanucleotides, for example, have entered into the spaces inside CNTs, as have segments of RNA.[32]

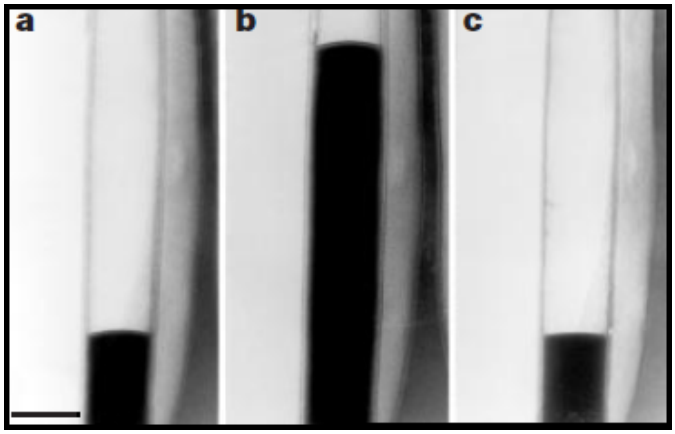

Figure 9: A gallium-CNT "nanothermometer," visualised by scanning electron microscopy, showing the changing level of the gallium meniscus at a) 58 °C, b) 490 °C, and c) 45 °C.[45]

1.2.3 DNA

Numerous approaches have been undertaken to control and manipulate DNA, either for the purposes of gene delivery (see Section 1.3), or for incorporation into nanostructures. In addition to interactions with dendrimers or with CNTs as described above, DNA tiles formed by nucleotide base-pairing have been formed into chiral tubes and ribbons,[46] while double-stranded DNA has been used to construct rigid tetrahedra[47] and truncated octahedra,[48] as well as "four-way junctions" being created by G-quadruplex formation (Figure 10).[49,50] These units could be incorporated into larger nanohybrid complexes as scaffold units to govern structure and orientation, or as functional units themselves.

Similar structures have been designed in which, with the covalent addition of other groups such as thiols, form cages capable of binding gold nanoparticles or a range of transition metals.[52,53] By covalently including protein binding ligands in a self-assembled, modified DNA nanostructure, distance dependent cooperativity can be probed with nanometre-scale precision,[54] while triplex-DNA has been used to create nanostructures with unique, individually addressable sites, potentially allowing sub-nanometre targeting by nucleotide recognition (Figure 10).[55]

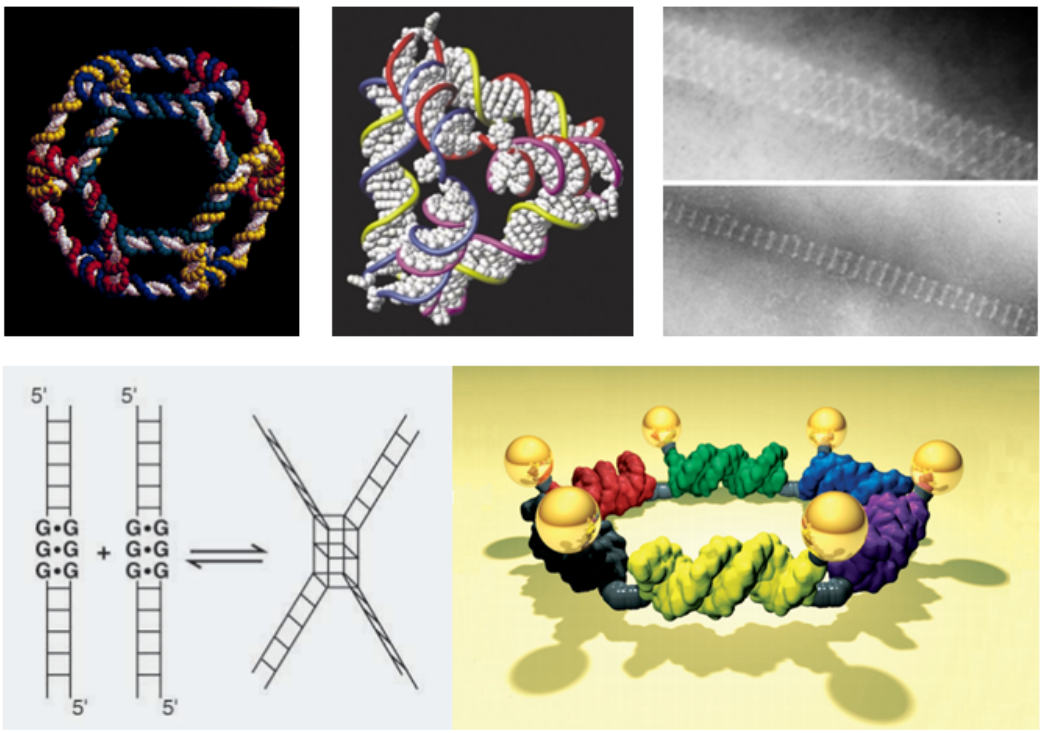

Figure 10: Truncated octahedron (top-left)[48] and a tetrahedron (top-centre)[47] created by complementary base-pairing, chiral DNA nanoribbons (top-right),[46] four way junction created by G-quadruplex formation between two double-stranded DNA oligonucleotides (bottom-left)[49] and a hexamer self-assembled from covalently modified DNA, able to template the arrangement of gold nanoparticles (bottom right)[51]

In addition to control over the placing of ligands, or nucleotide-specfic binding, non-specific DNA complexes can be formed using a number of techniques such as electrostatic attraction between cations and DNA's anionic backbone. The need for highly efficient, readily synthesisable DNA-binding molecules becomes apparent when examining their uses in gene therapy.

1.3 Gene Therapy and DNA Binding

Gene therapy offers considerable potential as a means of treating heritable genetic diseases, and as a novel treatment for non-hereditary diseases such as some cancers. The various approaches all share the common aim of introducing either modified DNA into the target cells or, in the case of damaging mutations, introducing the naturally occurring, "wild-type" form

of the gene. The following pages will explore some common means of gene binding, packaging and delivery, and outline some of the processes that must be considered when designing gene-therapeutic agents and other DNA binding molecules.

While the genes that govern a particular process are, in many cases, identified by correlating an error in function with an observed or induced mutation, many have been isolated based on similarities between the encoded protein and proteins of known function.[20] It should be noted that typically, the introduction of a working copy does not replace a defective gene, rather the additional material complements it: coding for the desired protein and so regulating a biochemical process that was hitherto unregulated or incorrectly regulated. In cases where pathology results from the production of an undesirable protein, or an otherwise acceptable protein in undesirable amounts, the gene's expression could, theoretically, be inhibited by introducing DNA or RNA complementary to the messenger RNA (mRNA) complicit in the production of the protein. The resultant double-stranded hybrid would be unable to take part in translation of the mutant genetic code, and the defective protein would no longer be produced.[56] Recent investigations have successfully demonstrated that double stranded short interfering RNA (siRNA) can have a similar effect, demonstrating a reduction of up to 50% in the expression of a specific protein.[57]

Mammalian cells cultured *in vitro* will take up DNA directly from their growth medium, albeit only at low levels, as will yeast and plant cells if first treated to remove their cell walls. Uptake can be promoted by preparing the DNA as its calcium salt, by increasing membrane permeability with the application of a high-voltage pulse, or by direct injection of DNA into the cells' nuclei using a fine-tipped pipette.[20]

Once inside the nucleus, the foreign DNA may remain distinct from the target cell's genetic material and is known, in this case, as an episome. Alternatively, the new genes may be attached to the resident chromosomes by foreign

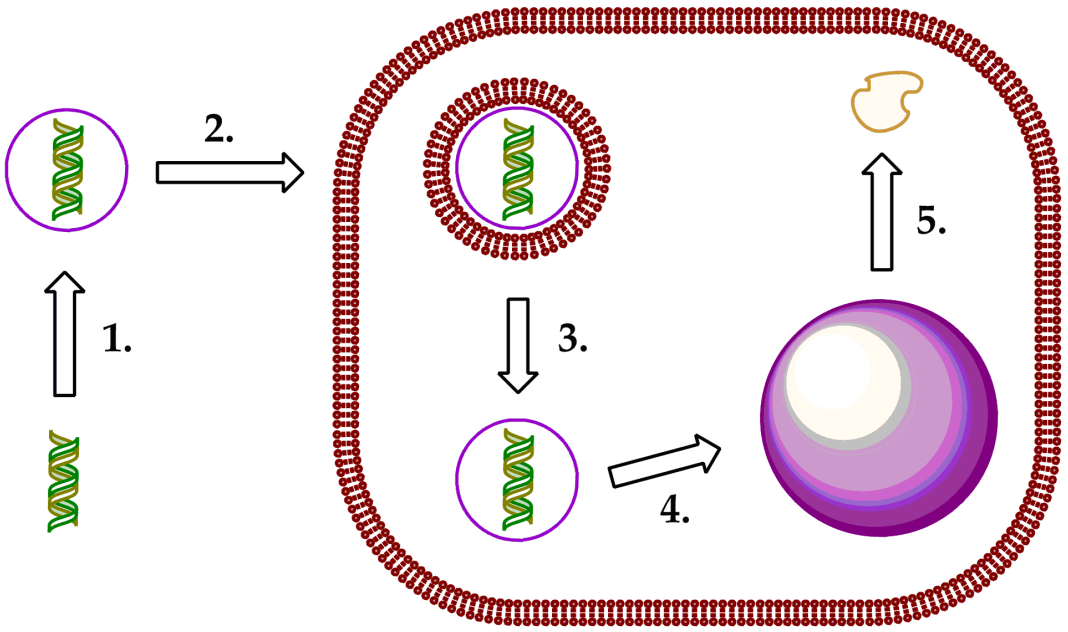

Figure 11: Vector-mediated transfer of DNA into a cell and the resulting expression of the gene, showing (1.) protection/complexation of the DNA with the vector of choice, (2.) transport across the cell membrane and encapsulation of the DNA and vector within an endosome, (3.) escape from the endosome, (4.) transport to the nucleus and decomplexation of the DNA from the vector, and (5.) expression of the gene, producing the desired protein.[54]

integrase enzymes introduced for that purpose, or by the cell's normal DNA repair and recombination pathways. Insertion may be site-specific or may be seemingly random, disrupting the host cell's genetic sequence and, in effect, causing mutations. Such non-specific addition can interfere with the coding of essential proteins, impairing the correct functioning of otherwise healthy cells and, in some cases, producing carcinogenic effects. In one French trial, several children developed a leukemia-like illness after integration of the therapeutic DNA disrupted other, previously healthy genes.[56] Alternatively, incorporation may be of no detriment to the host cell and, in the course of normal growth, these cells may replicate their now modified genome. In organisms that propagate by sexual reproduction, if this new genetic material makes its way into the gametes it will be inherited by any offspring; something between 0.1% and 1% of the DNA of mice is formerly viral DNA that has now become integrated into the genome.[20] While the deliberate incorporation of alien genes into somatic cells is of little social and ethical

concern beyond the immediate medical effects, the introduction of transgenic material into the human germ-line, leading to heritable genetic modifications, is currently considered to be cause for caution and, accordingly, research directly involving gene therapy using human gametes is not permitted in most jurisdictions.[56]

1.3.1 Viral Vectors

There are myriad ways to improve the absorption and expression of DNA by cells. The uptake of "naked" or untreated DNA can be increased in several ways, including those outlined above, or by techniques such as massage of the target organs.[58] Free DNA, however, does not persist *in vivo* if not taken up by cells; when incubated in blood, the majority of any unprotected DNA will degrade within 2 hours.[59] Viruses, being well adapted to transmit foreign DNA into cells, can be used to bind and package DNA, and then to "infect" unhealthy cells with this desirable genetic material.[20] Virus based gene therapy has been successfully used in the treatment of adenosine deaminase deficiency (ADA), one cause of SCID (severe combined immunodeficiency, or"'bubble-boy disease").[20,60,61] T-lymphocytes were isolated from the patient and infected *in vitro* with a retrovirus bearing the working adenosine deaminase gene. Regular injections of these transgenic immune cells led to a significant improvement in the patient's health. Similar ex vivo methods have been explored for other conditions in which, as in ADA, the defect is confined to a single gene and the pathological effect of the error is limited to a single type of easily accessible cell.[20,56]

In contrast, some conditions require an *in vivo* approach to treatment. Cystic fibrosis (CF) and Duchenne Muscular Dystrophy (DMD) are both frequently presented as possible candidates for gene therapy. While both conditions are the result of monogenic defects and would, conceivably, be treatable through the introduction of working CFTR and dystrophin genes respectively, in neither case are the target cells of a single type, nor are they easily

manipulated *in vitro* and then reintroduced, as in blood cell disorders.[56]

Retroviruses & Lentiviruses

In general, retroviruses are only able to infect replicating cells, as the viral genome must become incorporated into the target cells' chromosomes and is only able to do so during mitosis. This renders retroviral vectors of little use for conditions such as CF or DMD where the target cells replicate slowly, if at all. Lentiviruses exist as a sole exception in the family Retroviridae, having developed the ability to replicate without the cell division process. A lentivirus such as HIV could, therefore, be modified and used to transduce DNA into non-dividing cells. A further difference from the majority of retroviruses is that HIV infects only one type of cell (specifically, T lymphocytes) due to protein interactions between the virus' coat and the cell surface during infection. By modification of the virus surface proteins, this specificity can be tuned to target other cells. HIV-based vectors have been prepared in which 75 % of the original genome has been removed in order to reduce any risk of possible pathological effects *in vivo*, leaving only the genes necessary to enable the transduction of DNA into non-dividing cells. Concerns remain, though, that the modified virus may undergo recombination with related viruses, resulting in an infectious, pathological hybrid.[56]

Adenoviruses

Rather than containing RNA, which must then be transcribed into DNA after entry to the target cell, adenoviruses contain double-stranded DNA. Not needing mitosis and its associated biochemical process in order to manifest the desired genes, adenoviruses are able to infect non-replicating cells. In cells that do go on to replicate, the additional DNA is present as distinct episomes, rather than becoming integrated into the host cell's DNA, reducing

fears of germ-line contamination and oncogenic effects. Some show a degree of specificity for the respiratory tract and, accordingly, are well suited to treatment of cystic fibrosis. One adenovirus implicated in the common cold and thus ideally suited to infecting pulmonary tissue has been modified to carry a working copy of the CFTR gene,[20] though as the additional genetic material is not incorporated into any progeny of the target cells, repeat dosage was necessary. Adenoviruses, however, tend to provoke a strong immune response and, after multiple doses, this response can become increasingly severe. Even modification of the virus to minimise this effect is not always successful, and an adenovirus-based delivery method has led to the death of one patient suffering from ornithine transcarbamylase deficiency during Phase I clinical trials, due to an inflammatory reaction to the vector.[56]

1.3.2 Non-Viral Vectors

In addition to problems of pathology and other undesirable biological effects, it may be impractical to transduce long segments of DNA using viral vectors. As many human genes are indeed very large, either truncated versions must be engineered that maintain the full functionality of the original or, alternatively, non-viral vectors capable of transfecting large sections of DNA must be explored.[20]

Without the integrase enzymes present during retroviral transduction, non-viral vectors are not capable of incorporating a significant proportion of their load into the target cells' chromosomes. While this may be of some concern when treating the most prolific cells, in the case of CF or DMD it is not an issue; the target cells in these conditions replicate slowly, if at all, and passing the additional genetic information along to their progeny is therefore of little importance. Maintaining the foreign DNA as distinct episomes also carries the advantage of avoiding disruption of viable genetic material, hopefully reducing the incidence of gene therapy induced cancers. Aside from these common advantages, the range of available non-viral methods

is as broad and varied as that of viral vectors. The common factor linking these approaches is the presence of cationic groups in the complexing agent. The electrostatic interaction between the cationic moiety and the anionic phosphate backbone of the DNA helix serves to provide a strong attraction, binding the DNA to the vector and allowing the transport of the genetic material to be facilitated by the binding agent's specific physicochemical properties. In addition, the resulting charge-neutralisation causes collapse and compaction of the oligonucleotide which further assists in the process of cell membrane trafficking.[35]

Lipoplexes

As biological molecules present naturally in a wide array of forms, lipids, with or without significant synthetic modification, present themselves as candidates upon which further DNA-binding and delivery agents can be based. Lipids typically self-assemble due to their predominantly hydrophobic nature, and the cationic head group present naturally in many fatty acids or phospholipids will interact favourably with DNA. Such groups can also be introduced synthetically. Cationic lipid-DNA complexes, or lipoplexes, lack the immunogenicity and possible pathogenicity of viral vectors. In addition they are biodegradable and relatively easy to prepare. Lipoplexes also promise a degree of tuneability through covalent modification or blending of different lipids, with the charge, structure of the hydrophobic portion, and spacing between the charged and hydrophobic moieties all playing a part in DNA-binding and transfection capacity.[62] After complexation, the resulting DNA-containing liposomes interact electrostatically with anionic cell-surface glycoproteins and then fuse with the phospholipid membrane, enabling passage of the lipoplex into the interior of the cell.[35,63] Uptake of intravenously injected lipoplexes is rapid; within five minutes of injection nearly two-thirds of the total concentration of a DNA-lipid complex could be found in the liver and lungs alone, with less than 3 % remaining in the blood. This can be contrasted with free DNA, of which 36 % remained

after five minutes, before rapidly degrading.[59] Once inside the cell, the packaging afforded by the charge-neutralisation effect of the cationic lipids further facilitates transport of the DNA through the cytoplasm. The interior of the cell is not homogeneous, and it is thought that cytoskeletal elements function in a manner akin to molecular sieves, inhibiting the diffusion of large molecules. Highly-compacted nucleotides will, therefore, be able to diffuse through the cell more rapidly.[35]

While lipoplexes typically do not exhibit the negative immunological effects associated with viral vectors, at higher concentrations the cationic lipids used can exhibit cytotoxicity, leading to cell death.[63] Increasing the concentration of the cationic lipids does, however, improve the degree of transfection[63] presumably in part due to improved packaging of the DNA and perhaps in part due to the proton-sponge effect.[64] Upon entry into the cell, the DNA-lipoplex will, for some time, exist within an endocytic vesicle or endosome, a bubble of cell membrane within which the cell can partition and control the chemical environment and diffusion of foreign substances. Cells will then acidify these vesicles, and exit from the endosome is essential if the genetic material is to avoid degradation, and move through the cytoplasm in order to gain access to the nucleus. The acidification of the endosome can be manipulated in order to facilitate this exit; protonatable sites in the vector will act to buffer the endosomal environment, forcing the cell to introduce ever-increasing concentrations of ionic solutes. The resulting osmotic swelling eventually leads to the bursting of the endosome and discharge of its contents into the cytoplasm. This process can be aided by the addition of promoters such as chloroquine, however, as with the cationic lipids themselves, higher concentrations of chloroquine will lead to cytotoxicity and cell death.[65] The efficacy of chloroquine in aiding transfection has been taken to support the endocytosis-based model for lipoplex entry.[66] It has also been demonstrated that in some cases lipoplexes or nucleotides are able to pass through the endosome or cell membrane using a "flip-flop" mechanism, in which lipids in the lipoplex are exchanged with those in the membrane.[67,68]

Trials involving lipoplex-based aerosols monitored the presence of CFTR DNA and mRNA in nasal epithelia, and quantified the expression of the gene by measuring the conductance and absorbance of chloride and sodium ions respectively. Levels of expression were transient, and low, but were comparable to those observed when investigating adenovirus based vectors. Unlike the adenovirus, however, the lipoplex aerosol did not trigger an immune response.[56]

Polyplexes

Cationic polymeric molecules, both biologically-derived and entirely synthetic, have been explored as DNA-binders. Akin to the naming logic behind the term "lipoplexes," these polymer-DNA complexes are commonly known as "polyplexes." Gene delivery was initially demonstrated in 1975, both *in vitro* and *in vivo*, using a lysine-based polymer. In their simplest polylysine form, molecular weights above 3000 Da are required for effective DNA complexation. Further investigations, modifying lysine oligomers with the addition of other peptides or non-biologically derived molecules such as imidazole, have demonstrated improved DNA-binding and reduced cytotoxicity.[35]

As with lipoplexes, it is the cationic nature of the protonated amine moieties on lysine that enables binding of the anionic DNA phosphate backbone. Accordingly, high-molecular weight, highly-branched polyethylenimine (PEI - Figure 12) has demonstrated considerable transfection efficiency.[35] Again, the structure of this polymer-based vector has been modified in order to improve its DNA-binding capacity, and reduce its cytotoxicity - demonstrated, in PEI, as being due to compromise of cell surface membrane and mitochondrial membrane integrity.[35,69] Derivatisation with polyethylene glycol (PEG) known as "PEGylation," inhibits unfavourable interactions between the vector and blood components by creating a hydrophilic surface on the polyplex.

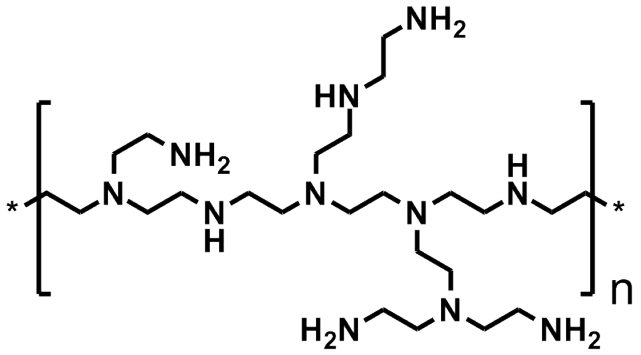

Figure 12: Portion of a branched polyethyleneimine (PEI) structure

Complex Dissociation

Contrary to initial expectations, the acetylation or addition of dextran groups to PEI vectors has been shown to improve gene transfection capacity, in one instance by a factor of nearly 60.[70] It would be thought that the functionalisation of otherwise protonatable nitrogen atoms would reduce gene delivery by preventing efficient binding of DNA in the polyplex. While it is indeed the case that reducing the potential net charge of the polymer will reduce its affinity for DNA, this seems, to an extent, to be beneficial for gene expression, presumably due to facilitating dissociation of the complex after delivery into the cell. The introduction of biodegradable moieties into the vector is a further means of reducing the strength with which the DNA is bound, and, if these groups are carefully selected, only after entry into the cell. A polylysine derivative, containing a number of cysteine residues was held together in part by disulfide bonds, allowing the vector to break down after entry to the cell.[71] In PEGylated polyplexes, the polymer is hydrolysable,allowing the vector to degrade once inside the cell.[72]

Charge-density

While the net cationic charge is an important factor in the tolerance of the cells to a non-viral vector, it would appear that spreading out this charge has the capacity to reduce cytotoxicity without compromising transfection efficiency.

Modified lipoplexes, in which the ammonium cations were replaced with arsonium or phosphonium groups, possessed lower charge-density due to the larger ionic radius of As^+ and P^+ as compared to N^+. Another alternative that has been explored is the replacement of the ammonium group with pyridinium, allowing the charge to be delocalised around the aromatic ring.[35] The incorporation of arginine units into peptide-based polyplexes contributes towards a reduced cytoxicity relative to lysine, due to resonance across the guanidinium cation.[6,73] Molecules in which the same net charge is more spread out demonstrate an increased transfection efficiency *i.e.*, reducing the charge density while maintaining the overall charge of the molecule actually improves transfection as well as reducing the vector's toxicity.[35] The need for efficient gene delivery, and the clear problems with the use of viral vectors *in vitro*, highlights the importance of research into novel DNA-binding compounds.

1.3.3 DNA-binding Dendrimers

Just as highly-branched polyethyleneimine polymers demonstrate a higher capacity for DNA binding than those based on linear PEI,[35] vectors based on dendrimers have shown a high degree of DNA-binding and gene transfection capability. Dendritic polyamidoamine (PAMAM) has been shown to efficiently bind DNA, and has been commercialised as an *in vitro* gene transfection agent, while dendritic polylysines have been developed that show comparable levels of transfection with reduced toxicity.[74]

Dendrons and dendrimers provide well-defined polymer-type properties, allowing for control over both the degree and extent of any branching and thus the overall molecular weight and number of surface groups. Modification of the dendrimers' primary and secondary structure has been shown to affect the morphology of the resulting DNA-dendrimer complexes: treatment of hydroxyl terminated PAMAM dendrimers with methyl iodide results in permanently cationic dendrimers which produce more highly

compact polyplexes,[75] while PAMAM dendrimers heated to "fracture" their spherical structure (Figure 13) have been shown to form toroid shaped units when bound to DNA.[76] These toroidal complexes have demonstrated improved transfection ability, and have been commercialised as Superfect®.[77]

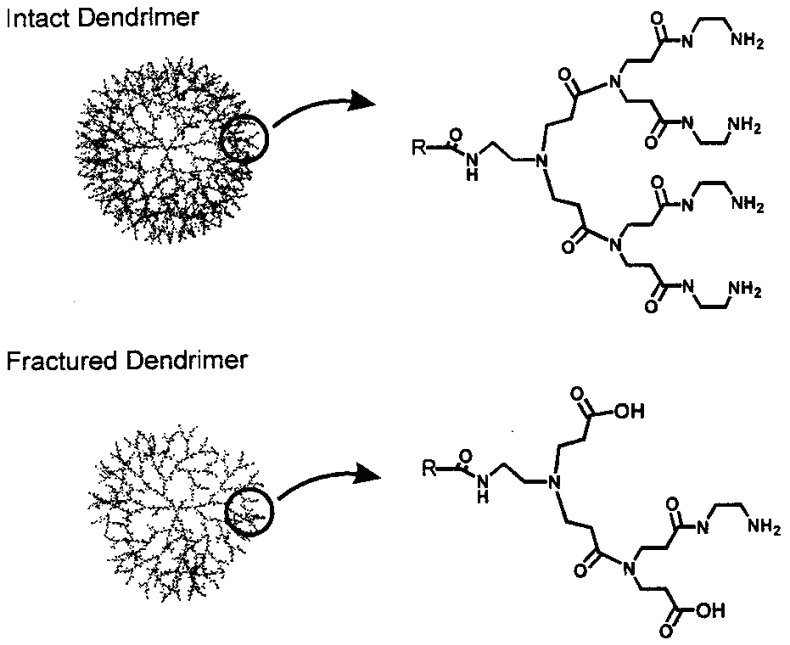

Figure 13: Unmodified (top) and "fractured" (bottom) PAMAM dendrimers, showing secondary structure (left) and primary chemical structure (right).[76]

A number of groups have investigated the surface modification of otherwise nitrogen-poor dendrons.[78,79] Using standard Newkome and Fréchet syntheses,[80–82] well-characterised and well understood dendrons can be produced in high yields; simple coupling to amine-rich terminal groups then provides a cationic surface capable of efficient binding of DNA (Figure 14).[79] Such strong binding is not typically cause for concern in the construction of structural nanohybrids. However, in dendrimers destined for use in gene therapy, the considerable strength with which these multivalent polyamines form complexes with DNA has, in some cases, been demonstrated to be detrimental to transfection, with the delivery and expression of the packaged genes hindered by low rates of decomplexation inside the cell. Attempts have been made to aid the dissolution of these complexes, either by introducing hydrolysable groups into the dendrimer's

shell,[83] or by reducing the ionic strength of the surface groups by replacing a polycation such as spermine with a less protonatable alternative such as *N*,*N*-di-(3-amino-propyl)-*N*-(methyl)amine (DAPMA).

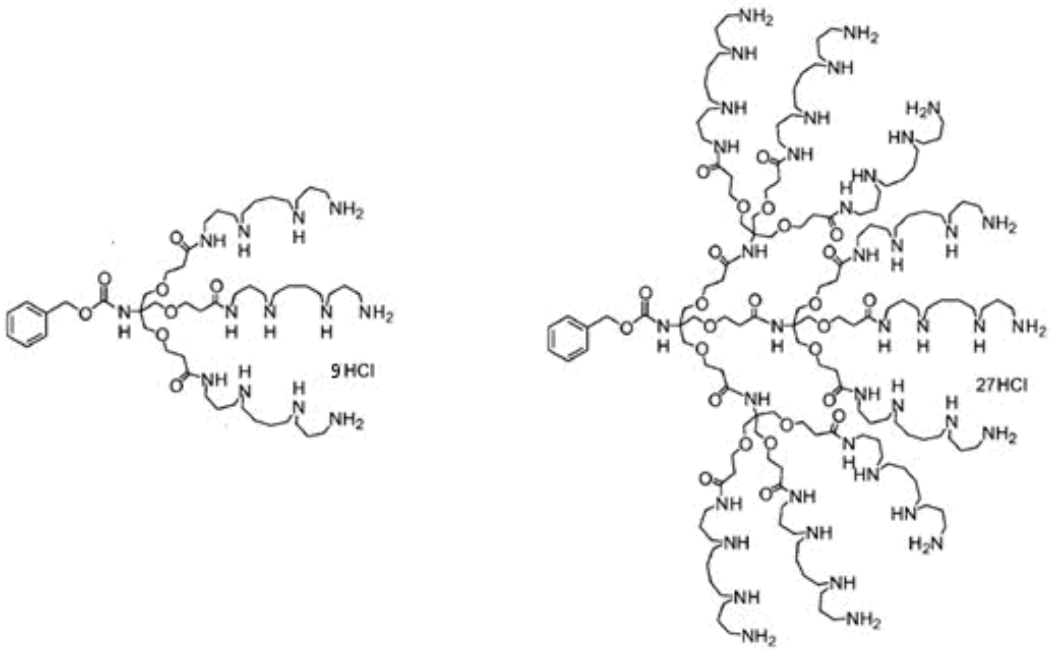

Figure 14: G1 & G2 amide Newkome ether dendrons, with spermine-based surface groups.[84]

Synthetic vector design has considered not just covalent branching, but also the potential provided by self-assembled multivalency.[85] Just as multiple cationic lipids act cooperatively during lipoplex formation, amphiphilic dendrimers and dendrons will, if possible, assemble into highly-charged aggregates, further enhancing their DNA-binding ability. Steric hindrance must be taken into account, with more linear, planar molecules often being more able to form aggregates but perhaps losing some of their covalent branching and multivalency in return.[78] Study of a library of asymmetric diphenylacetylene dendrons demonstrated that increased branching in the hydrophobic heads of otherwise self-assembling molecules discouraged formation of dimers, presumably due to the increase in steric bulk.[21] The tendency of dendritic molecules to self-assemble or to dissociate in response to their covalent structure and external environment can be harnessed to increase or decrease the effective multivalency of the dendrimer aggregates.

Through careful tuning of the steric properties and the protonatability of the component dendrons, the morphology of the resulting DNA-polyplexes can be made pH responsive, with clear implications for controlled release or uptake of DNA.[86]

Dendrons have been synthesised that self-assemble "inside-out" in the presence of DNA, with their branched, cationic head groups facing toward the centre of the polyplex while their tails face outwards.[15] In such structures, the DNA acts as the core of this non-covalently formed hybrid, while the tails of the component dendrons, now the surface of the complex, can be functionalised with tissue targeting groups or, potentially, functionalities designed to promote interaction with other nanoscale structures (Figure 15).

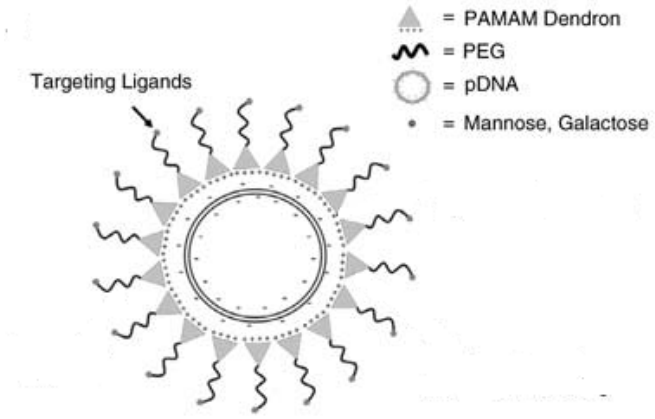

Figure 15: Non-covalent nanohybrid, consisting of plasmid DNA, asymmetrical PAMAM dendrons, PEG "tails" and cell-surface protein targeting ligands.[15]

1.3.4 Carbon Nanotubes as Vectors, and as Nanoscale Building Blocks

Modifying the core of such DNA binding dendrons and dendrimers to promote their supramolecular interaction with carbon nanotubes could provide an interesting means of facilitating DNA-CNT binding without significant divergence from established synthetic methods, nor any need for covalent modification of the nanotubes.

Previously, DNA-CNT hybrids have relied on covalent modification in order

to produce functionalised carbon nanotubes (f-CNTs). The addition of, for example, amine groups both solubilises the nanotubes and provides a mechanism for non-covalent interaction with DNA; at biological pH the amines are largely protonated and, as in lipo- and polyplexes, the resulting cations interact favourably with DNA (Figure 16).[87]

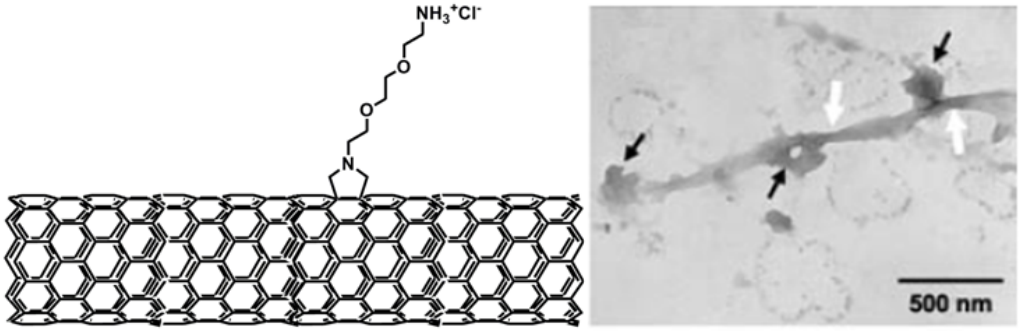

Figure 16: Ammonium functionalised CNT (left) and an f-CNT complexed with DNA (right). These f-CNT-DNA complexes have demonstrated effective transfection of DNA into cells.[87,88]

While carbon nanotubes are not, as such, toxic, when introduced into murine lung tissue *in vivo* CNTs above 20 μm in length have demonstrated "asbestos-like" properties, leading to inflammation and scarring.[89] It may be desirable, therefore, to restrict the selection of carbon nanotubes used in gene delivery to those below this length limit, especially if they are to be used to treat pulmonary tissue.

Evidence suggests that, unlike most other non-viral vectors, the mechanism of delivery does not proceed via endocytosis.[35] The rigidity and length of the nanotubes make encapsulation within an endosome implausible. In addition, CNT-based vectors have been shown to enter the cell even after treatment of the cells with sodium azide or 2,4-dinitrophenol, both of which inhibit endocytosis and any other active, energy-dependent route of uptake. It had been hypothesised that carbon nanotubes are able to pass directly through the cell membrane without causing sufficient damage to result in cell death.[88] Molecular modelling suggests that functionalised nanotubes first

orient themselves parallel to the cell surface, lying along the membrane. Lipid flipping then allows the nanotube to rotate through ninety degrees, leaving it perpendicular to, and transecting, the cell membrane.[90] A reversal of the procedure should then leave the nanotube either outside or inside the cell. Analysis by transmission electron microscopy has shown that once f-CNTs have entered the cell, they tend to become localised in the nucleus.[88]

As stated above, covalent modification of the carbon nanotube surface may have detrimental effects on the properties of the bulk material. It may, therefore, be desirable to explore routes that allow functionalisation of the carbon nanotubes by non-covalent means, facilitating strong CNT-DNA binding without the need for harsh treatment of the nanotubes. The creation of a three-component nanohybrid, in which an additional molecule is capable of strong non-covalent binding to both carbon nanotubes and DNA could satisfy these aims. Molecules capable of non-covalent interaction with both DNA and carbon nanotubes could be thought of as a loosely attached bridging unit, or a nanoscale glue.

Hirsch *et al.* have demonstrated that their perylene bisimide (PBI) dendrimers (Figure 17) are capable of adsorption onto the surface of single-walled carbon nanotubes, disrupting the nanotube bundles and effectively solubilising the carbon nanotubes in pH 7.0 buffered aqueous solutions.[36] Several dendrimers were investigated, with asymmetric dendrimers providing the best solubilising effect. It was theorised that this was due to a greater degree self-assembled multivalency, with the formation of the dendrons into micelle type structures encouraging the carbon nanotubes to dissolve.[91]

A number of molecules based on the pyrene moiety have also been shown to solubilise carbon nanotubes via π-π interactions between the aromatic unit core and the CNTs' extended aromatic systems.[39,92,93]

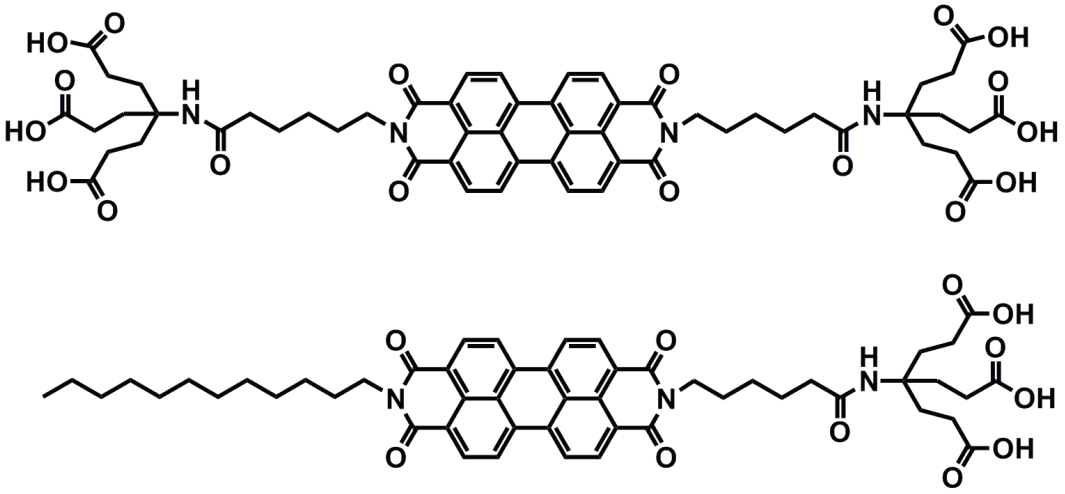

Figure 17: Symmetric, bolaamphiphilic (top) and asymmetric, amphiphilic (bottom) first generation perylene bisimide dendrimers, capable of solubilising SWCNTs.[36]

1.4 Aims

These dendritic perylenes and pyrenes show clear potential for functionalisation with polyamine groups, *via* the type of amide coupling routes and dendron syntheses previously demonstrated in the Smith group.[94] This approach would afford dendrons or dendrimers capable of supramolecular interaction with both DNA and carbon nanotubes, providing an interesting means of facilitating DNA-CNT binding without significant divergence from established synthetic methods, nor any need for covalent modification of the nanotubes. This will open up a fully non-covalent route for the creation of DNA-CNT nanohybrid complexes. It should then be possible to investigate the physical behaviour of these complexes. Ultimately, such an interaction may be used to produce non-endocytic gene-delivery agents without any need for covalent functionalisation of the carbon nanotubes. Alternatively, programmable DNA-DNA interactions could be used to control the complexation of DNA PBI CNT nanohybrids into even larger units in solution, or existing "DNA origami" techniques could be used to produce complex scaffolds onto which pristine nanotubes could be patterned while maintaining their desirable physical and electronic properties.

The use of dendritic molecules suggests great potential for fine-tuning the degree of binding of these complexes; in contrast to the poorly defined DNA binding sites on f-CNTs it should be possible to control the number and binding strength of sites on the non-covalently functionalised nanotubes by modifying the degree of aggregation of the dendritic molecules, as well as the number of surface amine groups.

The formation of micellar structures by aromatic dendrimers has been documented in previous studies, and has been implicated in enhanced carbon nanotube binding due to an alternative dendrimer-CNT binding mode.[36] The addition of surface polyamine groups may affect the degree of micelle formation, as might the binding of DNA to these micelles, and consequently increase or decrease the degree to which the micelles are capable of binding CNTs.

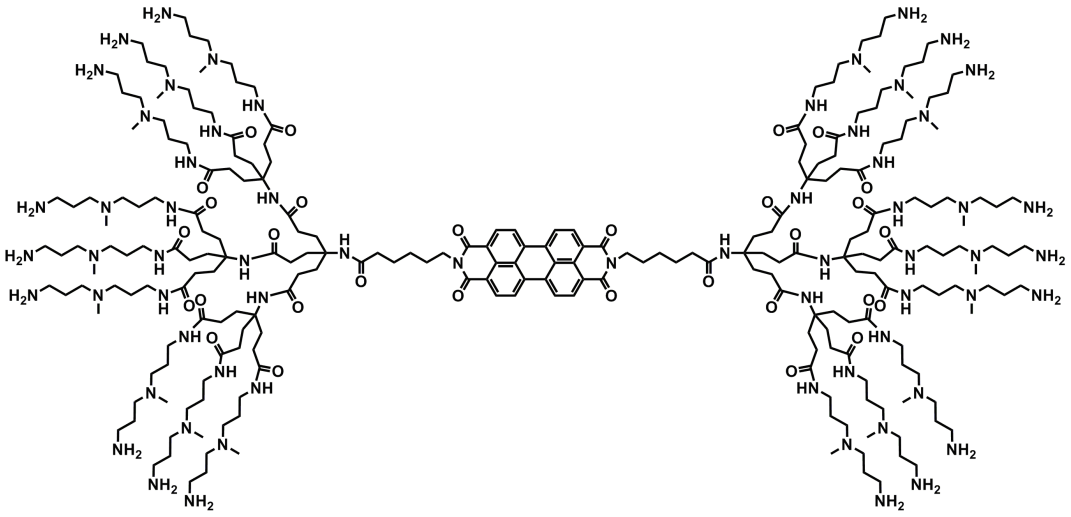

Figure 18: G2 perylene bisimide dendrimer, with DAPMA based surface groups.

Investigating the synthetic modification of Hirsch's perylene bisimide dendrimers, as well as their binding to both carbon nanotubes and DNA, will be of significant interest (Figure 18). Out of consideration for possible gene-therapeutic applications, and in the interest of comparison with similar dendritic molecules synthesised in the Smith group, the surface groups of both the perylene bisimide dendrimers and the perylene dendrons will be terminated with DAPMA rather than spermine, as discussed above. This

approach is also synthetically beneficial, with the absence of secondary amines in DAPMA (in contrast to the two present in the spermine molecule) reducing the complexity of the protection steps required in the synthesis.

2 Synthesis

2.1 G1 DAPMA-Terminated Perylene Bisimide Newkome Dendrimers

Hirsch's perylene bisimide dendrimers were chosen for modification due to their demonstrated affinity for single-walled carbon nanotubes. Synthesis of these molecules was largely carried out as reported in the literature, albeit with some procedural modifications deemed necessary due to unavailability of the required reagents. The surface groups were then modified to bear multiple polyamine groups *via* an amide-coupling route.

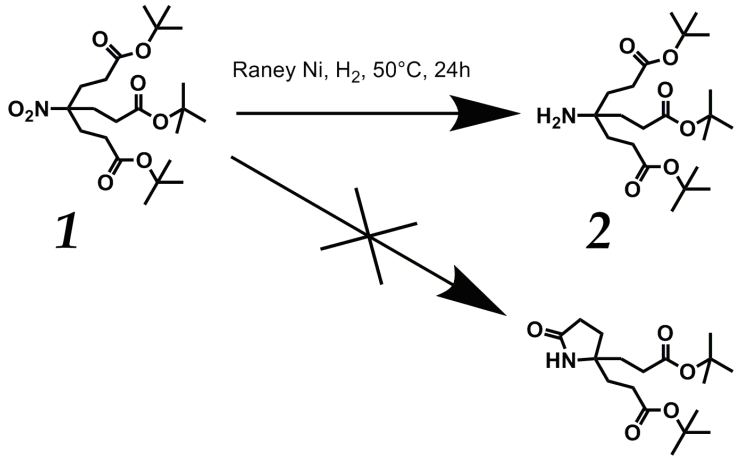

Scheme 1: Synthesis of "Behera's amine," **2**, also showing the undesirable cyclic product.

Synthesis of the dendritic branching unit follows the method described for the preparation of "Behera's amine" by Newkome, Behera et al. in 1991.[80] The nitro functionalised dendron was prepared by Michael addition of *tert*-butyl acrylate to nitromethane, with Triton B, a common surfactant, acting as a base. The reaction proceeded in good yield, with the product isolated *via* recrystallisation from ethanol. During hydrogenation of this dendron to produce **2**, some problems were encountered, with significant percentages of a cyclic impurity produced (Scheme 1). After purification by chromatography, further quantities of this impurity seemed to form during storage.

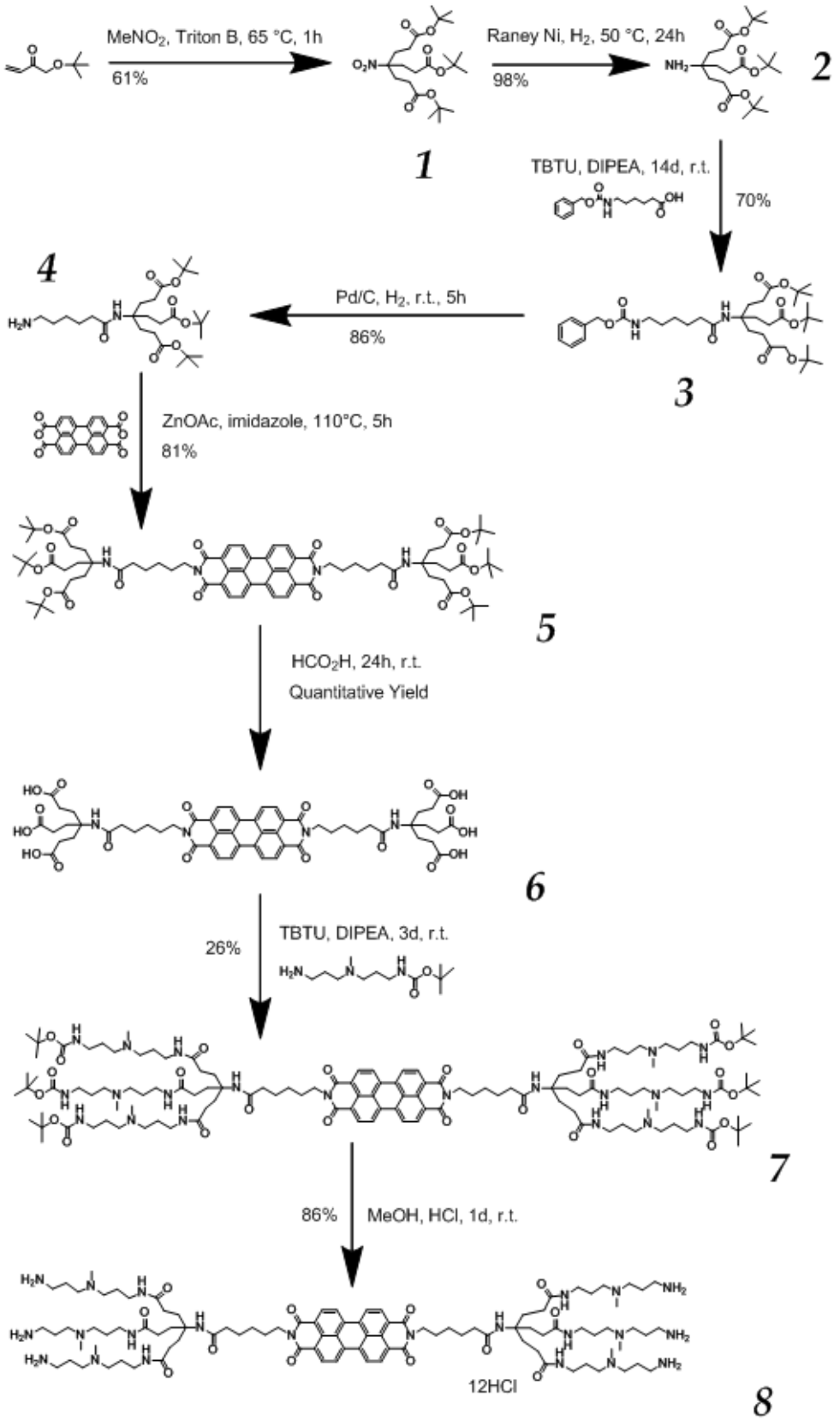

Scheme 2: Synthesis of a DAPMA-terminated G1 dendrimer, *8*, based on Hirsch's PBIs.

The synthesis was modified to take into account further work reported by Newkome and Weis in 1996. The temperature at which hydrogenation was carried out was lowered from 60 °C to below 55 °C. In addition, their recommendation that *in vacuo* solvent removal be carried out below 50 °C was taken into account.[81] Following these amendments, the procedure produced the amine in high yield and with minimal impurities, with no need for purification (Figure 19). The product was then stored in a dry, nitrogen filled flask (in order to avoid water condensing inside the flask upon cooling) at *ca.* -18 °C in order to minimise any risk of cyclisation during storage.

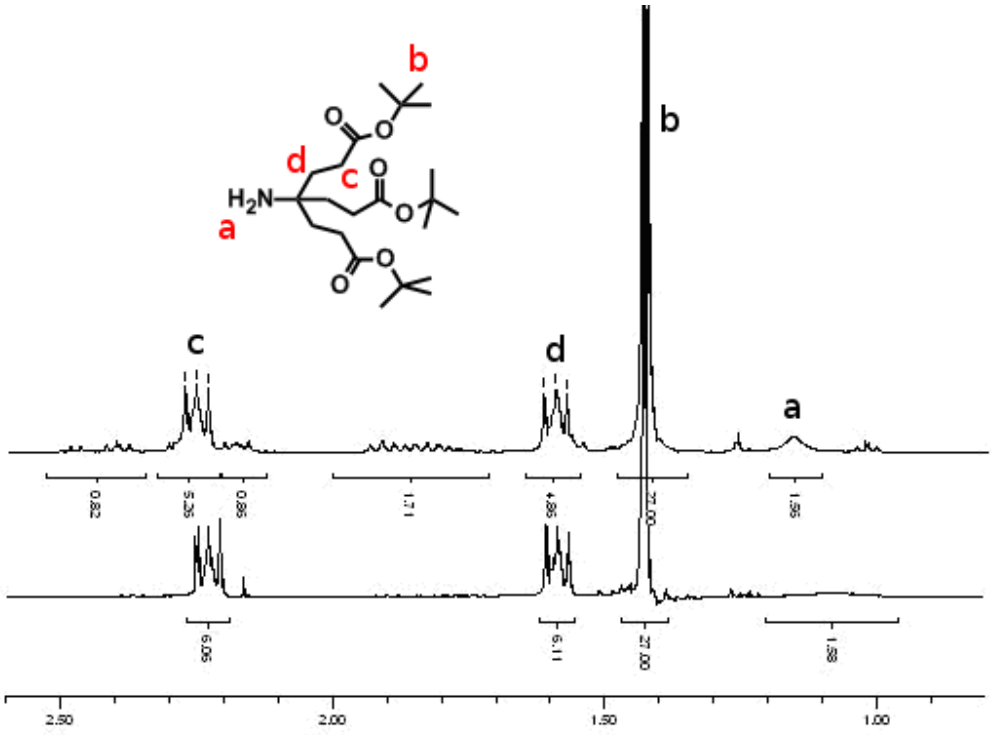

Figure 19: ^{1}H NMR spectra of "Behera's amine" showing significant impurities (top) and the pure product produced by hydrogenation at lower temperatures (bottom).

Further difficulty was encountered during the addition of the 6-carbon spacing unit (**2**, Scheme 2); introduced by Hirsch *et al.* in order to distance the aromatic perylene unit from the bulky side groups and so facilitate aggregation of the dendrimers, and carbon nanotube binding.[95] The reported synthesis required hydroxybenzotriazole (HOBt), a commonly used peptide coupling reagent, and dicyclohexylcarbodiimide (DCC) (Scheme 3).[96,97]

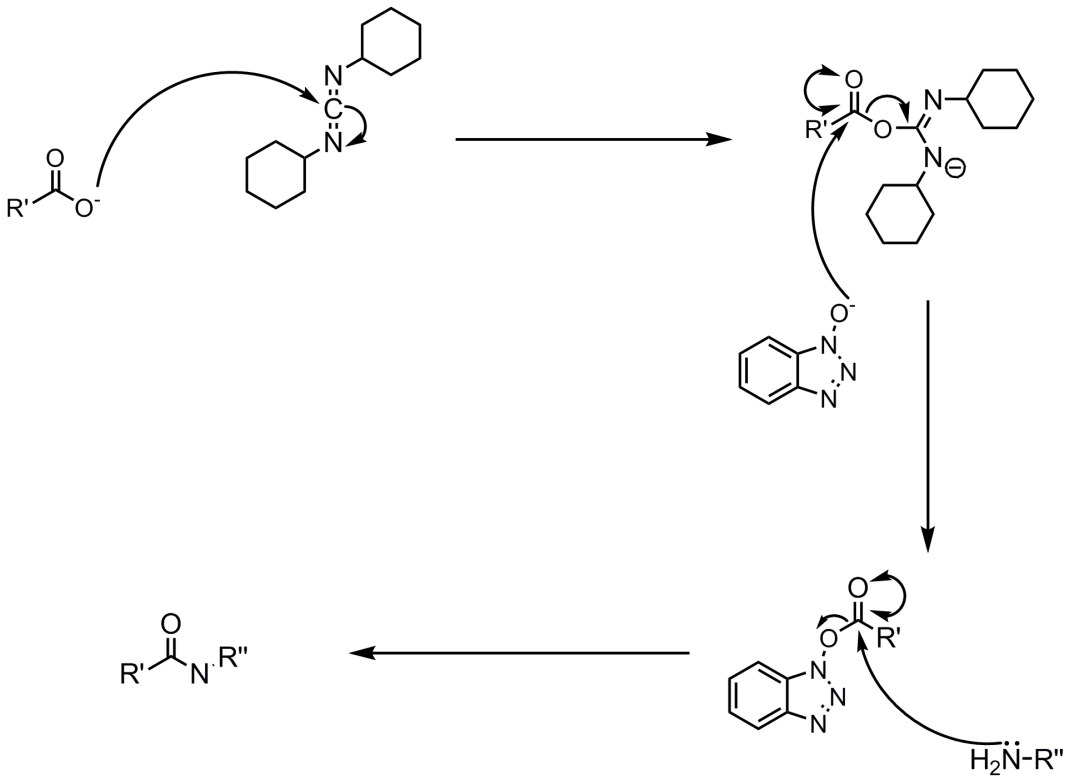

Scheme 3: Mechanism of amide coupling facilitated by HOBT and DCC.

HOBt was unavailable at the time due to reclassification as an explosive material, with restrictions on transportation and storage Accordingly, a method based on 2-propanephosphonic acid anhydride (T3P) was used in its place (Scheme 4). While amide-coupling using T3P can be more sensitive to moisture than HOBt-based procedures, the by-products of the reaction are water-soluble. T3P was readily available as a solution in ethyl acetate, and several test reactions were carried out (Table 1).

Reagents	Time	Temperature	Yield
HOBt, DCC, DMAP[95]	14d	r.t.	92%
T3P, Et3N	4d	r.t.	10%
T3P, DIPEA	1d	r.t.	19%
T3P, DIPEA	5d	40 °C	17%
T3P, DIPEA	16d	r.t.	21%

Table 1: Yields of amide coupling reactions between Behera's amine and Z-caproic acid, comparing HOBt with various T3P conditions.

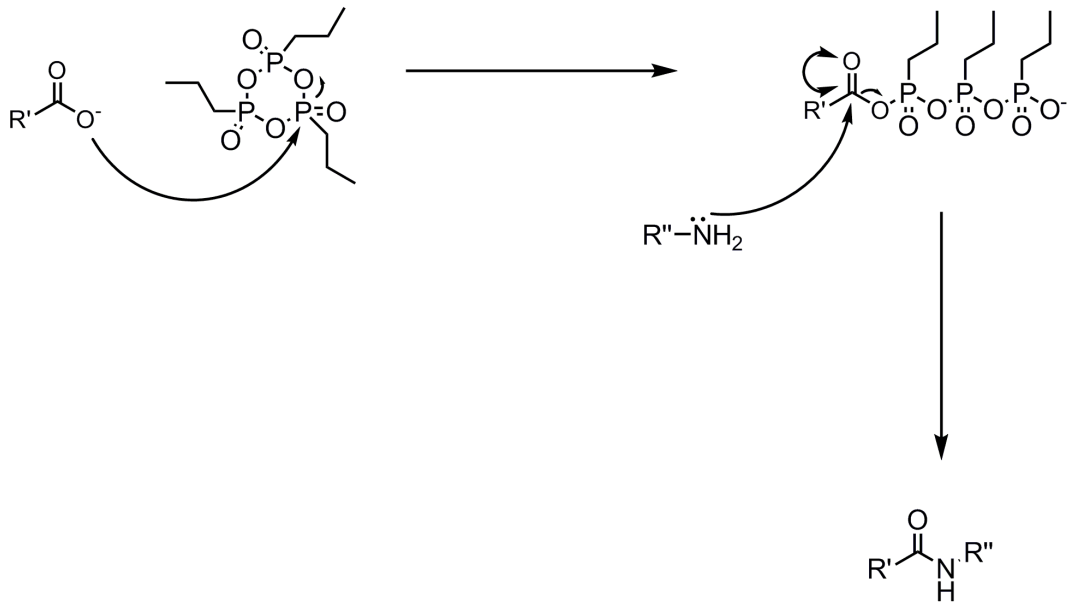

Scheme 4: Mechanism of amide coupling facilitated by T3P.

Unfortunately, using T3P gave poor yields. The long reaction times, even for the reported HOBt route, are due to the sterically hindered, neopentyl nature of the dendron. It was unclear if low yields with T3P were a result of poorly optimised methodology and production of side-products, or if they were also a consequence of steric hindrance, with the reaction requiring more time to reach completion. A change of amide-coupling reagent from T3P to tetramethyl-O-(benzotriazol-1-yl)uronium tetrafluoroborate (TBTU), which is known to assist sterically hindered amide couplings, provided vastly improved yields.[98] Structurally and mechanistically, TBTU bears more resemblance to HOBt than to T3P (Scheme 5).

The yields obtained, while a significant improvement over the T3P-based methodology, were still lower than those reported using HOBt (Table 2). However, given the unavailability of the latter reagent, TBTU was used for all further amide couplings.

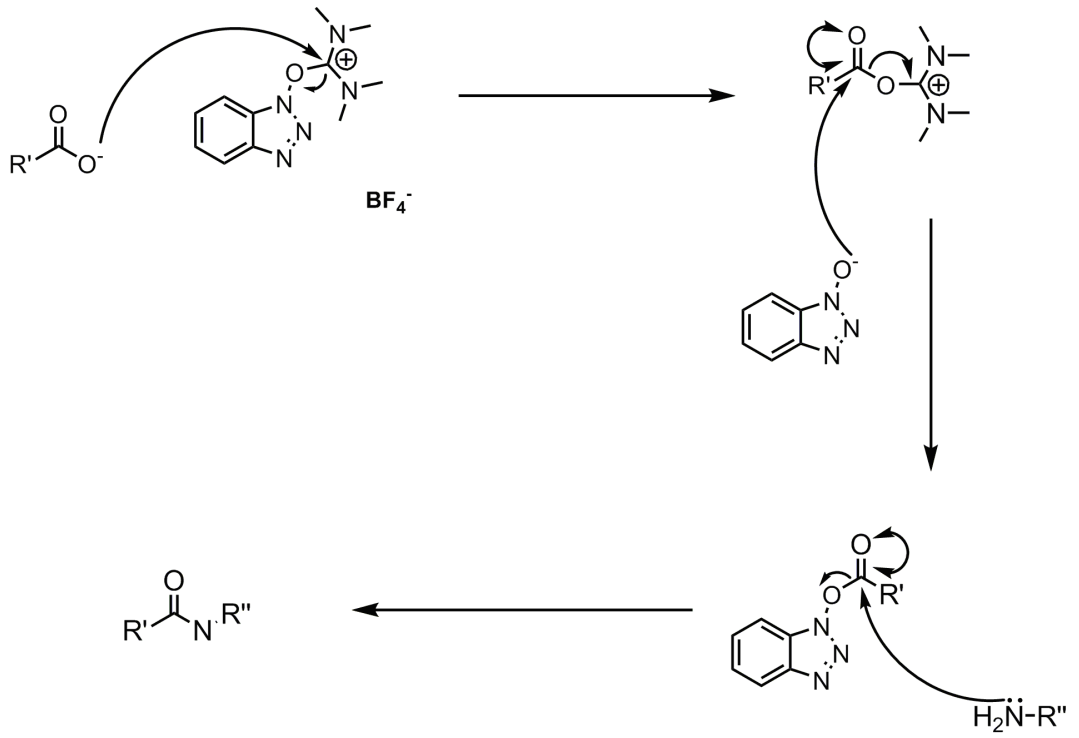

Scheme 5: Mechanism of amide coupling facilitated by TBTU, showing no need for additional coupling reagents such as DCC or DMAP.[99]

Reagents	Time	Temperature	Yield
HOBt, DCC, DMAP[95]	14d	r.t.	92%
T3P, DIPEA	16d	r.t.	21%
TBTU, DIPEA	12d	r.t.	70%

Table 2: Yields of amide coupling reactions between Behera's amine and Z-caproic acid.

The branched dendrons, now complete with spacer units, were then coupled to a perylene core *via* Lewis acid mediated imide formation (Scheme 6). Using molten imidazole as a solvent provides both a basic environment and efficient leaving group; the reaction was, therefore, carried out at 110 °C. Zinc acetate, present in sub-stoichiometric quantities, acts as a Lewis acid catalyst.[95,100] Purification was acheived by column chromatography, with the now strongly coloured products clearly visible to the naked eye. Accordingly, identification of perylene containing fractions did not require further visualization techniques. Both mono- and disubstituted products

were obtained and were clearly identifiable by NMR.

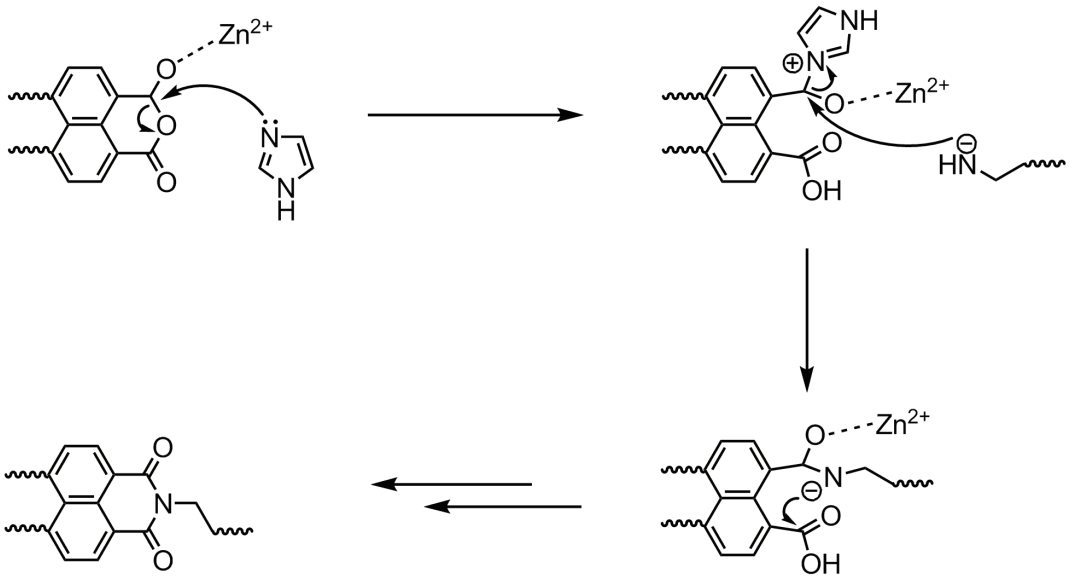

Scheme 6: Mechanism of imidazole and Lewis acid mediated cyclic imide formation.

After deprotection of the disubstituted *tert*-butoxycarbonyl (Boc) protected G1 dendrimer with formic acid, NMR and mass spectroscopy both indicated that the desired compound had been isolated. Fluorescence spectra were measured, in pH 7.0 buffer, at two concentrations. Upon aggregation, PBI dendrimers show a shift in their absorption and fluorescence wavelengths. This typically leads to two distinct maxima, and the proportions of aggregated and non-aggregated perylenes can be monitored by observing the relative absorbance or fluorescence of these frequencies. Accordingly, the absorption and fluorescence spectra are concentration dependent.[101] The fluorescence spectra measured corresponded to concentrations roughly one order of magnitude lower than expected. This may be attributable to the strongly hygroscopic nature of the amphiphilic dendrimers, resulting in the absorption of a significant mass of water from the air during handling. Indeed, when the remaining product was reweighed some time after the deprotection had been carried out, the mass was found to be was roughly ten times the expected value. When synthesising further samples, great care was taken to remove all solvent under high-vacuum and to keep the resulting dry film under argon, following which all fluorescence spectra obtained

correlated closely with those reported in the literature.

Large quantities of Boc-protected *N*,*N*-di-(3-aminopropyl)-*N*-(methyl)amine (Boc-DAPMA) were available, having been previously synthesised by others, from DAPMA and di-(*tert*-butyldicarbonate) in tetrahydrofuran (THF), and purified by extraction from dichloromethane (DCM) using 10 % citrate.

Initial attempts at amide-coupling of Boc-DAPMA to the carboxylic acid terminated PBI dendrimer, ***6***, were unsuccessful, producing an insoluble pink powder that could not be characterised. Molecular sieves were employed in an attempt to remove excess water and so assist in driving the reversible coupling reaction to completion, however this merely resulted in staining and crumbling of the sieves, degradation of which may account for the uncharacterisable, insoluble powder obtained from the reaction. A further attempt to produce the desired product, this time omitting the use of molecular sieves, and using the well-defined, pure and dry ***6*** that had been kept under argon produced a deep-red solution that was then purified by size-exclusion chromatography over Bio-Beads® to give the hexa-substituted amide. However, further purification was required: while the chromatography procedure used was successful in separating the desired product from less substituted side products, the resulting solution was contaminated with large quantities of an aromatic compound.

While a repeat of the above chromatography procedure did not appear to remove the remainder of this undesirable aromatic residue, eluting over Sephadex® with methanol provided the amide free of any impurity readily observable by ^{1}H NMR or UV/Vis spectroscopy (Figure 20). As may be expected when working with compounds so prone to intermolecular association, significant broadening of chemical shift peaks was observed in the ^{1}H NMR spectrum of this compound. In addition, and presumably due to the same factors, no ^{13}C NMR spectrum could be obtained, even after decreasing the concentration of the sample in order to reduce the degree of π-π stacking between perylene moieties, and considerably lengthening the

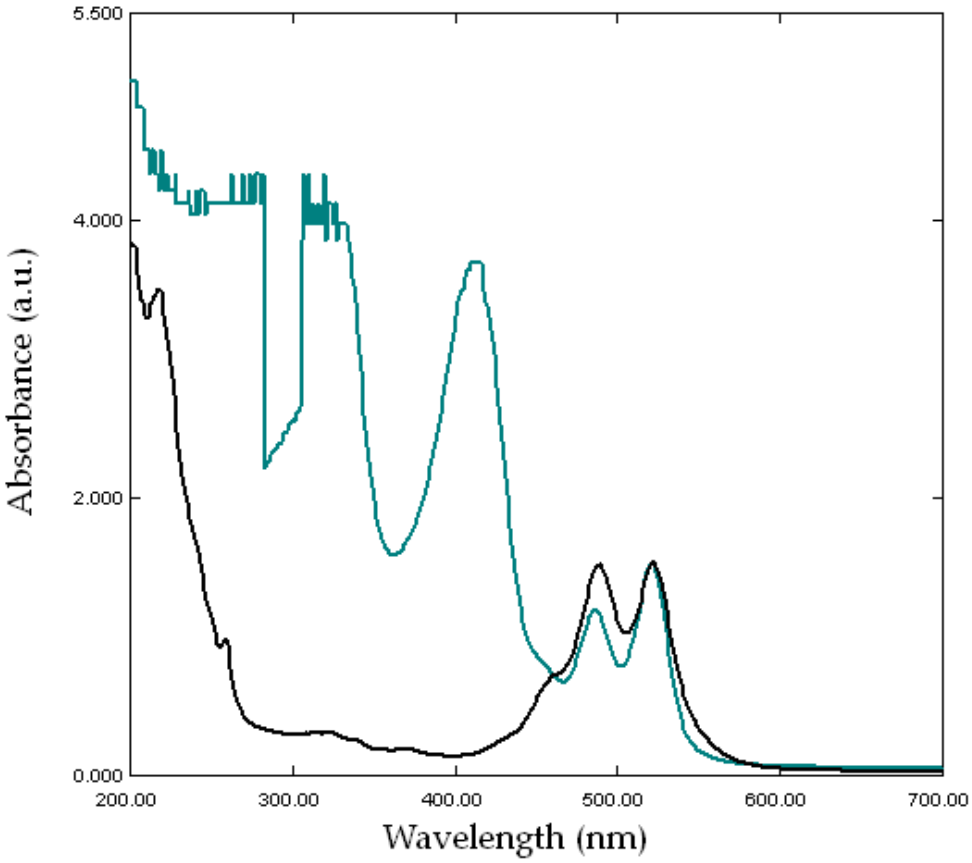

Figure 20: UV/Vis absorbance spectra of G1-PBI-BocDAPMA, **7**, contaminated with large quantities of an aromatic impurity (light blue), and after purification over Sephadex® (black).

duration of the NMR experiment.

The butoxycarbonyl protecting groups were removed by stirring **7** in methanol acidified with gaseous HCl, providing the deprotected DAPMA-terminated dendrimer as its hydrochloride salt. Once again, significant broadening of chemical shifts in ^{1}H NMR spectra of the compound made accurate assignment of specific protons difficult, with the relative integration of some peaks difficult to determine accurately. ^{13}C NMR produced no observable peaks across a wide range of concentrations. Mass spectrometry, however, clearly showed the desired product as *2+*, *3+*, *4+* and *5+* ions. No significant impurities appeared to be visible by ^{1}H NMR, nor were any chromophore bearing impurities observed in the UV/Vis spectrum of the compound. Accordingly, no further purification was carried out.

2.2 G2 DAPMA-Terminated Perylene Bisimide Newkome Dendrimers

The second-generation, DAPMA-terminated dendrimer was synthesised in order to investigate the effects of the degree of multivalency and increased steric bulk upon the PBI dendrimers' affinity for DNA.

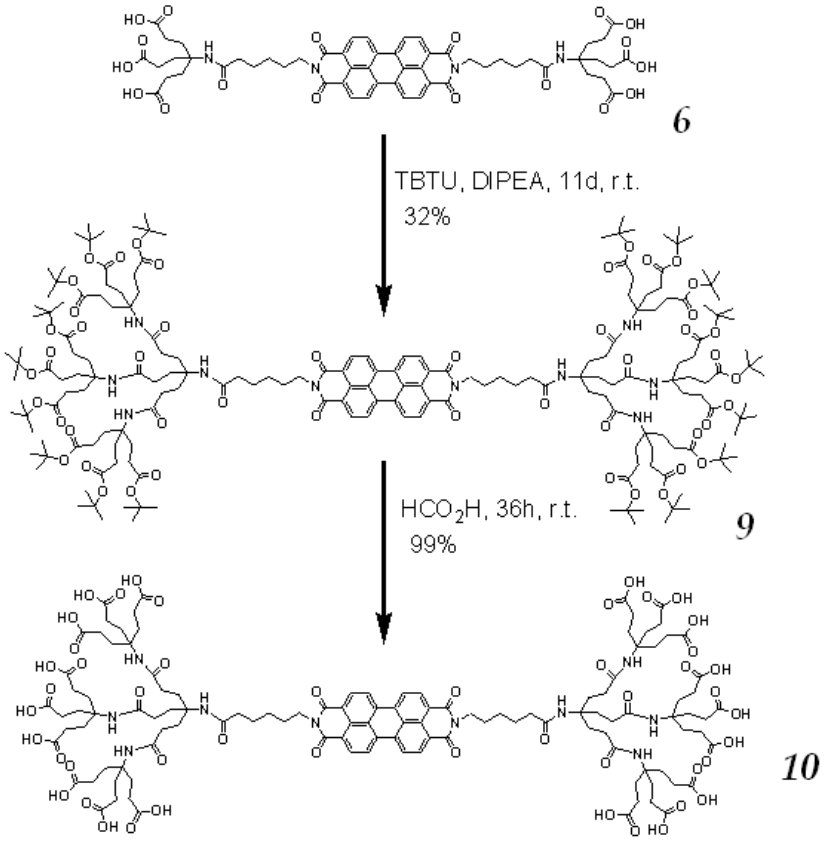

Scheme 7: Synthesis of DAPMA-terminated G2 dendrimers based on Hirsch's PBIs - initial steps

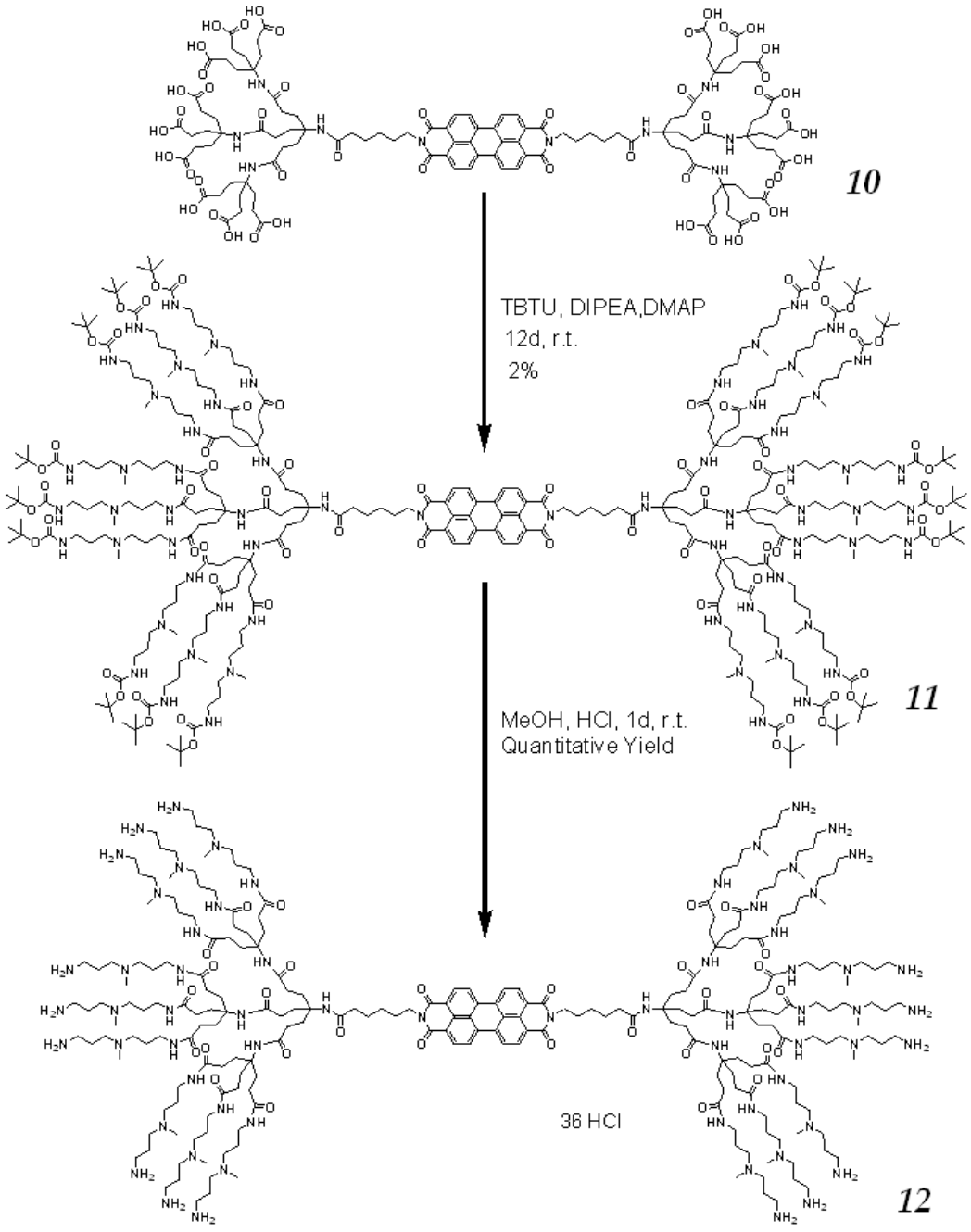

Scheme 8: Synthesis of DAPMA-terminated G2 dendrimers based on Hirsch's PBIs - final steps

The G1 carboxyl-terminated dendrimer ***6***, synthesised as described above, was used as the starting point for the synthesis. A convergent approach was used, coupling "Behera's amine" to the periphery of the dendrimer using a TBTU-based coupling methodology. The resulting G2 dendrimer, ***9***, a *tert*-butyl ester, was purified by column chromatography in ethyl acetate (EtOAc), giving the desired product in reasonable yield. The *tert*-butyl protecting groups were then removed in formic acid in quantitative yield to give the G2 carboxyl-terminated dendrimer, ***10***, ready to be coupled to Boc-protected DAPMA (Schemes 7 and 8).

The coupling of Boc-DAPMA to the G2 carboxyl-terminated dendrimer was largely carried out as described above in the synthesis of the G1 Boc-DAPMA derivative, albeit with the reaction time extended in order to encourage the complete substitution of reaction of the eighteen peripheral groups (in contrast to the G1 dendrimer's six peripheral amides). However, while the first generation dendrimer was readily soluble in a 1:1 mixture of DCM and pyridine, this solvent system failed to solubilise the G2 dendrimer. While the reagent in question was fully soluble in MeOH, alcohols are unsuitable solvents for this reaction due to the potential formation of esters. After screening a range of solvents, a 3:2 mixture of pyridine and dimethyl sulfoxide (DMSO) was deemed suitable. As in the synthesis of the G1 dendrimer, the product was isolated as a red solid which was then separated by size-exclusion chromatography over Bio-Beads®, eluting with DCM. Again, as with the Boc-DAPMA coupling to the first-generation dendrimer, which was carried out simultaneously, the earlier fractions (those containing the larger molecules, expected to be the substituted product) were contaminated with a UV chromophore containing impurity. Size-exclusion chromatography, eluting over Sephadex® with methanol, once again provided the desired product free of observable impurities, along with what appeared to be the incompletely substituted amide, isolated as a second fraction (Figure 21).

Analysis of the resulting fractions by ^{1}H & ^{13}C NMR failed to provide clear

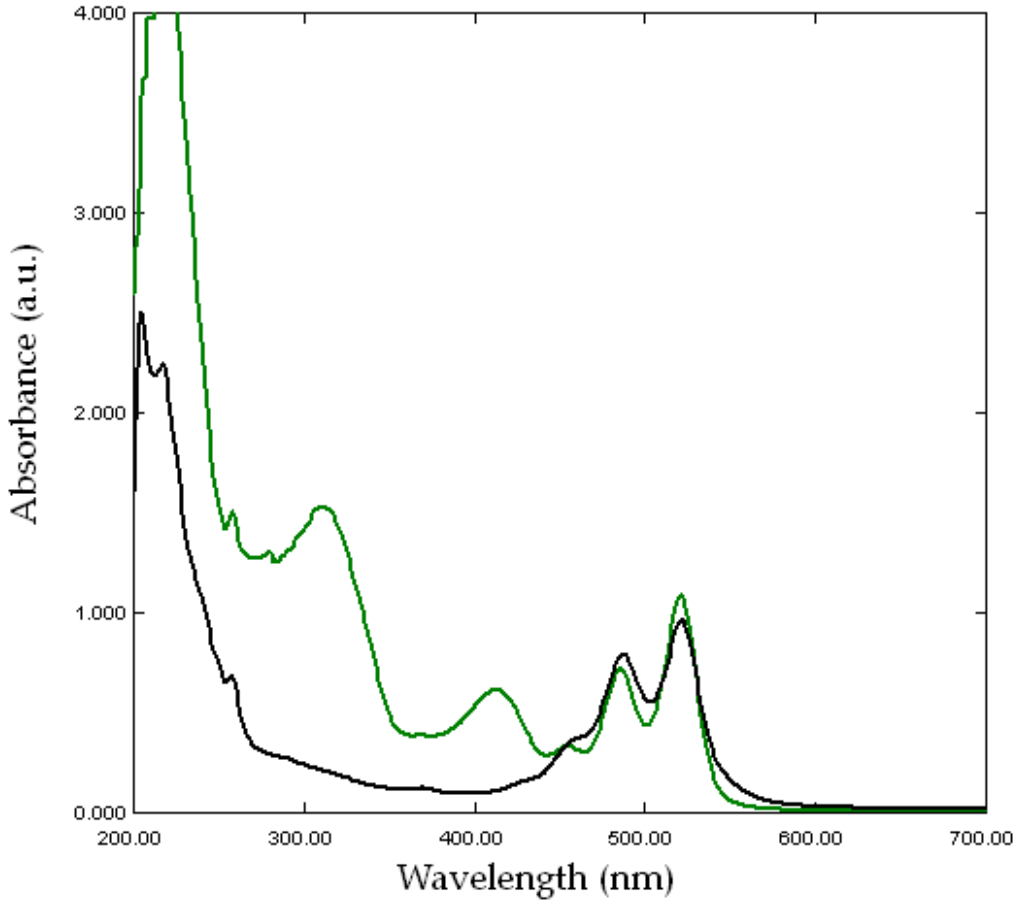

Figure 21: UV/Vis absorbance spectra of ***11*** after purification over Sephadex® showing the first (black) and fifth (green) fractions, with the latter still clearly containing a proportion of the aromatic impurity.

and conclusive evidence regarding the degree of substitution of the products. Formation of aggregates in solution due to stacking of the perylene cores leads to significant broadening of peaks, leading to difficulty in ascertaining the accurate chemical shift and integration of the signals. This broadening is particularly prevelant for those peaks relating to the carbon or hydrogen nuclei in the perylene core and, accordingly, the relative magnitude of the Boc and perylene integrals is difficult to calculate precisely.

Analysis of these samples by mass spectrometry also proved challenging; neither electrospray ionisation (ESI) nor matrix-assisted laser desorption ionisation (MALDI) provided spectra showing the molecular ion peak. Again, this was presumed to be related to the formation of aggregates by the Boc-

protected dendrimers (as some difficulty had been noted obtaining spectra for the G1 analogue, **7**) as well as being in part due to the considerable mass of these compounds, with the fully substituted dendrimer, ***11***, having a mass of 6545 Da.

UV/Visible spectrophotometry, in addition to confirming the removal of any impurities possessing UV chromophores, showed a significant difference between the two fractions when prepared as equimolar solutions in methanol (Figure 22). The proportion of peak heights in perylene bisimides has been shown to correlate with the degree of stacking of the compounds: the peak around 480 nm correlates with π-π stacked perylene units, while the peak around 520 nm correlates with unstacked perylenes. Accordingly, the strong 480 nm peak in the spectrum of the second fraction is indicative of a reduction in stacking. In previously published work, a G2 octadecacarboxylic acid-terminated perylene bisimide exhibited less stacking than its G1 analogue due, presumably, to the greater steric hindrance provided by the higher degree of branching, as well as electrostratic repulsion due to greater charge.

The apparent difference in stacking between the two solutions could, therefore, be the result of electrostatic repulsion of charged groups, steric clash, or differences in molarity. Should one or other fraction be incompletely substituted, the change would affect these three properties in the following ways:

Molarity An incompletely substituted fraction would have a lower Mw than predicted and, accordingly, a solution of equal w/v concentration would be of lower molarity than expected (and of lower molarity than a solution prepared containing the fully substituted product). This solution would, therefore, demonstrate reduced stacking.

Steric Clash It would be expected that an incompletely substituted product would possess less steric bulk, a barrier to stacking. Accordingly, like its first generation counterpart, a greater proportion of the compound would be present in the stacked form.

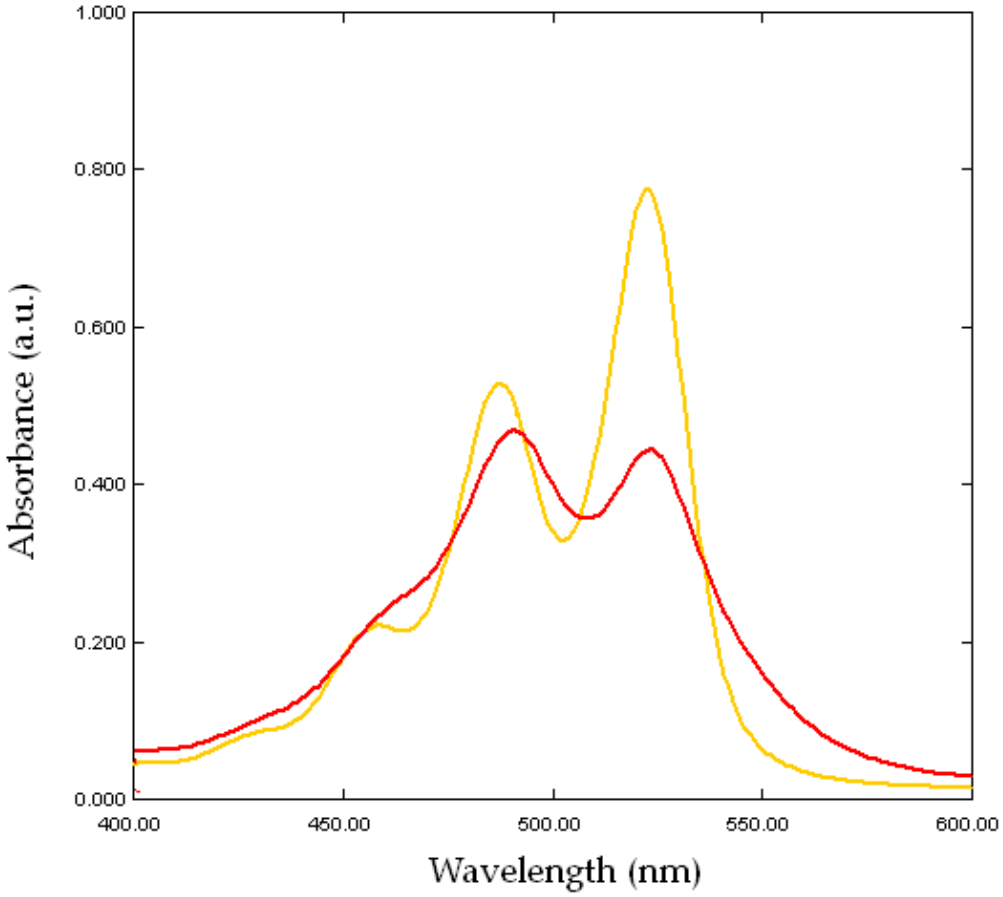

Figure 22: UV/Vis spectra of the first (red) and second (orange) fractions of ***11*** obtained by size-exclusion chromatography, after removal of solvent *in vacuo* and preparation of solutions of equal w/v. *N.B.* In the absence of any other data, when preparing solutions it was assumed that both fractions contained only pure, fully-substituted second generation Boc-DAPMA substituted perylene bisimide. Should this not be the case, the solutions will not be equimolar.

Charge The presence of charged groups should, through electrostatic repulsion, decrease the stacking of the perylene units. Both the starting material and the desired product contain chargeable moieties; in the case of the starting material some of the carboxylic acid groups will deprotonate in solution, affording anionic dendrimers, while the desired product carries protonatable secondary and tertiary amines some of which should, in methanol acquire protons and impart a cationic character to the molecule. The situation is complicated by the possibility that one or both fractions contain partially but incompletely substituted material, in which case the dendrimers may possess a net positive or negative charge or no charge at

all, depending on whether each molecule is predominantly cationic, anionic or zwitterionic.

A variable pH experiment was designed in order to test the hypothesis that one of the fractions may consist of the incompletely substituted G2 dendrimer. By modifying the pH of the solution and protonating or deprotonating any amine or carboxyl moieties, the degree of stacking of the dendrimers, and thus their UV/Vis spectrum, should be changed due to the resulting increase or reduction in charge. As a significant reduction of the solution pH could lead to removal of the Boc protecting groups and thus alteration of the dendrimers' stacking properties through covalent modification, the pH was instead raised by the addition of triethylamine to the solutions. Triethylamine was chosen both due to having a sufficiently high pKa (10.75 in water) to deprotonate both acidic carboxyl groups and protonated Boc-DAPMA, and the presumed lack of any other obvious interactions with the solute; *cf.* pyridine which, in addition to possessing a lower pKa, could be thought to affect aggregation of the dendrimers through π-π stacking interactions with their perylene cores.

In both cases, addition of base increases the stacking of the dendrimers. These experiments seem to indicate that neither fraction contains pure starting material: the neutral or negatively charged carboxylic acid terminated dendrimer should stack less or the same amount upon the addition of base, depending on the initial degree of deprotonation. However, in both cases an increase in pH appears to increase the proportion of stacked material, suggesting a decrease in the overall charge of each molecule. This would be consistent with deprotonation of cationic amine terminated dendrimers. As the appearance of these fractions differs so markedly by eye and by UV/Vis spectroscopy, it seems reasonable to suggest that, while both could contain protonatable amines, the first fraction is more fully substituted than the other.

Upon deprotection in acidified methanol, the first fraction behaved similarly to the G1 counterpart, with the deep-red solution turning slightly cloudy.

After removal of the solvent, and addition of neutral methanol, the product dissolved to give a red solution, albeit with an insoluble red film remaining undissolved.

Deprotection of the second fraction provided further information on the pH dependence of the material: upon acidification, the orange solution turned red, roughly corresponding to a relative decrease of the 523 nm absorbance and indicating stacking of the perylenes. This would suggest that significant protonation was leading to an overall decrease in charge, indicating the presence of acidic groups on the dendrimer. After stirring, a pale peach coloured solution was produced in addition to a considerable quantity of black solid. After separation, it was demonstrated that this black material would not dissolve in acidified methanol but dissolved in neutral methanol to give a red solution.

It would appear that both fractions contained a mixture of variously substituted Boc-DAPMA terminated dendrimers, with the first fraction consisting primarily of at least one more fully substituted product. This would also be consistent with the mechanism of size-exclusion chromatography, after which it would be expected that the more fully substituted, and thus larger, compounds would be the first to pass through the column. The soluble and insoluble portions of the first fraction were separated *via* glass pipette, with the soluble portion then being characterised as much as was possible given the low mass recovered (*ca.* 0.004 g).

3 Investigations

3.1 DNA Binding Capability of G1 DAPMA-Terminated Perylene Bisimide

The N/P charge ratio describes, on average, the number of nitrogen cations required to bind each phosphate anion. In contrast to a simple ratio of molecular concentrations, the charge ratio provides a measure of binding efficiency that is directly comparable between binders, irrespective of the number of protonatable nitrogen atoms per molecule. The use of the charge ratio as a measurement also avoids any problems associated with calculating the molecular weight of the DNA oligo- or polynucleotides used in any assay; the calf-thymus DNA used in many binding assays tends to be very polydisperse and calculating the number of nucleotide bases and, accordingly, the number of phosphate units, present in the sample is a considerably easier undertaking than determining the average length of each "DNA molecule". For these calculations, the average "molecular weight" of the nucleotide base pair residues was taken to be 660 Da.[102]

Typically, the association of cationic molecules with DNA is measured by indirect means. Binding to the phosphate backbone is not accompanied by any quantifiable change in the NMR, UV/Vis, or fluorescence spectra of the DNA and, accordingly, other means must be used to measure the magnitude of any ionic interactions.

One frequently used method, sensitive to small changes and providing data comparable between similar DNA-binders is the ethidium bromide fluorescence assay.[84] Ethidium bromide (EthBr) is a fluorescent dye, commonly used as a DNA stain.[104] Upon intercalating between DNA base pairs, the fluorescence of EthBr increases dramatically. While in aqueous solution, fluorescence is quenched by proton exchange with the solvent - however in the solvent free, hydrophobic environment between the base

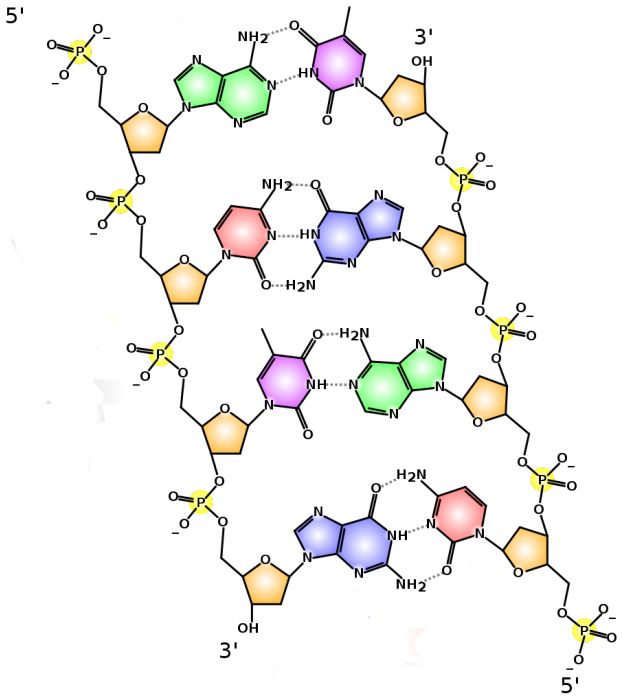

Figure 23: Diagram of double-stranded DNA, showing nucleotide bases (green, purple, blue and red) deoxyribose sugars (yellow) and anionic phosphate groups.[103]

pairs, EthBr fluoresces with around 20 to 100 times its quenched intensity, depending on the excitation wavelength chosen.[105,106]

While the intercalation of ethidium bromide distorts double-stranded DNA by causing unwinding of the double helix,[107] intercalation of drugs or other molecules,[108] or binding of cationic species to the phosphate backbone displace the bound EthBr, forcing it into solution.[84] The degree of binding of the cationic species can, therefore, be measured by monitoring the reduction in fluorescence of the ethidium bromide as it is quenched by the solvent.

In many cases, including previous studies by the Smith group, the excitation of ethidium bromide has been achieved using light of or around 540 nm.[109] While this direct excitement of the ethidium cation's chromophore was adequate and appropriate in these experiments, when investigating PBIs the fluorescence of the perylene moiety overlaps significantly at the observed fluorescence wavelengths (around 595 nm) when excited by light at 540 nm.

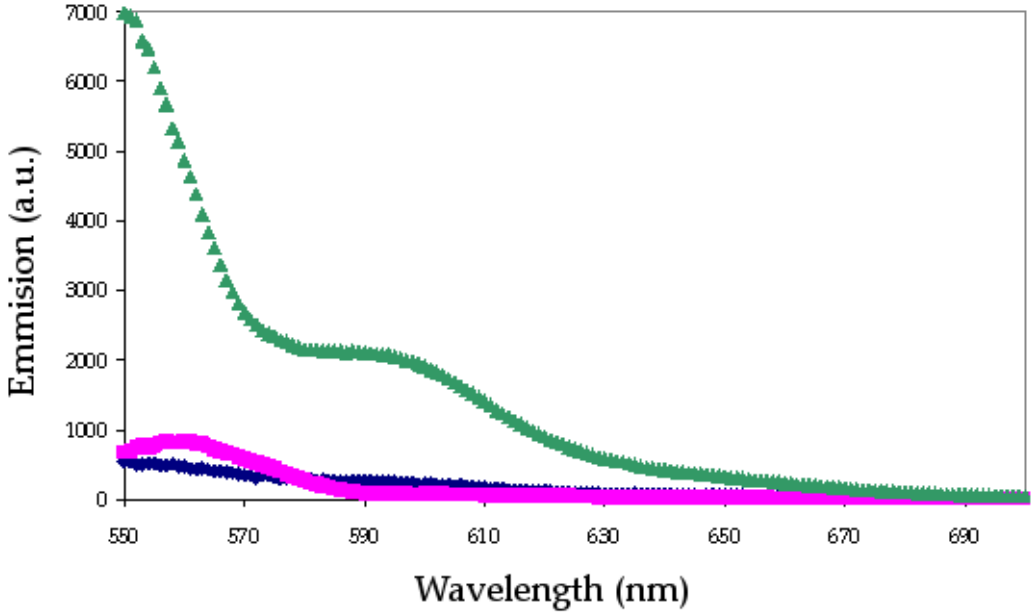

Figure 24: Comparison of DAPMA-terminated G1 perylene dendrimer emission, exciting at 260 nm ♦, 280 nm ■, and 540 nm ▲. Peaks below 570 nm are due to scattering of the excitation wavelength, or its overtones. In the region to be studied (around 595 nm) note the strong perylene emission when exciting at 540 nm, and the minimal emission when exciting at 260 nm or 280 nm.

Published work by Blagbrough and Geall[100] suggests an alternative range of excitation wavelengths around 260 nm. Their investigations show that excitement in this region will produce results comparable to those obtained using excitation at a higher wavelength, with equivalent percentage reductions in fluorescence upon addition of their cationic binder. Furthermore, the excitement of ethidium bromide at these lower wavelengths contains both direct and indirect components due to energy transfer from DNA, which also possesses a chromophore in this region. Upon displacement from the DNA, this additional excitation pathway is no longer available. This method results in a much greater absolute reduction in fluorescence upon displacement and, accordingly, a more sensitive assay than when directly exciting EthBr using higher wavelengths.

Preliminary investigations suggested that excitation at 280 nm, rather than at 260 nm, provided both strong initial fluorescence of the EthBr, and minimal fluorescence of the perylene moiety at the observed emission

wavelengths (Figures 24 and 25).

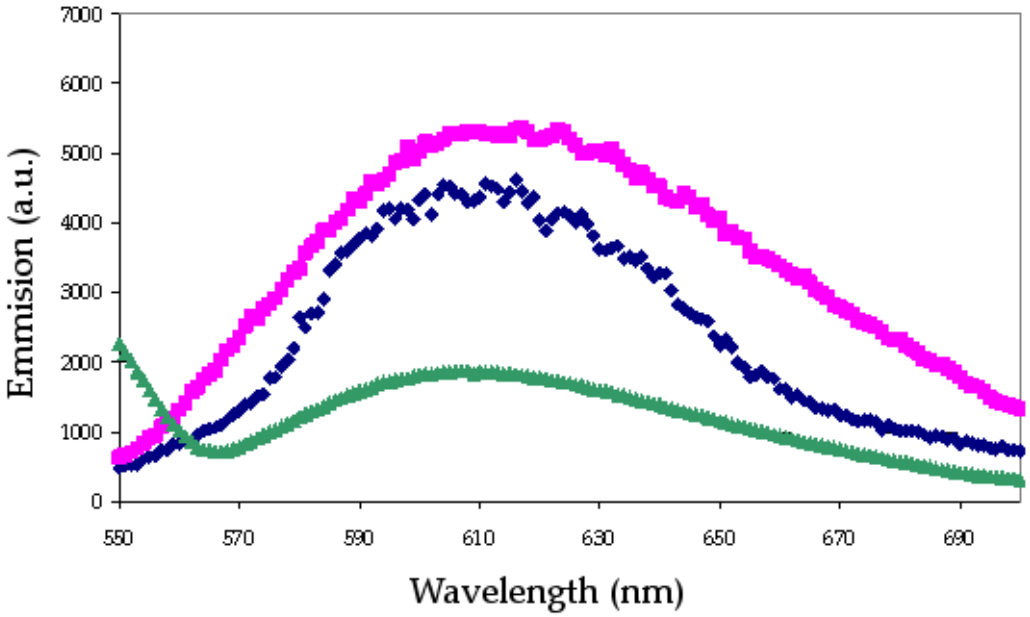

Figure 25: Comparison of ethidium bromide excitation, in the presence of DNA, exciting at 260 nm ♦, 280 nm ■, and 540 nm ▲, and demonstrating the increased fluorescence emission intensity when using lower excitation wavelengths.

Initial investigation, exciting at 280 nm and titrating a 10 μM solution of the DAPMA-terminated G1 perylene dendrimer reached the apparent baseline after the addition of just 20 μl of perylene solution, equivalent to an overall concentration of 0.1 μM (Figure 26).

In order to study the concentration range representing the greatest change in ethidium bromide fluorescence, and to avoid the perylene fluorescence that was observed to impinge on the spectrum at higher concentrations, the titration was then repeated using a 1 μM solution of the perylene dendrimer, producing a curve from which C_{50} and CE_{50} values could be calculated (Figure 27). The C_{50} indicates the concentration of DNA binder required to cause a 50% reduction in fluorescence, while the CE_{50} represents the charge excess at this concentration, defined as the concentration of cations or the nominal positive charge present divided by the nominal negative charge, in this case the concentration of phosphate anions.[102] The data for each titration can be averaged to produce a single mean curve, and the CE_{50} then noted for

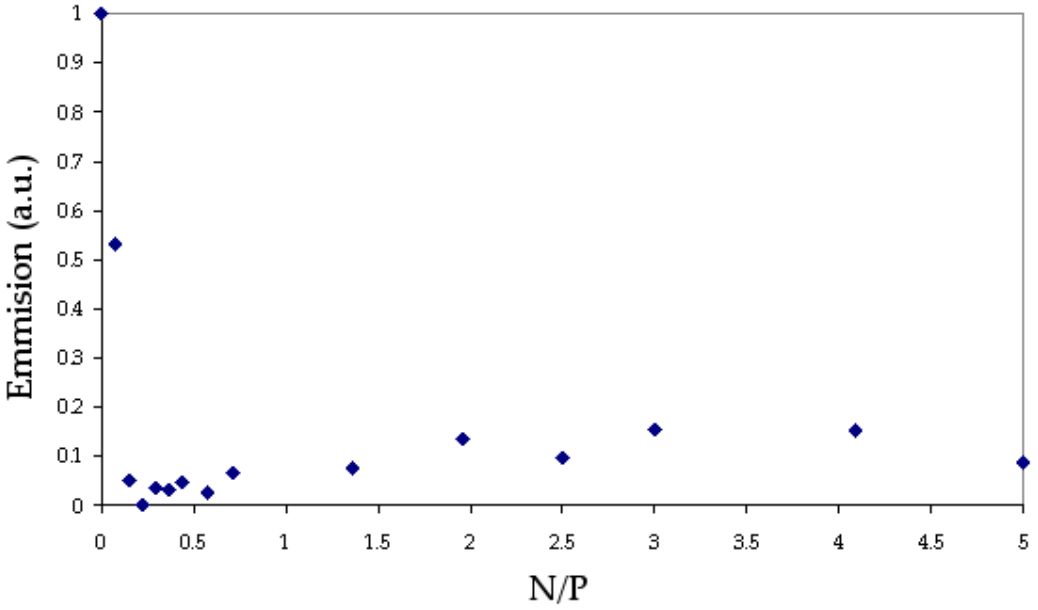

Figure 26: Titration of a 10 μM DAPMA-terminated G1 perylene dendrimer solution into a solution of 8 μM DNA with 5.18 μM EthBr. Note the initial rapid drop in fluorescence as the majority of the ethidium bromide is displaced from its intercalation sites, followed by the gradual rise as the concentration of perylene increased and its fluorescence begins to impinge on the region under observation. Samples were excited at 280 nm and emission observed at 595 nm.

this average. A separate CE_{50} value for each titration was calculated, and an average calculated from these figures (Table 3).

	C_{50} (μM)	CE_{50}
	0.070	0.10
	0.032	0.05
	0.023	0.03
	0.058	0.09
	0.049	0.07
	0.046	0.07
Mean	0.046	0.07

Table 3: C_{50} and CE_{50} values calculated from six ethidium bromide exclusion assays, in each case titrating 1 μM *8*. One further titration was discarded due to significant errors.

The particularly low CE_{50} value calculated for this dendrimer suggests either

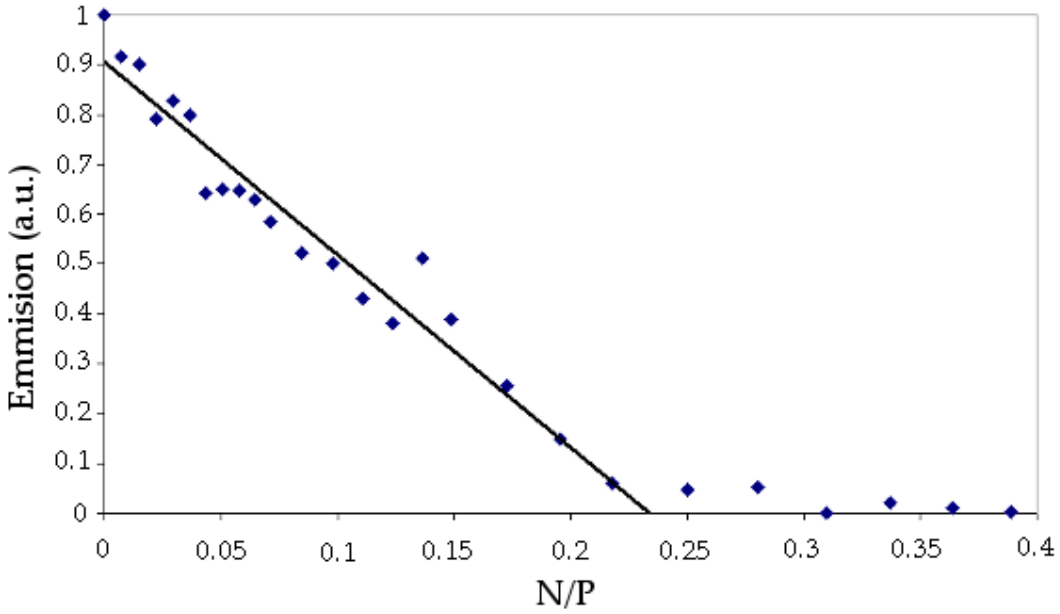

Figure 27: Titration of a 1 μM DAPMA-terminated G1 perylene dendrimer solution into a solution of 8 μM DNA with 5.18 μM EthBr. Note the region between N/P = 0, and N/P = 0.22 (340 μl perylene solution added, total concentration = 0.15 μM) where additional perylene displaces increasing quantities of ethidium bromide and reduces the overall fluorescence of the sample. The CE_{50} corresponds to N/P at 50 % of the maximum fluorescence emission.

a particularly strong DNA binding ability, or an artifact of the indirect method used to quantify the binding interaction.

3.2 Intercalation of PBIs into dsDNA

In the case of a simple polyamine such as DAPMA, spermine, or simple dendritic molecules bearing those moieties such as those used in previous studies by Smith *et al.* (Figure 28), the only relevant supramolecular interactions present in solution are the intercalation of EthBr into DNA, and the ionic interaction between the phosphate backbone of the DNA and the cationic protonated nitrogens of the polyamine. However, the structure of the dendrimers under investigation suggests a further possible interaction; previous work by Kerwin, Federoff *et al.* has investigated the interaction of perylene bisimides' aromatic cores with various DNA polynucleotides.[110,111] It is conceivable that intercalation of the perylenes into the DNA double-helix would displace EthBr upon binding, adding a further, non-ionic binding

mode observable by the ethidium bromide assay.

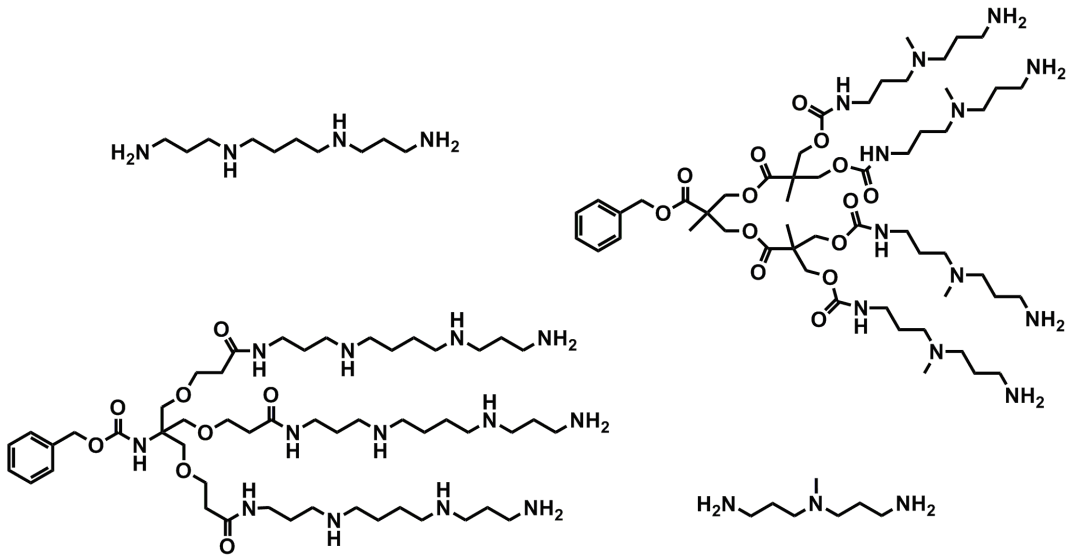

Figure 28: Spermine (top left), spermine dendron (bottom left),[79] DAPMA (bottom right)[112] and DAPMA dendron (top right).[113]

Kerwin *et al.* measured the intercalation of their perylene bisimide compounds by monitoring the disruption of perylene-perylene stacking.[111] Upon addition of increasing concentrations of dsDNA, they observed a change in the UV/Vis spectrum of the perylene moiety, indicating a decrease in the proportion of stacked perylene aggregates, and an increase in the proportion of individualised PBI units (Figure 29). Their conclusions were supported by a lack of the observed shift when investigating a more sterically bulky PBI, and an increased shift when titrating G-quadruplex DNA, which possesses a more open structure and so would be thought to interact more easily with the perylene units.

An analogous experiment was designed to determine the degree of intercalation of the cationic dendrimers under investigation. Double-stranded calf thymus DNA, as used in the DNA binding assays described above, was titrated into a 1 μM solution of ***8*** in 0.01 M SHE buffer (Figures 30 and 31).

After normalisation, the shifts in absorbance indicate a degree of intercalation over the concentration range studied. The absorption of the sample at 500 nm, corresponding to the stacked perylenes in solution (*cf.* Figure 29 and

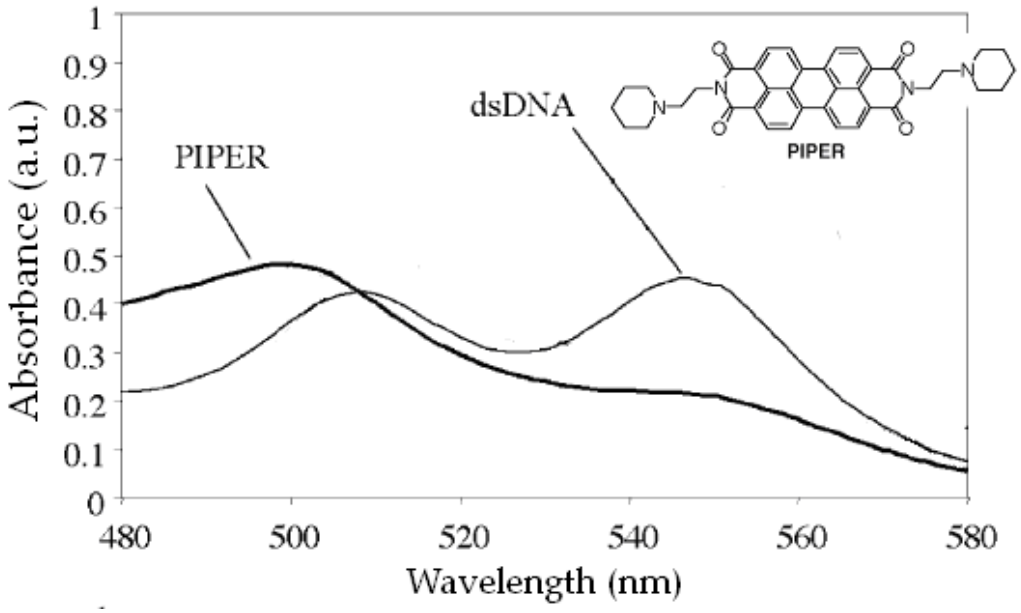

Figure 29: UV/Vis absorption spectra of a perylene bisimide alone, and in the presence of excess double-stranded DNA. The change in relative absorption of the two peaks is indicative of individualisation of the perylene units, presumably due to intercalation into the DNA.[111]

30) decreases over the course of the titration, while the absorption at 538 nm, corresponding to individualised perylenes, increases. These changes suggest intercalation of the dendrimers' core perylene units between the DNA nucleotide bases, being the most likely mechanism for separation of the aromatic, π-π stacking perylenes. The data represented in Figure 31 span the relative concentrations at which the DNA-binding assays were carried out, suggesting that in those experiments a degree of intercalation would likely have been occurring. This should contribute to the observed N:P ratio, although without further data, namely the relative concentration at which no more individualization of the perylene moieties occurs, it is not possible to determine the degree of intercalation and, therefore, what percentage of the total dendrimer-DNA interactions results from this contribution.

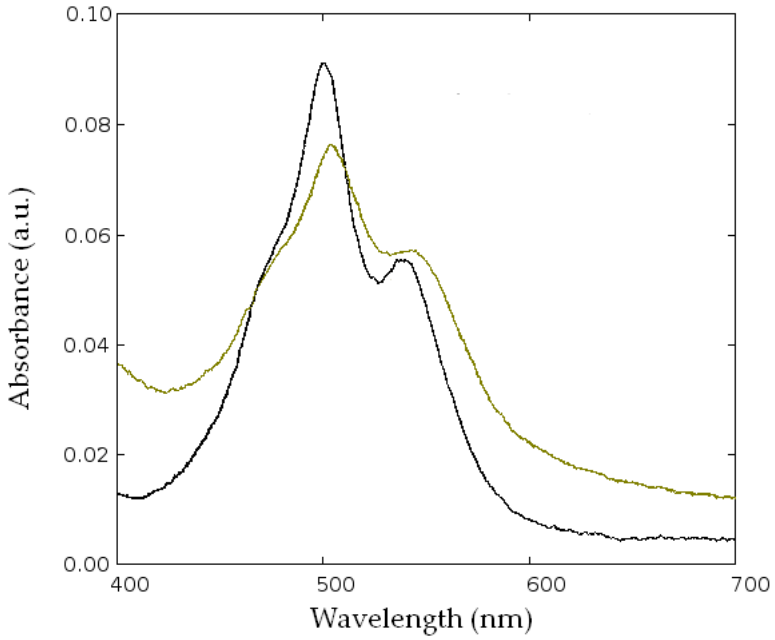

Figure 30: UV/Vis absorption spectra of *8* before (black) and after (green) the addition of double-stranded calf thymus DNA, indicating a degree of intercalation and resulting individualisation of the perylene moities. Data not normalised to account for UV/Vis absorption of DNA.

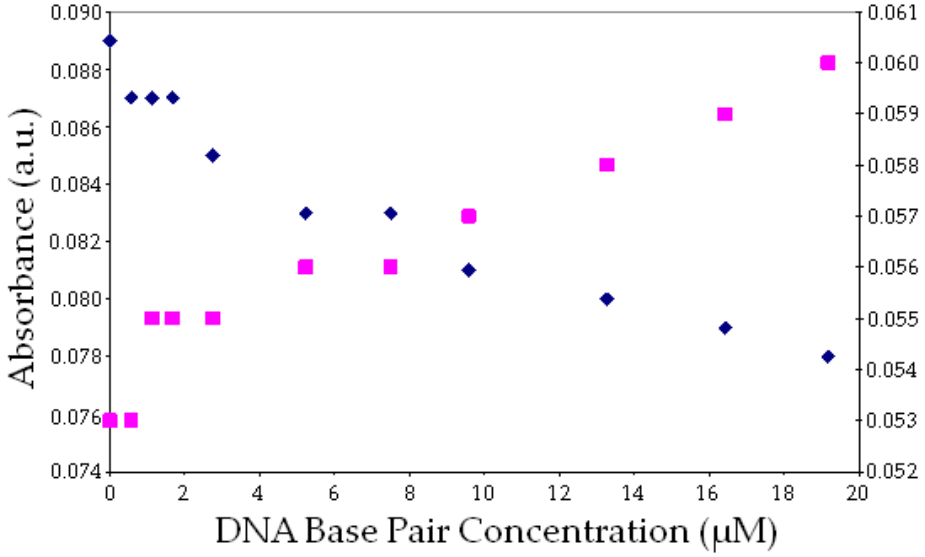

Figure 31: Changes in UV/Vis absorbance of 1 μM DAPMA-terminated perylene dendrimer at 500 nm ♦ (left axis) and 538 nm ■ (right axis) upon addition of calf-thymus DNA. All solutions made using 0.01 M SHE buffer. All data normalised according to UV/Vis absorbance of calf-thymus DNA dilutions in 0.01 M SHE buffer.

3.3 Low CE_{50} as an artifact of methodology

One further interaction that could plausibly contribute to an exceptionally low CE_{50} value is the possible π-π stacking of perylene and ethidium moieties. Removal of free ethidium from solution by interaction with perlyene would shift the DNA-EthBr intercalation equilibrium in favour of dissociation, distorting the results of the displacement assay and making the dendrimer appear to be a better DNA-binder than is in fact the case (Figure 32).

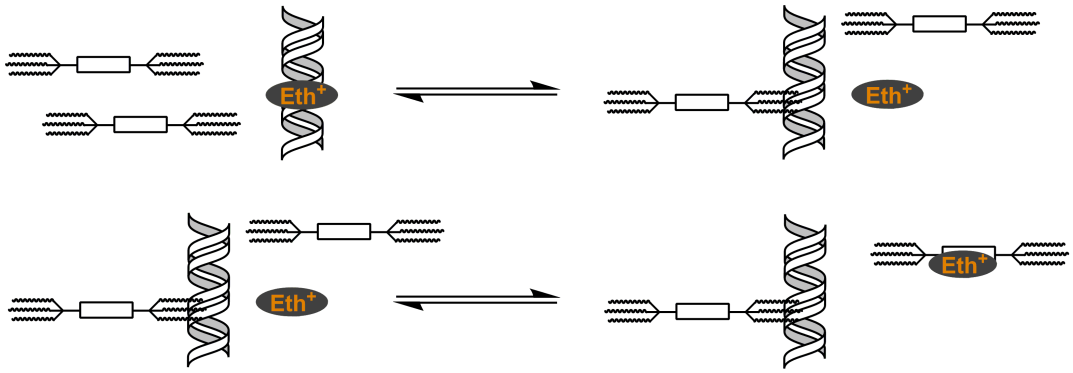

Figure 32: Representation of the interactions between perylene dendrimers, DNA, and ethidium moieties, and the equilibria present in solution. The diagram shows the displacement of the ethidium cation upon binding of the cationic dendrimer to the minor groove of the DNA (top) and the further interaction between the aromatic ethidium cation and the electron-rich perylene moiety at the core of the dendrimers (bottom). Removal of free ethidium from solution in the lower equilibrium shifts the upper equilibrium to the right, distorting the results of the exclusion assay and making the dendrimer appear to be a better DNA-binder than is in fact the case.

Unlike the intercalation of the perylene core into DNA, this EthBr-perylene interaction does not represent an additional DNA-binding mode, rather its contribution to the CE_{50} is an artifact of the indirect means used to monitor the degree of DNA binding.

No obvious means could be found to measure and quantify the π-π stacking of ethidium bromide and DNA. Preliminary studies suggested that any stacking interactions between the perylene dendrimers and EthBr did not individualise the perylene units to a degree observable using UV/Vis spectroscopy, nor would these interactions produce a significant change in

the fluorescence of the ethidium bromide when combined with the perylenes in aqueous solution.

3.4 DNA Binding Capability of G2 DAPMA-Terminated Perylene Bisimide

As with its G1 analogue, ***8***, the DNA binding strength of the G2 DAPMA terminated perylene bisimide dendrimer, ***12***, was indirectly measured using an ethidium bromide displacement assay.

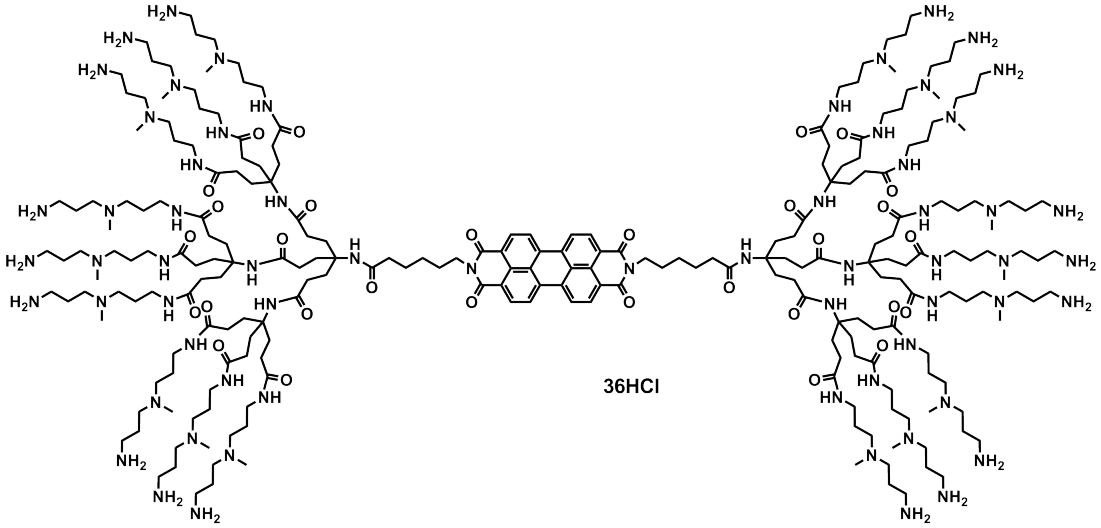

Figure 33: G2 DAPMA terminated perylene bisimide dendrimer, ***12***, shown as its hydrochloride salt.

Due to concerns comparable to those expressed during the investigation of the G1 dendrimer, regarding the fluorescence emission of the perylene moiety beginning to impinge upon the assay at higher concentrations, the assay was carried out at a 1 μM concentration of ***12***. The low mass of material available made precise determination of the concentration difficult. However, after dissolving the available solid in 0.01 M SHE buffer, the UV/Vis absorption of the resulting solution was compared with that of various concentrations of ***8***, its G1 counterpart. It was reasoned that, broadly, the absorbance of the perylene core would correspond to the concentration of that moiety in solution, regardless of the generation of the dendrimer's shell. However, as discussed previously (Section 2.2) the maxima of the perylene absorbance are not an accurate reflection of concentration, and their relative heights vary depending on the degree of aggregation of the compound. A wavelength on the edge of the perylene absorption region, at 700 nm, was found to follow the

Beer-Lambert law, with its absorbance increasing linearly with concentration. The concentration of the G2 solution was therefore found to approximate to 5 μM, allowing dilution to afford the desired 1 μM solution.

Expressed as a charge-excess, N/P, the concentration of protonated groups is clearly much higher in the second generation dendrimer than in its first generation counterpart. It was of some surprise therefore, when, upon addition of a concentration of the G2 DAPMA-PBI comparable to the C_{50} of the G1 dendrimer, the fluorescence had only diminished by around one-third.

	C_{50} (μM)	CE_{50}
	0.090	0.40
	0.120	0.54
	0.097	0.43
Mean	0.102	0.46

Table 4: C_{50} and CE_{50} values calculated from three ethidium bromide displacement assays, in each case titrating 1 μM G2-DAPMA-PBI ***12***.

In contrast to the mean values obtained from titrations of the G1-DAPMA-PBI, ***8***, (C_{50} = 0.046 μM, CE_{50} = 0.07), the G2 dendrimer's C_{50} of 0.102 μM and CE_{50} of 0.46 are unexpectedly low, especially considering the expected increase in binding, observable in similar, albeit non self-assembling systems. Apart from the inaccurate method of determining the initial solution concentration, which might be expected to account for some but not all of this effect, it seems plausible that the observed reduction in binding affinity would be, at least in part, the result of the increased size of the dendrimer. Just as Hirsch *et al.* demonstrated that their smaller or less symmetrical perylene dendrimers were more able to solubilise CNTs due to increased micelle formation, these larger dendrimers may exhibit a reduction in their self-assembled multivalency. Both the steric bulk and increased charge of the branching units could be expected to hinder the formation of aggregates, preventing some of the self-assembled multivalent effect that has been implicated in the remarkably low CE_{50} of the first-generation DAPMA-terminated dendrimer (Section 3.1).

In addition to inhibiting perylene-perylene stacking, the increased bulk of

the second generation branching unit would also be expected to hinder intercalation of the dendrimer's core into dsDNA. Kerwin *et al.* demonstrated that larger perylene bisimides were less able to intercalate into double-stranded DNA,[111] and the increase in size from first- to second-generation may lead to a corresponding inhibition of the expected intercalation binding mode. Accordingly, this may account for a portion of the reduction in total binding.

3.5 CNT Binding Capability of G1 DAPMA-Terminated Perylene Bisimide

The binding of carbon nanotubes by perylene-CNT π-π stacking is not measured by assay. Qualitatively this interaction can be observed through the formation of stable carbon nanotube solutions; Hirsch *et al.* have shown that amphiphilic perylene dendrimers can solubilise and individualise CNTs to a significant extent.[36]

Carbon nanotubes shaken or sonicated in water or in SHE buffer solution will not separate considerably, and will rapidly clump and settle in the vial. 2 ml of a 10 μM solution of the first-generation, DAPMA-terminated dendrimer, ***8***, was sonicated with 0.09 mg of carbon nanotubes, producing a stable deep-red solution.

Titration of CNT-perylene solutions into a perylene solution of equivalent concentration should allow the nature of the solubilisation to be probed. The UV/Vis spectra produced by the titration show an increased absorbance at all wavelengths, presumably due to absorption and scattering by the carbon nanotubes (Figure 34). At all observed wavelengths the increase in absorption appeared to be linear with respect to concentration, following the Beer-Lambert law and so supporting the hypothesis that the carbon nanotubes were present in solution rather than as a suspension. At no point, however, were the van Hove singularities characteristic of individualised CNTs observable; these appear as jagged regions in the UV/Vis spectrum.[36] This would suggest that, while solubilised, within the range of concentrations and perylene-CNT ratios studied nanotubes were not individualised to an observable degree, existing instead as bundles of several nanometres in diameter.

Solutions of carbon nanotubes were prepared in 0.01 M SHE buffer using sodium dodecylbenzenesulfonate (SDBS) as a surfactant. The UV/Vis spectra of these solutions were measured and subtracted from those of the perylene-

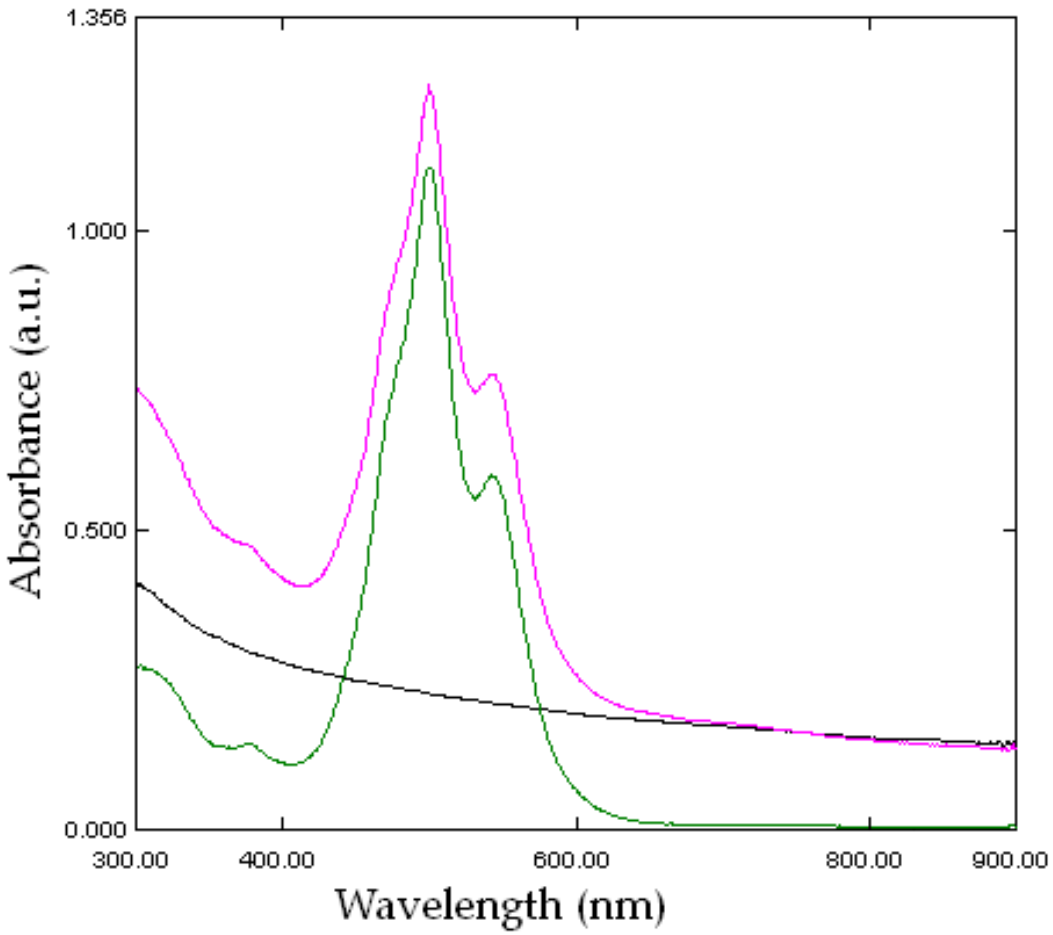

Figure 34: UV/Vis absorption of 10 μM DAPMA-terminated G1 perylene dendrimer (green), the same perylene solution with 0.01 g L^{-1} single-walled carbon nanotubes (pink), and a solution of 0.01 g L^{-1} single-walled carbon nanotubes in 0.7 mM SDBS (black).

CNT titration in order to normalise the spectra with respect to the carbon nanotubes.

Data were normalised at 500 nm and 543 nm, values representing the absorption of light by stacked perylenes and unstacked, individualised perylene units respectively. Upon increasing concentration of CNTs there appeared to be a corresponding increase in the proportion of unstacked perylenes, though to be due to the disassembly of perylene aggregates upon interaction with the surface of the carbon nanotubes. However, the data also appeared to show an increase in the proportion of stacked perylenes suggesting that the increase was due to, or was within, any errors in the normalisation (Figure 35).

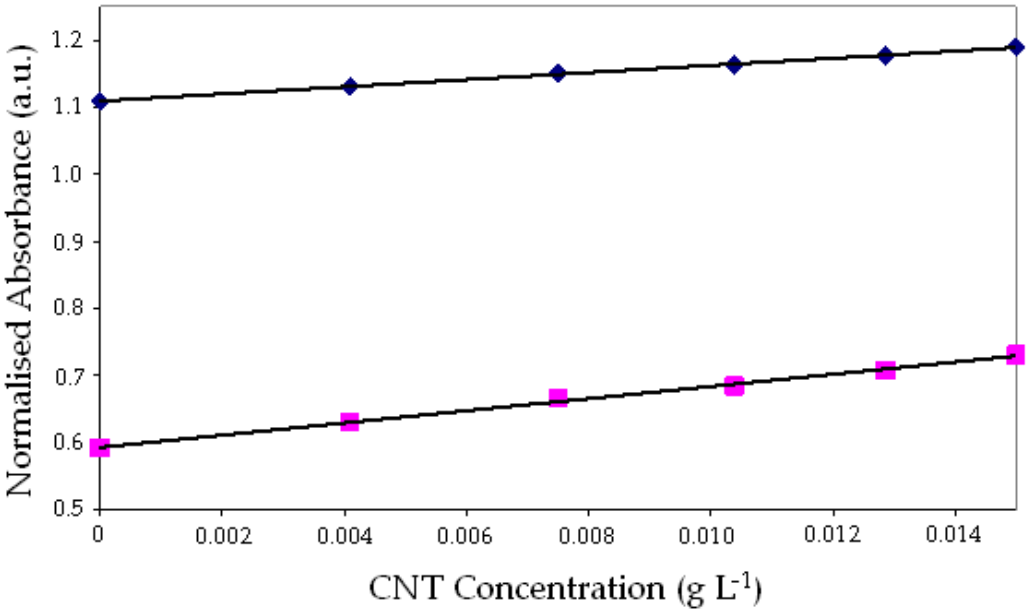

Figure 35: UV/Vis absorbance of perylene core at 500 nm ♦ and 543 nm ■, with respect to increasing carbon nanotube concentration. Data normalised to remove carbon nanotube absorbance.

Interaction between the nanotubes and polyamine-terminated perylene dendrimers was further probed via transmission electron microscopy. 0.0045 g L^{-1} carbon nanotubes were dissolved in a 10 μM solution of perylene in 0.01 M SHE buffer. Electron micrographs appeared to show carbon nanotubes, or bundles of nanotubes, coated periodically with large, globular perylene aggregates (Figure 36).

Micrographs were also taken of the residue from solutions of nanotubes, perylene, and plasmid DNA, which is known to provide clearer pictures than calf-thymus DNA when viewed using transmission electron microscopy. Unfortunately, the images obtained did not clearly show any DNA-dendrimer-CNT nano-hybrids; rather the structures formed appeared much the same as those without the presence of DNA, and no DNA, bound or free, was visible. These micrographs do not, therefore, seem to disprove the existence of such hybrid structures, rather is is possible that DNA was present and was bound to the CNT-perylene aggregates but was unable to be visualised under the conditions used in this experiment (Figure 37).

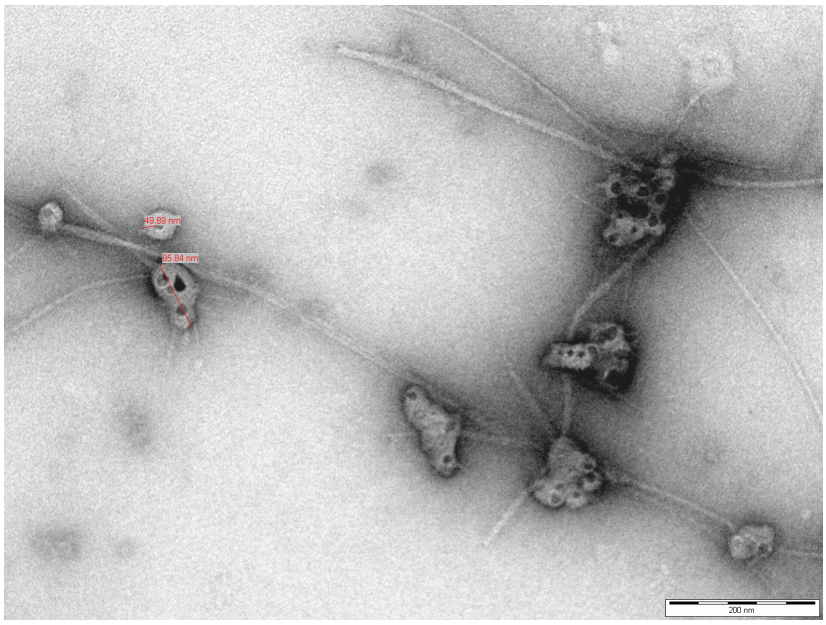

Figure 36: Transmission electron micrograph showing an 87,000 x magnification of the residue from a solution of DAPMA-terminated perylene dendrimer and single-walled carbon nanotubes.

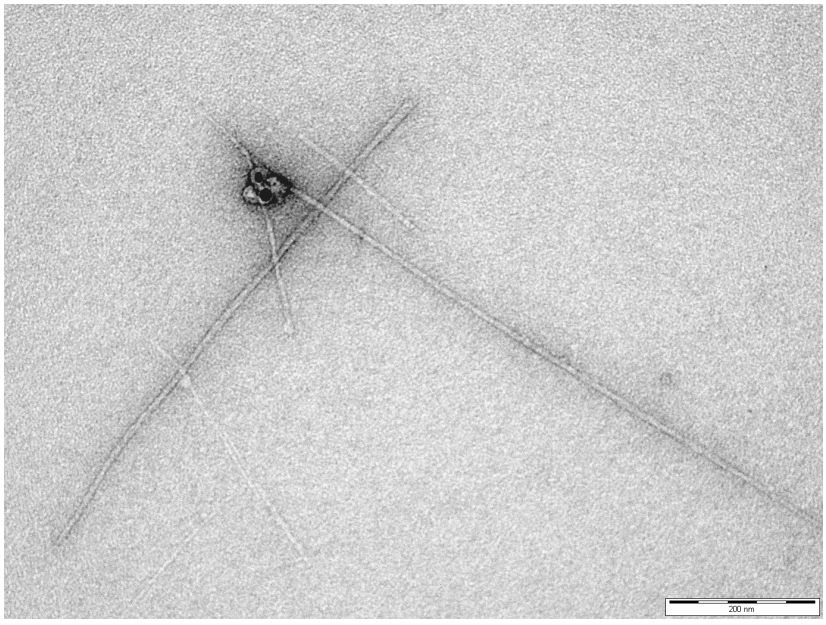

Figure 37: Transmission electron micrograph showing an 87,000 x magnification of the residue from a solution of DAPMA-terminated perylene dendrimer, SWCNTs, and plasmid DNA.

3.6 Effect of Carbon Nanotubes on DNA Binding Capability of G1 DAPMA Terminated Perylene Bisimide

While it has hopefully been shown that DAPMA-terminated peryene bisimide dendrimers are capable of interaction with both CNTs and DNA, it does not necessarily follow that in solutions containing all three components the desired three-component nanohybrids would be formed. Any number of factors may discourage the formation of CNT binding to an existing DNA-PBI polyplex, or of DNA binding to perylene-coated CNTs. Given the plausibility of a perylene-DNA intercalation interaction forming at least part of the total binding of DNA to the dendrimers, as discussed (Section 3.1), it might be thought that the addition of carbon nanotubes to the DNA-PBI solutions under investigation may inhibit such an interaction by preferentially binding the perylene cores of the dendrimers. Alternatively, should the DNA perylene core intercalation be particularly strong, the presence of DNA might cause separation of the perylene units from the CNTs, leading to a reduction in solubility and, accordingly, carbon nanotubes clumping and settling from solution.

A simple method was devised in order to test the effect of carbon nanotubes on the binding of *8* to DNA. An ethidium bromide displacement assay was carried out as described above, but with the addition of 2.5 mg L^{-1} single walled CNTs to the titrating mixture. This concentration was chosen as close to the maximum carbon nanotube concentration sustainable by a 1 μM solution of *8*. This, then, provides the highest proportion of CNT-perylene hybrids possible. The C_{50} and CE_{50} of this CNT perylene mixture were then calculated from the resulting curve (Table 5).

	PBI C_{50} (μM)	CE_{50}
PBI (Mean)	0.046	0.07
PBI-CNT Mixture	0.049	0.07

Table 5: Comparison of C_{50} and CE_{50} of G1 DAPMA-Terminated PBI ***8*** (Section 3.1) and a mixture of this dendrimer with single walled CNTs in a 1 μM to 2.5 mg L^{-1} ratio.

While this single experiment gives a C_{50} a little lower than that calculated as the mean of the assays performed with a 1 μM solution of ***8*** alone, the value calculated is within a fraction of the standard deviation of the earlier experiment (a difference of 0.003 μM, in contrast to a standard deviation of 0.176 μM). It would be hard to conclude, therefore, that this experiment demonstrates any significant decrease in the DNA affinity of the first-generation DAPMA-terminated dendrimer, ***8***, when bound to carbon nanotubes.

In order to further probe such DNA-PBI-CNT systems, an additional assay was performed in which the CNT concentration of the solution was altered while keeping the concentration of ***8*** constant. Portions of 0.125 mg L^{-1} CNTs, 5.08 μM EthBr, 4 μM DNA and 0.05 μM ***8*** were added to a solution of 5.08 μM EthBr, 4 μM DNA and 0.05 μM ***8***. This concentration of ***8*** was chosen due to its proximity to the C_{50}, reasoning that in this region any fluctuations in the fluorescence of ethidium bromide, suggesting a reduction or increase in the DNA affinity of the PBI, would be most visible.

Across a CNT concentration range of 0.06 mg L^{-1}, a slight decrease in ethidium bromide fluorescence was observed, suggesting an increase in the strength of DNA binding by ***8***. Conceivably, this could be attributable to increased aggregation of perylene units around the carbon nanotubes raising the degree of self assembled multivalency of the dendrimers. However, as discussed earlier, the ethidium bromide displacement assay is not a direct measure of cationic binding, and it may be possible that the polyaromatic nature of the CNTs introduced into the solution acts to shift the free/bound

ethidium ion equilibrium in favour of the free form, leading to a reduction in EthBr fluorescence without an actual increase in the DNA binding capability of the dendrimer.

4 Conclusions

The first-generation perylene bisimide dendrimer was, once elements of the synthesis had been optimised, produced in reasonably high yields. The remarkably high binding affinity demonstrated by the dendrimer (CE_{50} = 0.07, though these values are not always comparable between dissimilar compounds) shows great promise in designing similar, strongly DNA binding molecules. Previous research into dendritic molecules with aromatic cores or micelle inducing hydrophobic tails demonstrates the potential for self-assembled multivalency, and the strong DNA binding that can result from this. The weaker binding exhibited by the second-generation dendrimer appeared to lend some support to the idea that self-assembly contributed to the low C_{50} and CE_{50} of these molecules. Despite greater branching and higher charge per molecule, the G2 DAPMA-terminated dendrimer posessed a CE_{50} more than six-times greater than that of the first-generation dendrimer, or CE_{50} = 0.46 rather than the G1's CE_{50} = 0.07.

It seems highly plausible that some part of this particularly strong binding, and some part of the difference between first- and second-generation dendrimers, is attributable to intercalation of the perylene core moieties into the DNA double helix. This additional binding mode would also cause displacement of ethidium cations from DNA but may not be beneficial to efficient DNA packaging, lacking the collapse caused by charge-neutralisation upon electrostatic binding. This binding mode may also be undesirable in the formation of three-component nanohybrids, reducing the availability of the perylene cores for interaction with carbon nanotubes.

As discussed, another method of ascertaining the strength of DNA binding may be desirable, due to concerns regarding the applicability of the ethidium bromide displacement assay to these polyaromatic molecules.

While difficult to quantify, the binding of the perylene core to carbon nanotubes can be indicated qualitatively by the dispersion and solubilisation

of the CNTs in aqueous buffer. TEM evidence shows that, after deposition and drying, the nanotubes remain discretely distributed (Figure 38).

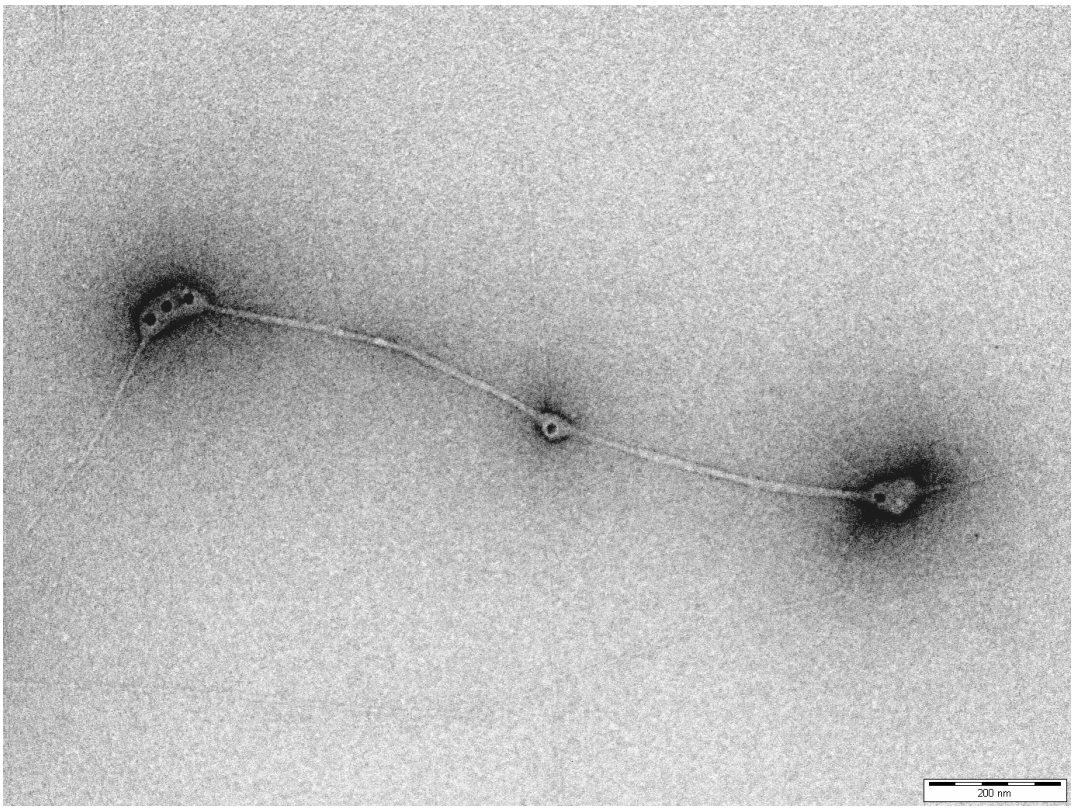

Figure 38: Transmission electron micrograph showing an 60,000 x magnification of the residue from a solution of DAPMA-terminated perylene dendrimer, SWCNTs, and plasmid DNA.

The addition of CNTs to a solution of DNA and *8* did not appear to significantly disrupt the binding of DNA, nor cause aggregation and precipitation of the nanotubes. While a significant shift in the binding affinity of the dendrimer may have been indicative of a change in the morphology of the PBI-DNA complexes, statistically it can be presumed that a proportion of the dendrimer aggregates bind to both DNA and carbon nanotubes. Indeed, the continued binding of both CNTs and DNA by the first-generation DAPMA terminated dendrimer suggests the formation of three-component nanohybrids in solution.

5 Future Work

5.1 Non-DAPMA Terminated PBIs

Further study of the means by which perylene bisimides cause exclusion of ethidium bromide is warranted by the possibility of perylene intercalation into the DNA double-helix, as described in Section 3.2.

The relative contributions of cationic binding and other potential EthBr displacement modes could be explored through investigation of dendrimers lacking the DAPMA polyamine functionality. This could consist simply of carrying out the EthBr displacement assay and UV/Vis intercalation experiments using the tert-butyl or carboxylic acid terminated dendrimers described above (compounds ***5*** and ***6*** respectively, or ***9*** and ***10*** for the second-generation dendrimer) or of novel molecules that retain the bulk of ***8*** and ***12*** while lacking protonatable amines, such as those terminated with alkyl, polyethylene glycol, or alcohol units.

5.2 Increasing Bulk

Previous studies reported in the literature indicate that perylene bisimides possessing increased bulk demonstrate reduced intercalation into dsDNA.[111] As the second-generation DAPMA-terminated dendrimers described in this thesis appeared to displace EthBr less efficiently than the less charged first-generation dendrimers, and as it is presumed that a component of this displacement results from intercalation, it would seem that increasing the generation, and thus bulk, of the dendrimers could significantly inhibit this binding mode. While synthesis of a third-generation DAPMA-terminated dendrimer would indeed increase this bulk further, the low yields obtained during the synthesis of ***12*** would seem to cast some doubt on the viability of obtaining a G3 DAPMA-terminated perylene bisimide in useful quantities without significant expenditure of time and material. In addition, such a

dendrimer would exhibit greater charge and possibly different aggregation behaviour to the first- and second-generation variants.

An alternative means of increasing steric hindrance around the perylene moiety would be the synthesis of a "bay-substituted" PBI, in which groups are added to the 1, 6, 7, or 12 positions of the perylene. (Figure 39). Either short, highly-branched alkyl groups, or long linear alkyl chains able to describe a large gyrodynamic radius should reduce the ability of the dendrimer to intercalate into dsDNA, aiding investigation into the nature of this interaction, and its contribution to the DNA binding ability demonstrated by the molecules whose investigation is described in this thesis. However, once again direct comparison may not be available due to potential changes in the size and morphology of dendrimer aggregates; if increased bulk around the dendrimers' cores inhibits attractive interactions between perylene units, the resulting reduction in self-assembled multivalency may also lead to a weakening of the electrostatic DNA binding mode. In addition, increased bulk around the bay area in such close proximity to the planar perylene moiety, as well as the resulting twisting of the planar aromatic system, may hinder CNT binding by the dendrimers, potentially reducing the degree to which they can solubilise and non-covalently functionalise nanotubes and participate in the formation of nanohybrids.[114]

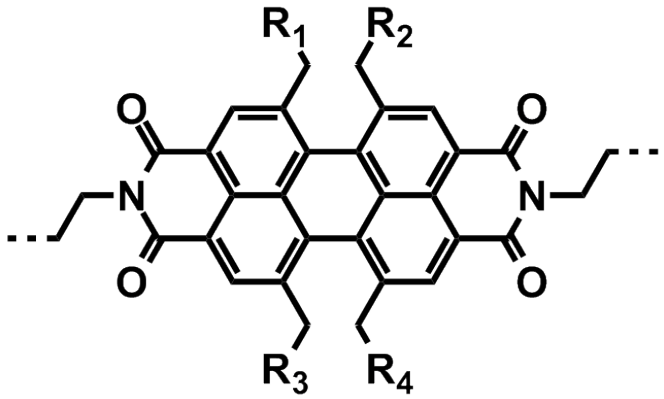

Figure 39: Bay-substituted perylene bisimide, showing functionalisation at the 1, 6, 7 and 12 positions.

5.3 Potential Sources of Error in the EthBr Exclusion Assay

During the course of the investigations described on previous pages, no means could be devised by which possible interactions between EthBr and perylenes could be monitored. As explained in Section 3.3, direct association between PBIs and ethidium cations in solution could alter the equilibrium between intercalated and free ethidium, introducing error into the binding assay. Perylene bisimide dendrimers such as ***5*** and ***9***, lacking polyamine units and so presumably unable to exclude EthBr from DNA *via* an electrostatic binding interaction with the DNA, could be modified to introduce additional bulk, possibly by methods such as those discussed above (Section 5.2). Should such dendrimers be demonstrated to be unable to intercalate into DNA, any ethidium bromide displacement measured by assay would, therefore, be the result of direct perylene-ethidium interactions.

5.4 Newkome-branching, DAPMA-terminated Pyrene Dendrons

Dendritic pyrenes, represent promising candidates for the efficient binding of DNA to carbon nanotubes. Should minor synthetic hurdles be overcome, the resulting dendrons whould presumably bind DNA with affinities at least as high as those reported previously for Newkome-branching DAPMA-terminated dendrons lacking the pyrene core.[84] A degree of aggregation may be expected in aqueous solution, resulting in a degree of self-assembled multivalency that could further improve DNA binding.

The affinity of the pyrene moiety for CNTs has been estalished.[39] Comparison of symmetrical, bolaamphiphilic dendrimers and analogous asymmetrical amphiphiles by Hirsch *et al.* suggested that wedge-shaped units able to self-assemble into micelle-like units demonstrated improved CNT binding relative to bulky, symmetrical molecules. Accordingly, it would be thought that a pyrene-based dendron should bind to both carbon nanotubes and DNA to a

reasonable degree, promoting the formation of nanohybrids.

A practical benefit associated with investigating the DNA binding of pyrene-containing molecules is that, unlike perylene, its fluorescence emission reaches a maximum at around 400 nm, with little fluorescence at 595 nm. Accordingly, difficulties associated with the fluorescence of the dendron impinging on the observed walvength during EthBr exclusion assays are of little concern. While neither the absorbance nor fluorescence emission spectra seem to be as sensitive to aggregation as those of perylene, the formation of pyrene dendron aggregates could be investigated by TEM, with appropriate staining.

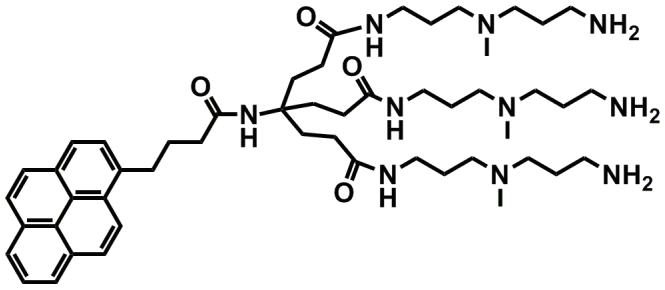

Figure 40: A first-generation Newkome-branching, DAPMA-terminated pyrene dendron.

6 Experimental

Materials and methods

All reagents were commercially available, and used as supplied unless otherwise stated. Water was de-ionised, and MilliQ water was prepared using a Millipore Simplicity 185. Boc-DAPMA was synthesised previously by Anna Barnard, and was used as supplied. TLC was performed on aluminium-backed plates coated with 0.25 mm silica gel 60, supplied by Merck; spots were visualised with the naked eye under visible light or under UV, and with staining where necessary. Column chromatography was performed using silica gel 60 with a pore size of 0.035 - 0.070 mm, supplied by Fluka. Size-exclusion chromatography was performed using Bio-Beads®SX-1 and Sephadex®LH-20.

Nuclear magnetic resonance spectroscopy was carried out using two JEOL 400 (^{1}H 400 MHz, ^{13}C 100 MHz) spectrometers. ^{13}C DEPT-135 experiments were performed where necessary. Chemical shifts (δ) are reported in parts per million (ppm) downfield of tetramethylsilane (TMS) and residual solvent was used as an internal reference ($CHCl_3$: 7.26 ppm & 77.16 ppm, MeOH: 3.31 ppm & 49.00 ppm, pyridine: 7.29 ppm). Electrospray Ionisation (ESI) and Atmospheric Pressure Chemical Ionisation (APCI) mass spectrometry were recorded using a Bruker micrOTOF MS. Matrix-assisted laser desorption ionisation (MALDI) mass spectrometry was recorded using a Bruker Ultraflex II MALDI-TOF/TOF mass spectrometer, with 2,5-dihydroxybenzoic acid (DHB) as the matrix. Infrared spectra were recorded using a JASCO FT/IR-4100 and values are expressed in cm^{-1}, while UV/Vis spectra were recorded using a Shimadzu UV 2401PC, with values expressed in nm. Fluorescence spectroscopy was carried out using a Hitachi F-4500 Fluorimeter, exciting at 280 nm and observing emission at 595 nm unless otherwise stated.

SHE Buffer

0.01 M SHE buffer was prepared from 1 M HEPES (0.5 ml, 0.5 mmol), trisodium EDTA (0.0035 g, 0.009 mmol) and NaCl (2.194 g, 37.54 mmol) in MilliQ water (250 ml).

Ethidium Bromide Displacement Assay

All calculations described herein involving calf thymus DNA take the fundamental unit as one base pair residue, containing two nucleotides, two phosphate groups, and two deoxyribose residues. The average mass of this unit is taken to be 660 Da.

Calf thymus DNA (0.001 g, 0.0015 mmol) was dissolved in 0.01 M SHE buffer (75 ml) to give a 40 μM stock solution. A portion (10 ml) was then further diluted with SHE buffer (40 ml) to give an 8 μM solution. Ethidium bromide (0.005 g, 0.013 mmol) was dissolved in SHE buffer (50 ml) to give a 25.4 μM stock solution. A portion (20 ml) was then further diluted with SHE buffer (30 ml) to give a 10.16 μM solution. Portions of each were mixed in in a 1:1 ratio to give a solution of 4 μM DNA and 5.08 μM EthBr. To this was titrated portions of the solution under investigation, prepared following the procedures outlined below. Fluorescence spectra of these titrations were measured, exciting the samples at 280 nm and observing the emission at 595 nm. The initial fluorescence emission was normalised to 1, while the minimum was normalised to 0.

Preparation of PBI-DAPMA Solutions for Ethidium Bromide Exclusion Assay

Due to the small quantities of material required, in all cases stock solutions of the dendrimer were prepared in MeOH to a known concentration.

The desired volume of solution was then removed using an adjustable micropipette, transferred to a clean vial, and the solvent removed *in vacuo* to give a red film. This solid residue was then dissolved in the appropriate volume of 4 μM DNA and 5.08 μM EthBr in 0.01 M SHE buffer, prepared as above, in order that the DNA and ethidium bromide concentrations remain constant throughout the course of the titration. The solutions were then used in the exclusion assay, as described above.

Intercalation Study

A stock solution of the dendrimer was prepared in MeOH to a known concentration. The desired volume of solution was then removed using an adjustable micropipette, transferred to a clean phial, and the solvent removed in vacuo to give a red film. This solid residue was then dissolved in the appropriate volume of a 57.47 μM DNA solution , to give a 1 μM solution of the perylene. An equivalent 1 μM solution of the perylene was prepared using 0.01 M SHE buffer, rather than the DNA solution.

The UV/Vis absorbance of the perylene solution in buffer was measured. Portions of the DNA/perylene solution were then added by micropipette, and the absorbance after each successive addition was recorded relative to the DNA concentration. Data were then normalised according to the UV/Vis absorbance of equivalent calf thymus DNA dilutions in 0.01 M SHE buffer.

Preparation of CNT Solutions

Single-walled carbon nanotubes (0.09 mg) were weighed into a vial, to which was added 10 μM G1-PBI-DAPMA in 0.01 M SHE buffer (2 ml) via micropipette. After sonication for 2 hours, homogenous red-grey solution had formed: CNTs (0.045 g L^{-1}) in 10 μM G1-PBI-DAPMA. Centrifugation at 4500 rpm for 45 minutes afforded a pale red solution over dark material.

Sonication restored the liquid to a homogenous red-grey solution, which was stable after one week, with minimal aggregation. After three months, some settling of black material was observed but the solution was easily restored by shaking, with no need for further sonication.

Titration of CNT Solutions

The 0.045 g L-1 solution of CNTs in 10 μM G1-PBI-DAPMA, prepared as described above, was titrated into 10 μM G1-PBI-DAPMA in 0.01 M SHE buffer (2ml) in a quartz cuvette. The UV/Vis absorbance of the resulting dilutions was measured. In order to probe possible changes in the absorbance of the perylene moiety upon CNT binding, data were normalised according to the UV/Vis absorbance of equivalent CNT solutions in SDBS. The solutions were prepared from a 0.1 g L^{-1} solution of CNTs in SDBS, itself prepared from SWCNTs (0.7 mg) and SDBS (2.4 mg, 0.007 mmol) in 0.01 M SHE buffer (7 ml).

Transmission Electron Microscopy

TEM studies were carried out using an FEI Technai 12 Biotwin at 120 kV, using a copper grid on a Formvar and carbon support. Samples were placed on the grid in solution, left for 3 minutes, and excess liquid removed. Samples were then stained using uranyl acetate (1 % in water) and left for a further 10 minutes before excess stain was removed and imaging was carried out. Samples consisted of: a 10 μM solution of G1-PBI-DAPMA containing 0.045 g L^{-1} CNT; a further portion of the same, centrifuged and the supernatant diluted by a factor of 10 using 0.01M SHE buffer before the addition of 0.01 g L^{-1} plasmid DNA; a 1:1 mixture of these two samples.

Di-tert-butyl 4-(3-*tert*-butoxy-3-oxopropyl)-4-nitroheptanedioate (*1*)[80]

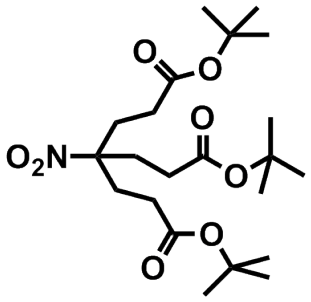

A solution of nitromethane (0.87 ml, 16.4 mmol) and Triton B (0.16 ml, 0.36 mmol) was stirred in THF (3.5 ml) at 60°C. *tert*-Butyl acrylate (7.4 ml, 51 mmol) was added dropwise in order to minimise any temperature increase; the temperature was monitored and kept below 70°C. After several minutes, two further portions of Triton B (each 0.16 ml, 0.36 mmol) were added. The yellow solution turned orange. The reaction was stirred for 1.5 h, after which the solvent was removed *in vacuo*, and the residue dissolved in chloroform (40 ml). The solution was washed with 10% aqueous HCl (10 ml), then with three portions of brine (each 10 ml). The organic phase was dried over magnesium sulfate and then filtered. The solvent was removed *in vacuo* and the residue recrystallised from ethanol. The resulting white crystals were recovered in two crops.

Yield 4.47 g (61 %). ^{1}H NMR ($CDCl_3$, 400 MHz) δ 1.43 (s, CH_3, 27H); 2.19 (s, CH_2, 12H). ^{13}C NMR ($CDCl_3$, 100 MHz) δ 28.16 (CH_3, 9C); 29.93 (CH_2CO, 3C); 30.47 (CCH_2, 3C); 81.29 ($C(CH_3)_3$, 3C); 92.32 (O_2NC, 1C); 171.21 (CO, 3C). ESI-MS (m/z): 468.26 (100%, $[M+Na]^+$).

Di-*tert*-butyl 4-amino-4-(3-tert-butoxy-3-oxopropyl)heptanedioate (2)[80]

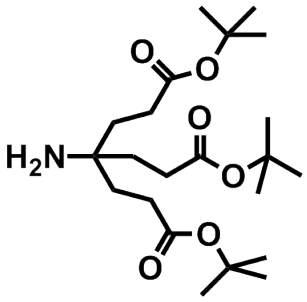

A slurry of 50% w/w Raney nickel in water (4.1 g, 34.93 mmol) was mixed with EtOH (25 ml). The resulting suspension was allowed to settle, and the supernatant was decanted. This procedure repeated twice more in order to obtain a suspension of Raney nickel in EtOH. This suspension was rinsed into the flask with a further portion of EtOH (50 ml). ***1*** (4.5 g, 10.10 mmol) was added. The flask was purged with nitrogen, then hydrogen. The solution was then stirred vigorously under hydrogen at 45 °C for 23 h, before being filtered over Celite and rinsed with MeOH. The solvent was then removed *in vacuo* at no more than 30 °C to give a translucent oil which, after several hours, became a white solid. No further purification was carried out, and the product was stored under nitrogen at -18 °C until required.

Yield 4.1 g (98 %). ^{1}H NMR ($CDCl_3$, 400 MHz) δ 1.14 (br s, NH_2, 2H); 1.39 (s, CH_3, 27H); 1.56 (t, CH_2, J = 8.4 Hz, 6H); 2.20 (t, CH_2, J = 8.4 Hz, 6H). ^{13}C NMR ($CDCl_3$, 100 MHz) δ 28.11 (CH_3); 30.00 (CH_2); 34.40 (CH_2-CO); 52.38 (H_2NC); 80.34 ($C(CH_3)_3$); 173.10 (CO). ESI-MS (m/z): 416.30 (100%, $[M+H]^+$).

di-tert-butyl 4-(6-(benzyloxycarbonylamino)hexanamido)-4-(3-tert-butoxy-3-oxopropyl)heptanedioate (*3*)

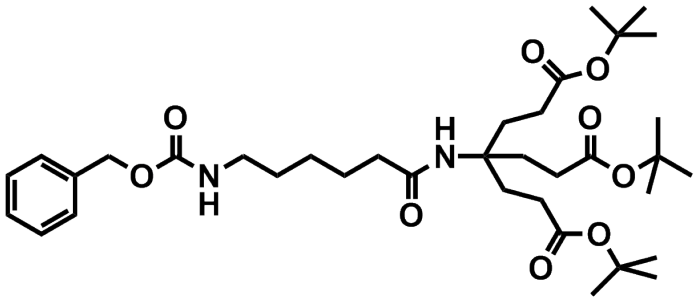

2 (0.33 g, 0.79 mmol), Z-caproic acid (0.27 g, 1.02 mmol) and TBTU (0.29 g, 0.90 mmol) were dissolved in DCM (15 ml) and cooled in ice. DIPEA (0.31 ml, 1.78 mmol) was added, with stirring. The solution was then stirred for 16 hours, slowly warming to room temperature, after which it was stirred at reflux for 11 days. During this time the reaction was monitored by TLC. The solvent was then removed *in vacuo*, and the residue redissolved in DCM (20 ml). This solution was then washed with water (40 ml), 1 M HCl (40 ml), 1 M Na_2CO_3 (40 ml), and then two further portions of water (2 x 40 ml). The solution was dried over $MgSO_4$, then filtered. The solvent was removed in vacuo and the resulting solid redissolved in 2:3 cyclohexane:EtOAc, before being eluted with the same over SiO_2. Solvent was removed in vacuo to give a solid, which was then redissolved in DCM and washed with $NaHCO_3$ in order to remove an aromatic impurity. The solvent was then once more removed *in vacuo*.

Yield 0.35 g (70 %). R_f = 0.65 (2:3 cyclohexane:EtOAc on SiO_2). ^{1}H NMR ($CDCl_3$, 400 MHz) δ 1.24 (m, CH_2, 2H); 1.34 (s, CH_3, 27H); 1.245 (m, CH_2, 2H); 1.52 (m, CH_2, 2H); 1.88 (t, CH_2, J = 8.0 Hz, 6H); 2.02 (t, CH_2, J = 7.2 Hz, 2H); 2.13 (t, CH_2, J = 8.0 Hz, 6H); 3.10 (q, CH_2, J = 6.4 Hz, 2H); 4.95 (br s, NH, 1H); 5.00 (s, C_6H_5-CH_2-O, 2H); 5.86 (s, NH, 1H); 7.23 (m, C_6H_5, 5H). ^{13}C NMR ($CDCl_3$, 100 MHz) δ 25.35 (CH_2, 1C); 26.42 (CH_2, 1C); 28.17 (CH_3, 9C); 29.74 (CH_2, 1C); 29.95 (CH_2, 3C); 30.05 (CH_2, 3C); 80.84 ($C(CH_3)_3$, 3C); 128.22,

128.61, 129.09, 136.76 (C_6H_5, 6C); 156.54, 172.49 (CONH, 2C); 173.07 (COO^tBu, 3C). ESI-MS (m/z): 663.42 (25%, $[M+H]^+$), 685.40 (100 %, $[M+Na]^+$).

Di-*tert*-butyl 4-(6-aminohexanamido)-4-(3-tert-butoxy-3-oxopropyl) heptanedioate (*4*)[80]

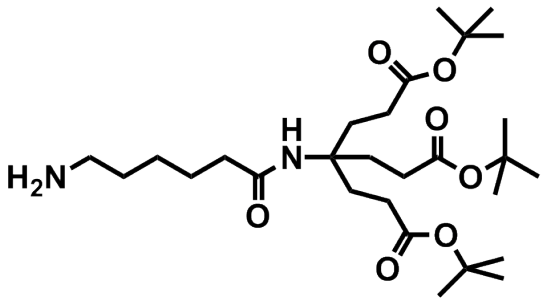

3 (0.35 g, 0.53 mmol) was dissolved in a sufficient volume of hot EtOH. 10 % palladium over carbon (0.05 g, 0.05 mmol) was added, with stirring. The flask was purged with nitrogen, then put under hydrogen and stirred at room temperature for 24 hours. The solution was then filtered over Celite, rinsed through with further EtOH. The solvent was then removed *in vacuo* to afford a clear film.

Yield 0.24 g (86 %). ^1H NMR ($CDCl_3$, 400 MHz) δ 1.10 (m, NH, 1H); 1.30 (m, CH_2, 2H); 1.39 (s, CH_3, 27H); 1.57 (m, CH_2, 2H); 1.92 (t, CH_2, J = 7.6 Hz, 6H); 2.08 (t, CH_2, J = 7.2 Hz, 2H); 2.17 (t, CH_2, J = 7.6 Hz, 6H); 2.65 (m, CH_2, 2H); 5.98 (m, NH, 1H). ^{13}C NMR ($CDCl_3$, 100 MHz) δ 25.59, 26.54 (CH_2, 2C), 28.15 (CH_3, 9C); 29.91 (CH_2, 3C); 30.04 (CH_2, 3C); 33.34 (CH_2, 1C); 37.46 (CH_2, 1C); 42.02 (CH_2, 1C); 57.37 (CONH-C-R_3); 80.74 ($C(CH_3)_3$, 3C); 172.53 (CONH, 1C); 173.01 (COO^tBu, 3C). ESI-MS (m/z): 529.38 (100%, $[M+H]^+$).

G1 Newkome Branching *tert*-Butyl Terminated Perylene Bisimide (*5*)[95]

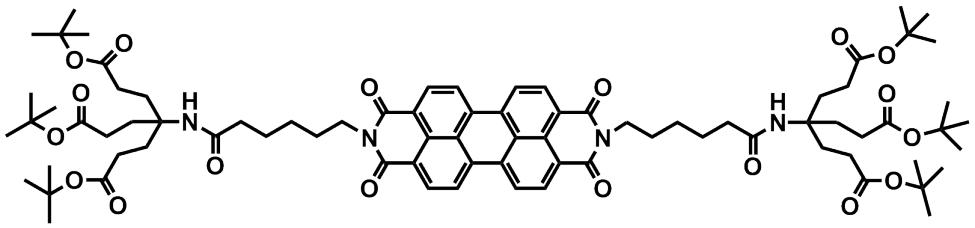

4 (0.24 g, 0.45 mmol), perylene tetracarboxylic acid dianhydride (0.092 g, 0.23 mmol), imidazole (1.5 g, 22 mmol), and zinc acetate (0.027 g, 0.15 mmol) were added to a flask, which was then heated to 110 °C with stirring. Upon melting of the imidazole, the resulting solution was stirred for 18 hours. Periodically, it was necessary to dislodge white needle-like crystals of imidazole forming in the top of the flask, in order to return them to the reaction volume. The solution was allowed to cool to room temperature and the resulting solid was dissolved in 95:5 DCM:MeOH. This was then eluted over silica with the same mixture of DCM and MeOH, to afford a red solid.

Yield 0.27 g (81 %). R_f = 0.56 (95:5 DCM:MeOH on SiO_2). ^{1}H NMR δ 1.26 (m, NH, 1H); 1.42 (s, CH_3, 54H); 1.48 (m, CH_2, 4H); 1.74 (m, CH_2, 8H); 1.97 (t, CH_2, J = 8.0 Hz, 12 H); 2.16 (t, CH_2, J = 7.8 Hz, 4H), 2.22 (t, CH_2, J = 8.0 Hz, 12H); 4.20 (t, CH_2, J = 7.6, 4H); 5.87 (s, NH, 1H); 8.56 (d, Ar-H, J = 8.4 Hz, 4H); 8.65 (d, Ar-H, J = 8.0 Hz, 4H). ^{13}C NMR δ 25.50 (CH_2, 2C); 26.73 (CH_2, 2C); 27.59 (CH_2, 2C); 28.16 (CH_3, 18C); 29.91 (CH_2, 6C); 30.01 (CH_2, 6C); 37.27 (CH_2, 2C); 40.42 (CH_2, 2C); 57.45 (CN, 2C); 80.72 ($C(CH_3)_3$, 6C); 122.76, 122.97, 125.64, 128.80, 130.89, 133.84 (Ar, 20C); 162.96 (CON, 4C); 172.81 (CONH, 2C); 173.01 (COOR, 6C). ESI-MS (m/z): 1436.7 (100 %, $[M+Na]^+$). APCI-MS (m/z): 1077.40 (100 %, $[M+H, -6^tBu]^+$).

G1 Newkome-Branching Carboxyl Terminated Perylene Bisimide (*6*)[95]

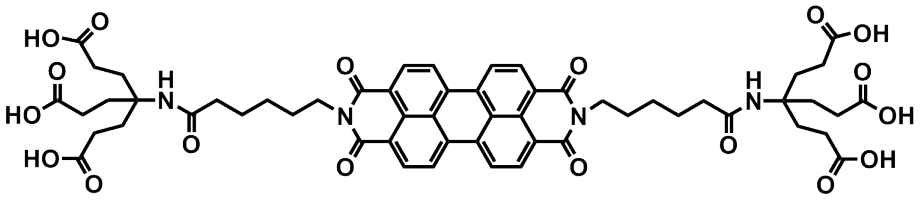

5 (0.25 g, 0.162 mmol) was dissolved in formic acid (20 ml) and stirred at room temperature for 21 hours. The solvent was then removed *in vacuo*. The resulting red solid was then put under a small volume of toluene, which was removed *in vacuo* in order to remove residual formic acid as an azeotrope.

Yield 0.23 g (Quantitative yield). ^{1}H NMR ($CDCl_3$/d5-pyridine, 400 MHz) δ 1.63 (s, CH_2, 4H); 2.00 (s, CH_2, 8H); 2.54 (m, CH_2, 4H); 2.74 (s, CH_2, 12H); 2.91 (s, CH_2, 12H); 4.40 (s, CH_2, 4H); 8.16, 8.18, 8.43 (m, Ar-H, 8H). ^{13}C NMR ($CDCl_3$/d5-pyridine, 100 MHz) δ 25.29 (CH_2, 2C); 26.47 (CH_2, 2C); 27.37 (CH_2, 2C); 29.82 (CH_2, 12C); 36.26 (CH_2, 2C); 39.79 (CH_2, 2C); 54.18 (CH_2N, 2C); 57.02; 122.11, 124.69, 12.86, 132.94 (Ar, 20C); 162.20 (CON, 4C); 172.16 (CONH, 2C); 175.28 (COOH, 6C). ESI-MS (m/z): 1077.39 (100 %, $[M+H]^+$).

G1 Newkome-Branching Boc-DAPMA-Terminated Perylene Bisimide (*7*)

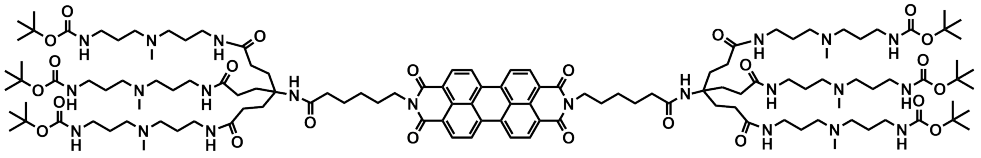

6 (0.095 g, 0.088 mmol) was dissolved in DCM (20 ml) and pyridine (20 ml). To this solution was added DIPEA (0.2 ml, 1.148 mmol), TBTU (0.189 g, 0.589 mmol), and DMAP (0.034 g, 0.278 mmol) with stirring. This was followed by Boc-DAPMA (0.407 g, 1.659 mmol), an oily gum that was dissolved in a small quantity of DCM and rinsed into the reaction vessel with a further portion of DCM. The translucent red solution was then put under nitrogen in order to minimise absorption of water from the air, and then stirred for 7 days. The progress of the reaction was monotired by TLC in 99:1 MeOH:Et_3N, with the product or a mixture of partially-substituted products appearing as a smeared region encompassing the length of the plate. This was in contrast to the starting material which failed to move from the baseline under these conditions. Solvent was removed *in vacuo* and the resulting red solid dissolved in the minimum quantity of DCM. The solution was then purified by size-exclusion chromatography over Bio-Beads®, eluting with DCM. A small quantity of red material remained at the top of the column, with the remainder passing through at various rates. As would be expected, the larger, more completely substituted material was present in the earliest fractions. These were recombined, the solvent removed in vacuo, and the the resulting red solid redissolved in DCM. Residual aromatic impurities were present in this material, some but not all of which was removed by a repeat of the size-exclusion chromatography procedure described above. Once again, the earliest, more pure, fractions were recombined and the solvent removed in vacuo. Finally, the remainder of the impurites were removed by further size-exclusion chromatography, this time eluting over Sephadex®with MeOH.

The resulting pure fractions were recombined and condensed in vacuo to give a red solid, which was further dried by lypohilisation: the solid was dissolved in ^{t}Bu-OH, freezed with liquid nitrogen, and the solvent was then sublimed *in vacuo*.

Yield 0.053 g (26 %). ^{1}H NMR (d-MeOD, 400 MHz) δ 1.41 (s, CH_3, 54H); 1.72, 1.95 (m, CH_2, 40 H); 2.25 (s, CH_2, 12H); 2.87, 3.02, 3.13 (m, CH_2, 52H); 3.27 (p, CH_3, J = 1.6 Hz, 18H); 3.99 (s, CH_2, 4H); 5.46 (s, NH, 12H), 7.94 (br m, Ar-H, 8H). ^{13}C NMR (MeOD, 100 MHz) δ 27.50 (CH_3, 18C), no other chemical shifts visible. ESI-MS (m/z): 814 (37 %, $[M+3H]^{3+}$), 611 (100 %, $[M+4H]^{4+}$]).

G1 Newkome-Branching DAPMA-Terminated Perylene Bisimide (*8*)

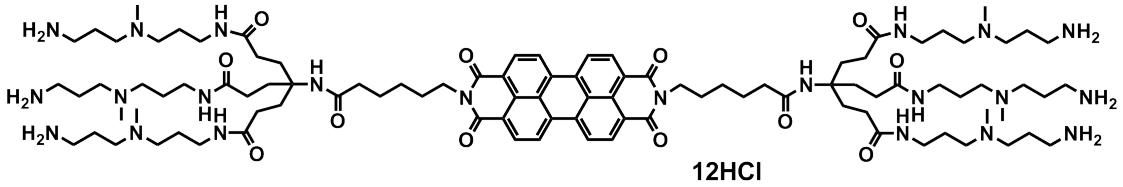

7 (0.053 g, 0.023 mmol) was dissolved in methanol (10 ml). With stirring, gaseous HCl was then bubbled through the deep-red solution for 40 seconds. Some cloudiness was observed in the solution. After 23 hours, stirring was ceased and the precipitate allowed to settle, affording an orange solution over a deep-red or brown precipitate. The solvent was removed *in vacuo* to give a red brown residue which was fully soluble in pure MeOH. The solvent was then once again removed *in vacuo* to give the solid.

Yield 0.044 g (86 %). ^{1}H NMR (d-MeOD, 400 MHz) δ 1.21, 1.41, 1.66, 2.02, 2.12 (br m, CH_2, 52H); 2.86, 2.94, 3.01, 3.10 (br m, CH_2, 60H); 3.24 (p, CH_3, J = 1.6 Hz, 18H); 3.63 (s, CH_2, 4H); 7.99 (br m, Ar-H, 8H). ^{13}C NMR (MeOD, 100 MHz) δ 23.49 (CH_2); 37.89 (CH_2); 40.59 (CH_2); 49.85 (CH_3); 54.38 (CN).

ESI-MS (m/z): 921 (34 %, $[M+2H]^{2+}$]), 614 (100 % $[M+3H]^{3+}$), 461 (85 % $[M+4H]^{4+}$), 369 [69 % $[M+5H]^{5+}$).

G2 Newkome Branching tert-Butyl Terminated Perylene Bisimide (*9*)

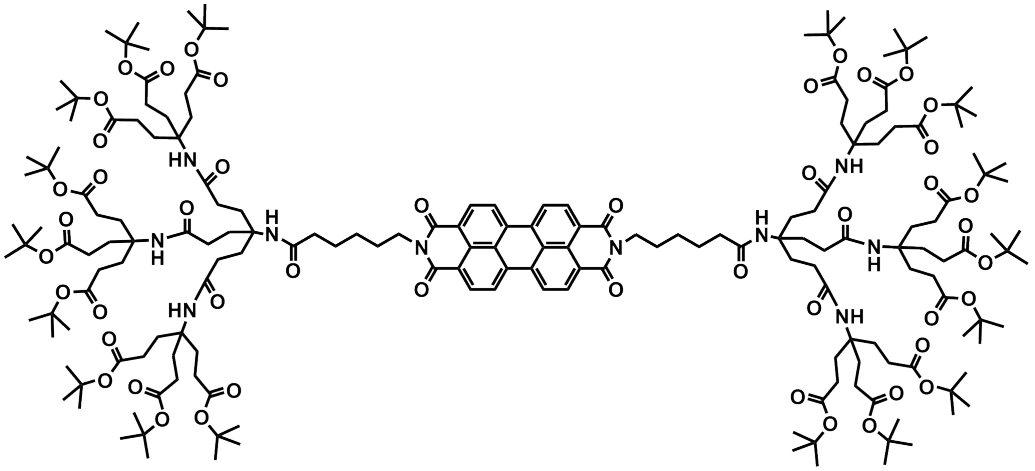

6 (0.095 g, 0.088 mmol) was dissolved in DCM (10 ml) and pyridine (10 ml). ***2*** (0.254 g, 0.611 mmol) and TBTU (0.184 g, 0.573 mmol) were added, with stirring. To this solution was added DIPEA (0.2 ml, 1.148 mmol). The opaque red solution was put under nitrogen in order to minimise the absorption of water from the air. In an attempt to improve the solubility of the components, THF (5 ml) and a further quantity of DCM (5 ml) were added. The progress of the reaction was monitored by TLC. After 11 days, the cloudy red-brown solution was condensed in vacuo and the resulting solid redissolved in the minimum quantity of DCM. This solution was then washed with 1.33 M $NaHSO_4$ (20 ml), saturated $NaHCO_3$ (20 ml), water (20 ml) and, finally, brine (20 ml). The solvent was then removed in vacuo, the product redissolved in EtOAc, and then purified by eluting with the same over SiO_2 to give a red solution. The solvent was once again removed in vacuo to give a red solid.

Yield 0.097 g (32 %). R_f = 0.94 (EtOAc on SiO_2). ^{1}H NMR ($CDCl_3$, 400 MHz) δ 1.20 (s, 20H), 1.37 (s, CH_3, 162H + m, CH_2, 4H); 1.67 (m, CH_2, 4H); 1.77 (m,

CH_2, 4H); 1.91 (m, CH_2, 48H); 2.16 (t, CH_2, J = 8.0 Hz, 52H); 4.17 (t, CH_2, J = 6.5 Hz, 4H); 6.19 (br m, NH, 6H); 7.29 (br s, NH, 2H); 8.60 (br m, Ar-H, 8H). ^{13}C NMR ($CDCl_3$, 100 MHz) δ 22.73, 25.26, 26.68 (CH_2, 6C); 28.13 (CH_3, 54C); 29.73, 29.85 (CH_2, 36C); 31.73, 31.88 (CH_2, 12C); 36.94 (CH_2CO, 2C); 40.56 (CH_2, 6C); 57.51 (CN, 6C); 57.83 (CN, 2C); 80.55 ($C(CH_3)_3$, 18C); 120.21, 123.28, 125.11, 128.82, 131.52 (Ar, 20C); 163.43 (CON, 4C); 172.73 (COOR, 18C); 173.00 (CON, 6C); 173.22 (CONH, 2C). ESI-MS (m/z): 1732 (100 %, $[M+2H]^{2+}$), 1155 (82 %, $[M+3H]^{3+}$).

G2 Newkome Branching Carboxyl Terminated Perylene Bisimide (*10*)

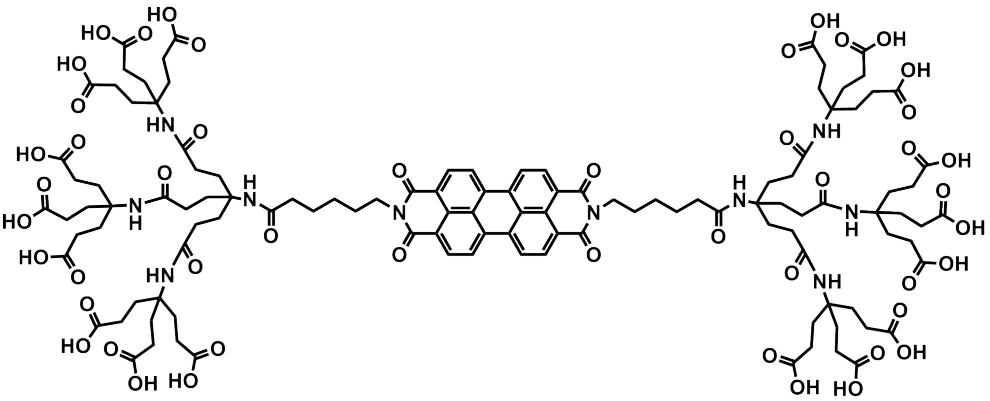

9 (0.097 g, 0.088 mmol) was dissolved in formic acid (5 ml). After 24 hours, residue on the inside of the flask was washed into the formic acid with DCM (3 ml). After a further 18 hours the solvent was removed in vacuo, and residual formic acid was removed as an azeotrope by dissolving the red solid in a mixture of methanol and toluene, which was then removed *in vacuo*.

Yield 0.068 g (99 %). ^{1}H NMR (MeOD/d_5-pyridine, 400 MHz) δ 1.19 1.49, 1.77, 1.94 (m, CH_2, 12H); 2.30, 2.40, 2.51 (m, CH_2, 100H); 4.22 (br s, CH_2, 4H); 8.18 (br m, Ar-H, 8H). ^{13}C NMR (MeOD/d_5-pyridine, 100 MHz) δ 29.40, 30.59, 30.74, 32.05, 35.79 (CH_2); 58.72 (CN); 175.67, 177.31 (OCNH). UV/Vis (MeOH): λ_{max} = 490 nm, 523 nm.

G2 Newkome-Branching Boc-DAPMA-Terminated Perylene Bisimide (*11*)

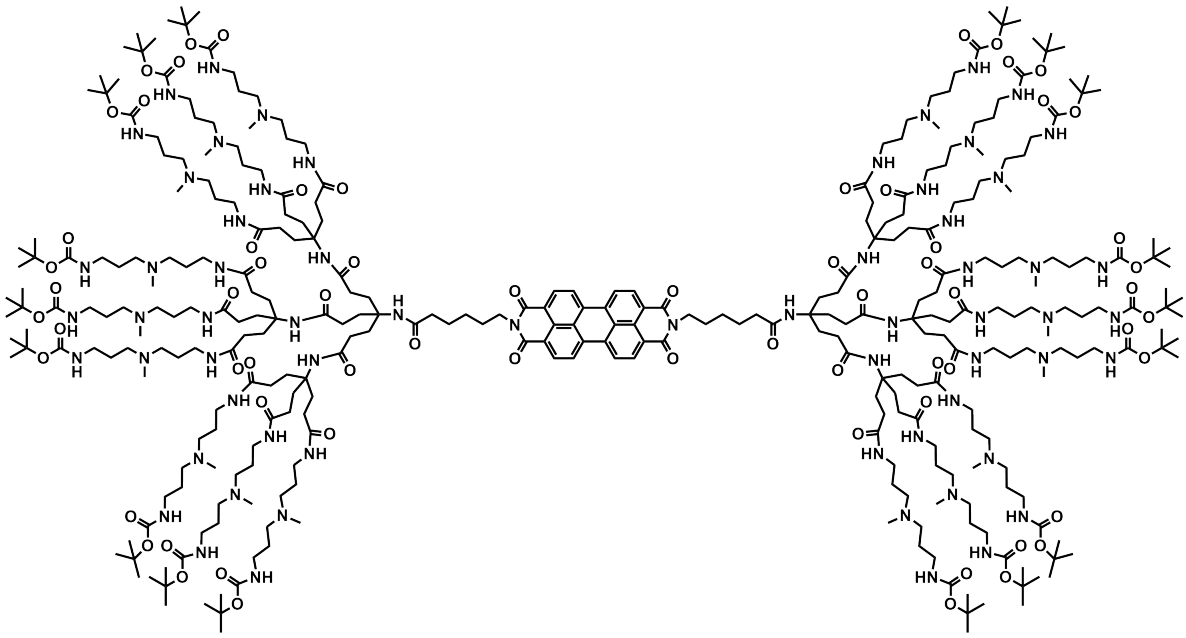

10 (0.068 g, 0.028 mmol) was dissolved in a mixture of DMSO (3 ml) and pyridine (2 ml) affording a deep-red solution. To this was added TBTU (0.205 mg, 0.638 mmol) and DMAP (0.034 g, 0.28 mmol). Boc-DAPMA (0.370 g, 1.508 mmol) was added dissolved in DMSO (2 ml) and DCM (2 ml). Initially, a small quantity of undissolved white powder was visible. After stirring for 5 minutes all components appeared to have dissolved, at which point DIPEA (0.2 ml, 1.148 mmol) was added. The progress of the reaction was monitored by TLC (99:1 MeOH:Et_3N on SiO_2). After 14 days, the solution was gently heated to encourage evaporation of the DCM. The remaining solvent was then removed by vacuum distillation. The resulting solid was then redissolved in DCM, which was removed in vacuo. Subsequent heating to 110 °C in vacuo was carried out in order to remove residual DMSO. The red solid was then dissolved in DCM (100 ml) and filtered to remove insoluble impurities, before being once again condensed in vacuo and then redissolved in DCM (20 ml) to give a dark red solution. This was then purified by

size-exclusion chromatography by eluting over BioBeads®with DCM. The fractions with highest R_f were then condensed in vacuo, dissolved in MeOH, and then further purified by additional size-exclusion chromatography over Sephadex®, eluting with MeOH.

Neither ESI nor MALDI-TOF mass spectrometry showed the desired product. ^{13}C NMR did not show any chemical shifts other than those attributable to the solvent, despite use of a high number of scans and extended relaxation delay.

Yield 0.004 g (2 %). ^1H NMR (MeOD, 400 MHz) δ 1.39 (s, CH_3, 162H); 1.84, 1.96, 2.19 (br m, CH_2, 162H); 2.66 (br s, CH_2, 6H); 2.92, 3.13 (br m, CH_2, 40H) 3.27 (p, CH_3, J = 1.6 Hz, 54H); 3.48 (s, CH_2, 36H); 7.67 (br m, Ar-H, 8H). UV/Vis (MeOH): λ_{max} = 490 nm, 523 nm.

G2 Newkome-Branching DAPMA-Terminated Perylene Bisimide (*12*)

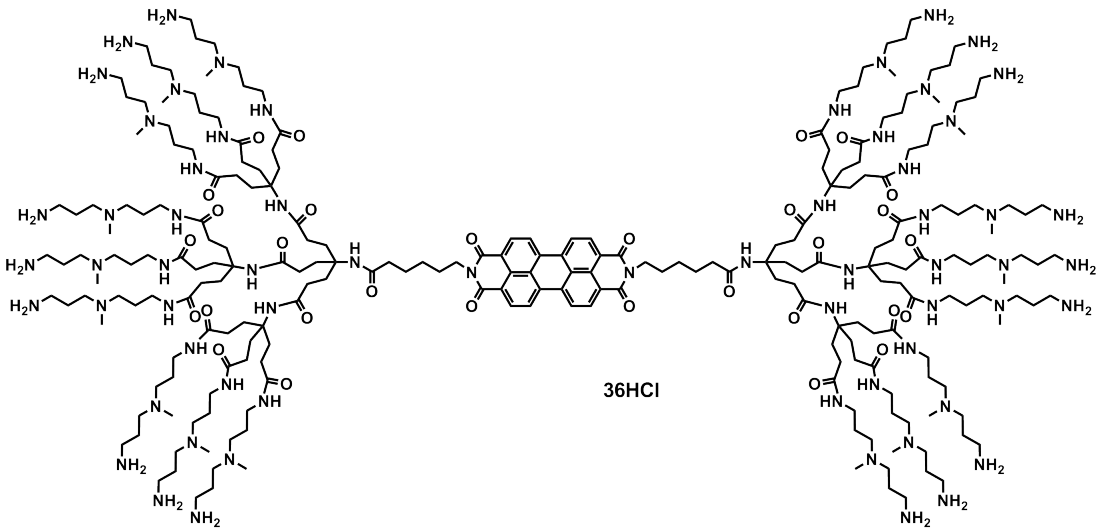

11 (0.004 g, 0.0006 mmol) was dissolved in methanol (5 ml). With stirring, gaseous HCl was then bubbled through the deep-red solution for 40 seconds.

Some cloudiness was observed in the solution. After 19 hours, the solvent was removed *in vacuo* to give a red solid. This was observed to be partially soluble in neutral MeOH, forming a pale-red or pink solution containing an insoluble red film suspended within.

Insufficient product was produced to obtain characterization by NMR.

Yield 0.004 g (Quantitative yield). UV/Vis (0.01 M SHE buffered water): λ_{max} = 499 nm, 543 nm.

References

[1] R. Chitta, A. Sandanayaka, A. Schumacher, L. D'Souza, Y. Araki, O. Ito and F. D'Souza, *Journal of Physical Chemistry C*, 2007, **111**, 6947–6955.

[2] A. Sandanayaka, E. Maligaspe, T. Hasobe, O. Ito and F. D'Souza, *Chemical Communications*, 2009, **46**, 8749.

[3] E. Ruiz-Hitzky, M. Darder and P. Aranda, *An Introduction to Bio-nanohybrid Materials*, Wiley-VCH Verlag GmbH & Co. KGaA, 2008.

[4] M. Kostiainen, G. Szilvay, J. Lehtinen, D. Smith, M. Linder, A. Urtti and O. Ikkala, *ACS Nano*, 2007, **1**, 103–113.

[5] M. Oba, K. Miyata, K. Osada, R. Christie, M. Sanjoh, W. Li, S. Fukushima, T. Ishii, M. Kano and N. Nishiyama, *Biomaterials*, 2011, **32**, 652–663.

[6] H. Hyun, Y.-W. Won, K.-M. Kim, J. Lee, M. Lee and Y.-H. Kim, *Biomaterials*, 2010, **31**, 9128–9134.

[7] K. Numata and D. Kaplan, *Biomacromolecules*, 2010, **11**, 3189–3195.

[8] A. Petitjean, R. Khoury, N. Kyritsakas and J.-M. Lehn, *Journal of the American Chemical Society*, 2004, **126**, 6637–6647.

[9] L. Berti, A. Alessandrini and P. Facci, *Journal of the American Chemical Society*, 2005, **127**, 11216–11217.

[10] D. Tomalia, H. Baker, J. Dewald, M. Hall, G. Kallos, S. Martin, J. Roeck, J. Ryder and P. Smith, *Polymer Journal*, 1985, **17**, 117–132.

[11] A. Patri, J. Kukowskalatallo and J. Bakerjr, *Advanced Drug Delivery Reviews*, 2005, **57**, 2203–2214.

[12] J. Baker, *Hematology / the Education Program of the American Society of Hematology. American Society of Hematology. Education Program*, 2009, 708–719.

[13] C. Backes, C. Schmidt, K. Rosenlehner, F. Hauke, J. Coleman and A. Hirsch, *Advanced Materials*, 2010, **22**, 788–802.

[14] S. Galeazzi, T. Hermans, M. Paolino, M. Anzini, L. Mennuni, A. Giordani, G. Caselli, F. Makovec, E. Meijer, S. Vomero and A. Cappelli, *Biomacromolecules*, 2010, **11**, 182–186.

[15] K. Wood, S. Little, R. Langer and P. Hammond, *Angewandte Chemie International Edition*, 2005, **44**, 6704–6708.

[16] B. Ravoo, *Dalton Transactions*, 2008, 1533.

[17] C.-Y. Chen, C.-J. Su, S.-F. Peng, H.-L. Chen and H.-W. Sung, *Soft Matter*, 2010, **7**, 61.

[18] S. Iijima, *Nature*, 1991, **354**, 56–58.

[19] J. Sha, J. Niu, X. Ma, J. Xu, X. Zhang, Q. Yang and D. Yang, *Advanced Materials*, **14**, 1219–1221.

[20] N. Chopra, R. Luyken, K. Cherrey, V. Crespi, M. Cohen, S. Louie and A. Zettl, *Science*, 1995, **269**, 966–967.

[21] M. Guillot, S. Eisler, K. Weller, H. Merkle, J.-L. Gallani and F. Diederich, *Organic & Biomolecular Chemistry*, 2006, **4**, 766.

[22] A. Robards, *Annual Review of Plant Physiology*, 1975, **26**, 13–29.

[23] H. Kroto, J. Heath, S. O'Brien, R. Curl and R. Smalley, *Nature*, 1985, **318**, 162–163.

[24] K. Novoselov, D. Jiang, F. Schedin, T. Booth, V. Khotkevich, S. Morozov and A. Geim, *Proceedings of the National Academy of Sciences of the United States of America*, 2005, **102**, 10451–10453.

[25] S. Iijima and T. Ichihashi, *Nature*, 1993, **363**, 603–605.

[26] D. Bethune, C. Klang, M. de Vries, G. Gorman, R. Savoy, J. Vazquez and R. Beyers, *Nature*, 1993, **363**, 605–607.

[27] A. Kis and A. Zettl, *Philosophical Transactions of the Royal Society A: Mathematical, Physical and Engineering Sciences*, 2008, **366**, 1591–1611.

[28] J. Mintmire, B. Dunlap and C. White, *Physical Review Letters*, 1992, **68**, 631–634.

[29] J. Vilatela and A. Windle, *Advanced Materials*, 2010, **22**, 4959–4963.

[30] J. G. Dempsey, *United States Patent 6981674*, 2006.

[31] A. C. Clarke, *The Fountains of Paradise*, Gollancz, London, 1979.

[32] R. Weisman and S. Subramoney, *Interface*, 2006, **15**, 42–46.

[33] D. Long, G. Wu and G. Zhu, *International Journal of Molecular Sciences*, 2008, **9**, 120–130.

[34] X. Zuo, C. Peng, Q. Huang, S. Song, L. Wang, D. Li and C. Fan, *Nano Research*, 2009, **2**, 617–623.

[35] M. Mintzer and E. Simanek, *Chemical Reviews*, 2009, **109**, 259–302.

[36] C. Backes, C. Schmidt, F. Hauke, C. Bottcher and A. Hirsch, *Journal of the American Chemical Society*, 2009, **131**, 2172–2184.

[37] W. Linert and I. Lukovits, *Journal of Chemical Information and Modeling*, 2007, **47**, 887–890.

[38] A. García, M. Herrero, S. Frein, R. Deschenaux, R. Muñoz, I. Bustero, F. Toma and M. Prato, *physica status solidi (a)*, 2008, **205**, 1402–1407.

[39] R. Chen, Y. Zhang, D. Wang and H. Dai, *Journal of the American Chemical Society*, 2001, **123**, 3838–3839.

[40] D. Tasis, N. Tagmatarchis, A. Bianco and M. Prato, *Chemical Reviews*, 2006, **106**, 1105–1136.

[41] C. Richard, F. Balavoine, P. Schultz, T. W. Ebbesen and C. Miokowski, *Science*, 2003, **300**, 775–778.

[42] P. Williams and G. Phillips, *Gums and Stabilisers for the Food Industry 15*, RSC Publishing, 2009.

[43] L. Zhang, T. Li, B. Li, J. Li and E. Wang, *Chemical Communications*, 2010, **46**, 1476.

[44] S. Granick and S. Bae, *Science*, 2008, **322**, 1477–1478.

[45] Y. Gao and Y. Bando, *Nature*, 2002, **415**, 599.

[46] J. Mitchell, J. Harris, J. Malo, J. Bath and A. Turberfield, *Journal of the American Chemical Society*, 2004, **126**, 16342–16343.

[47] R. Goodman, R. Berry and A. Turberfield, *Chemical Communications*, 2004, 1372.

[48] Y. Zhang and N. Seeman, *Journal of the American Chemical Society*, 1994, **116**, 1661–1669.

[49] F. Aldaye, A. Palmer and H. Sleiman, *Science*, 2008, **321**, 1795–1799.

[50] M. Gellert, M. Lipsett and D. Davies, *Proceedings of the National Academy of Sciences of the United States of America*, 1962, **48**, 2013–2018.

[51] F. Aldaye and H. Sleiman, *Angewandte Chemie International Edition*, 2006, **45**, 2204–2209.

[52] H. Yang, C. McLaughlin, F. Aldaye, G. Hamblin, A. Rys, I. Rouiller and H. Sleiman, *Nature Chemistry*, 2009, **1**, 390–396.

[53] P. Lo, P. Karam, F. Aldaye, C. McLaughlin, G. Hamblin, G. Cosa and H. Sleiman, *Nature Chemistry*, 2010, **2**, 319–328.

[54] S. Rinker, Y. Ke, Y. Liu, R. Chhabra and H. Yan, *Nature Nanotechnology*, 2008, **3**, 418–422.

[55] J. Tumpane, R. Kumar, E. Lundberg, P. Sandin, N. Gale, I. Nandhakumar, B. Albinsson, P. Lincoln, L. Wilhelmsson, T. Brown and B. Nordén, *Nano Letters*, 2007, **7**, 3832–3839.

[56] P. Sudbery and I. Sudbery, *Human Molecular Genetics, Third Edition*, Pearson Education, Harlow, 2009.

[57] M. Abbasi, A. Lavasanifar, L. Berthiaume, M. Weinfeld and H. Uludag, *Cancer*, 2010, **116**, 5544–5554.

[58] F. Liu and L. Huang, *Hepatology*, 2002, **35**, 1314–1319.

[59] R. Niven, R. Pearlman, T. Wedeking, J. Mackeigan, P. Noker, L. Simpson-Herren and J. Smith, *Journal of Pharmaceutical Sciences*, 1998, **87**, 1292–1299.

[60] R. Hirschhorn, G. Vawter, J. Kirkpatrick Jr. and F. Rosen, *Clinical Immunology and Immunopathology*, 1979, **14**, 107–120.

[61] J. Klawitter and Wisconsin State Laboratory of Hygeine, 2008, http://www.slh.wisc.edu/news/scid_080402.dot - Accessed December 2010.

[62] S. Ryhanen, M. Saily, T. Paukku, S. Borocci, G. Mancini, J. Holopainen and P. Kinnunen, *Biophysical Journal*, 2003, **84**, 578–587.

[63] P. Felgner, T. Gadek, M. Holm, R. Roman, H. Chan, M. Wenz, J. Northrop, G. Ringold and M. Danielsen, *Proceedings of the National Academy of Sciences of the United States of America*, 1987, **84**, 7413–7417.

[64] M. M. de Villiers, P. Aramwit and G. S. Kwon, *Nanotechnology in drug delivery*, Springer, 2009.

[65] M. Forrest, J. Koerber and D. Pack, *Bioconjugate Chemistry*, 2003, **14**, 934–940.

[66] J. Zabner, *Advanced Drug Delivery Reviews*, 1997, **27**, 17–28.

[67] S. Resina, P. Prevot, A. Thierry and C. Neylon, *PLoS ONE*, 2009, **4**, e6058.

[68] C. Lavigne and A. Thierry, *Biochimie*, 2007, **89**, 1245–1251.

[69] S. Moghimi, P. Symonds, J. Murray, A. Hunter, G. Debska and A. Szewczyk, *Molecular Therapy : the Journal of the American Society of Gene Therapy*, 2005, **11**, 990–995.

[70] N. Gabrielson and D. Pack, *Biomacromolecules*, 2006, **7**, 2427–2435.

[71] D. McKenzie, E. Smiley, K. Kwok and K. Rice, *Bioconjugate Chemistry*, 2000, **11**, 901–909.

[72] C. Ahn, S. Y. Chae, Y. H. Bae and S. W. Kim, *Journal of Controlled Release*, **80**, 273–282.

[73] S. Jones and J. Howl, *Regulatory Peptides*, 2004, **121**, 121–128.

[74] M. Ohsaki, T. Okuda, A. Wada, T. Hirayama, T. Niidome and H. Aoyagi, *Bioconjugate Chemistry*, 2002, **13**, 510–517.

[75] J. Lee, Y.-b. Lim, J. Choi, Y. Lee, T.-i. Kim, H. Kim, J. Yoon, K. Kim and J. Park, *Bioconjugate Chemistry*, 2003, **14**, 1214–1221.

[76] M. Tang and F. Szoka, *Gene Therapy*, 1997, **4**, 823–832.

[77] D. Smith, A. Hirst, C. Love, J. Hardy, S. Brignell and B. Huang, *Progress in Polymer Science*, 2005, **30**, 220–293.

[78] D. Joester, M. Losson, R. Pugin, H. Heinzelmann, E. Walter, H. Merkle and F. Diederich, *Angewandte Chemie International Edition*, 2003, **42**, 1486–1490.

[79] J. Hardy, M. Kostiainen, D. Smith, N. Gabrielson and D. Pack, *Bioconjugate Chemistry*, 2006, **17**, 172–178.

[80] G. Newkome, R. Behera, C. Moorefield and G. Baker, *The Journal of Organic Chemistry*, 1991, **56**, 7162–7167.

[81] G. Newkome and C. Weis, *Organic Preparations and Procedures International*, 1996, **28**, 495–498.

[82] H. Ihre, O. Padilla De Jesús and J. Fréchet, *Journal of the American Chemical Society*, 2001, **123**, 5908–5917.

[83] D. Welsh, S. Jones and D. Smith, *Angewandte Chemie International Edition*, 2009, **48**, 4047–4051.

[84] M. Kostiainen, J. Hardy and D. Smith, *Angewandte Chemie International Edition*, 2005, **44**, 2556–2559.

[85] D. Shah, T. Sakthivel, I. Toth, A. Florence and A. Wilderspin, *International Journal of Pharmaceutics*, 2000, **208**, 41–48.

[86] M. Guillot-Nieckowski, D. Joester, M. Stöhr, M. Losson, M. Adrian, B. Wagner, M. Kansy, H. Heinzelmann, R. Pugin, F. Diederich and J.-L. Gallani, *Langmuir*, 2007, **23**, 737–746.

[87] R. Singh, D. Pantarotto, D. McCarthy, O. Chaloin, J. Hoebeke, C. Partidos, J.-P. Briand, M. Prato, A. Bianco and K. Kostarelos, *Journal of the American Chemical Society*, 2005, **127**, 4388–4396.

[88] D. Pantarotto, R. Singh, D. McCarthy, M. Erhardt, J.-P. Briand, M. Prato, K. Kostarelos and A. Bianco, *Angewandte Chemie International Edition*, 2004, **43**, 5242–5246.

[89] C. Poland, R. Duffin, I. Kinloch, A. Maynard, W. Wallace, A. Seaton, V. Stone, S. Brown, W. MacNee and K. Donaldson, *Nature Nanotechnology*, 2008, **3**, 423–428.

[90] C. Lopez, S. Nielsen, P. Moore and M. Klein, *Proceedings of the National Academy of Sciences*, 2004, **101**, 4431–4434.

[91] A. Ebel, W. Donaubauer, F. Hampel and A. Hirsch, *European Journal of Organic Chemistry*, 2007, 3488–3494.

[92] D. Tasis, N. Tagmatarchis, V. Georgakilas and M. Prato, *Chemistry – A European Journal*, 2003, **9**, 4000–4008.

[93] C. Hunter and J. Sanders, *Journal of the American Chemical Society*, 1990, **112**, 5525–5534.

[94] S. Jones, G. Pavan, A. Danani, S. Pricl and D. Smith, *Chemistry – A European Journal*, 2010, **16**, 4519–4532.

[95] C. Schmidt, C. Böttcher and A. Hirsch, *European Journal of Organic Chemistry*, **2007**, 5497–5505.

[96] J. Sheehan and G. Hess, *Journal of the American Chemical Society*, 1955, **77**, 1067–1068.

[97] C. A. G. N. Montalbetti and V. Falque, *Tetrahedron*, 2005, **61**, 10827–10852.

[98] R. Poulain, A. Tartar and B. Deprez, *Tetrahedron Letters*, 2001, **42**, 1495–1498.

[99] M. M. S. Balalaie, *Journal of the Iranian Chemical Society*, 2007, **4**, 364–369.

[100] A. Geall and I. S. Blagbrough, *Journal of Pharmaceutical and Biomedical Analysis*, 2000, **22**, 849–859.

[101] C. Schmidt, C. Böttcher and A. Hirsch, *European Journal of Organic Chemistry*, 2009, 5337–5349.

[102] M. Kostiainen, G. Szilvay, D. Smith, M. Linder and O. Ikkala, *Angewandte Chemie International Edition*, 2006, **45**, 3538–3542.

[103] http://commons.wikimedia.org/wiki/File:DNA_chemical_structure.svg - Accessed December 2010.

[104] K. Kirsanov, E. Lesovaya, M. Yakubovskaya and G. Belitsky, *Mutation Research/Genetic Toxicology and Environmental Mutagenesis*, 2010, **699**, 1–4.

[105] J. Olmsted and D. Kearns, *Biochemistry*, 1977, **16**, 3647–3654.

[106] J. Lepecq and C. Paoletti, *Analytical Biochemistry*, 1966, **17**, 100–107.

[107] K. Utsuno and M. Tsuboi, *Chemical & Pharmaceutical Bulletin*, 1997, **45**, 1551–1557.

[108] B. Cain, B. Baguley and W. Denny, *Journal of Medicinal Chemistry*, 1978, **21**, 658–668.

[109] S. P. Jones, *Developing Synthetic Dendritic Vectors as Multivalent DNA Binders With Potential in Gene Therapy, PhD Thesis*, University of York, 2008.

[110] O. Fedoroff, M. Salazar, H. Han, V. Chemeris, S. Kerwin and L. Hurley, *Biochemistry*, 1998, **37**, 12367–12374.

[111] S. Kerwin, G. Chen, J. T. Kern and P. W. Thomas, *Bioorganic & Medicinal Chemistry Letters*, 2002, **12**, 447–450.

[112] H. F. Nelissen and D. Smith, *Chemical Communications*, 2007, 3039.

[113] A. Barnard and D. Smith, *Unpublished Work*.

[114] F. Würthner, *Pure and Applied Chemistry*, 2006, **78**, 2341–2349.